Coating of Structured Catalytic Reactors by Plasma Assisted Polymerization of Tetramethyldisiloxane

Adil Essakhi,[1] Brigitte Mutel,[2] Philippe Supiot,[2] Axel Löfberg,[1] Sébastien Paul,[1] Véronique Le Courtois,[1] Valérie Meille,[3] Isabelle Pitault,[3] Elisabeth Bordes-Richard[1]

[1] *Unité de Catalyse et de Chimie du Solide (UCCS), UMR 8181, Université Lille 1 Sciences et Technologies, 59655 Villeneuve d'Ascq cedex, France*

[2] *IEMN - UMR 8520, Groupe BioMEMS, Equipe P2M - Université Lille 1 Sciences et Technologies, 59655 Villeneuve d'Ascq cedex, France*

[3] *Laboratoire de Génie des Procédés Catalytiques CPE Lyon, 43 Boulevard du 11 novembre 1918, BP 82077, 69616 Villeurbanne cedex, France*

An original process based on cold plasma assisted polymerization of tetramethyldisiloxane (TMDSO) in the presence of O_2 was developed to cover substrates showing various shapes (plate and foam). In the frame of catalytic application, this coating has to act as a bonding layer for the deposition of active phase such as VO_x/TiO_2 well-known for its properties in NO_x and volatile organic compounds abatement and in the production of chemical intermediates. Good results were obtained by the deposition of a 5-μm thick polysiloxane film followed by a thermal treatment under air at 650°C and by a remote nitrogen plasma post treatment. This procedure led to a silica-like layer allowing its coating in an aqueous suspension of TiO_2. Such a multilayered material can be obtained homogeneously on the whole surface of a sample showing a 3D open geometry like metallic foam. Characterizations of the different steps of the elaborated multilayer material were performed by Fourier transformed infrared spectroscopy, Raman spectrometry, X-ray photoelectron spectroscopy, and electron probe micro-analyzer. **POLYM. ENG. SCI., 51:940–947, 2011.**

INTRODUCTION

Industrial heterogeneous catalysis technology use three main types of reactors: packed-bed reactors, fluidized-bed reactors, and recycle reactors. All of them offer a large internal surface area and a high free volume, but, in spite of these advantages, several drawbacks like a low-heat transfer coefficient (packed bed) and/or erosion/attrition of the catalyst powder (fluidized bed) have also to be noted [1, 2]. The microreactor technology is expected to present several advantages for chemical production compared to classical industrial reactors [3, 4]. For example in the case of strongly exothermic reactions like selective oxidation of hydrocarbons, packed bed reactors do not allow a good dissipation of the heat. The resulting formation of hot spots leads to an early deactivation of the catalyst as well as low selectivity to the targeted product due to the formation of by-products. To overcome these problems a possible solution is the use of structured reactors with coated catalytic walls [5]. The catalyst is thus deposited as a thin film (of a few microns) on metallic walls or structures by a dip-coating method. However, once deposited, the catalytic oxide film has to be both mechanically and chemically stable and to show catalytic properties similar to the corresponding powders. By now, good results were obtained with Al [6] or Al-alloy such as kanthal or FeCralloy but these materials are expensive. So the development of structured reactors will be possible if a technical solution based on cheap substrate is found. Austenitic stainless steel (SS) which is the common material for reactors [7] has to be modified in order to allow adhesion of catalysts like oxides. Another drawback is that under reaction, iron from SS may diffuse towards the active phase and poison it [8]. To by-pass this inconvenient, a way is to deposit a primer layer on the basis of plasma polymerization technology. Although organic compound with polymerizable structure are required for conventional way of polymerization, any organic or inorganic compound can be used in the frame of assisted plasma polymerization process. In this case, polymerization occurs because reactive species of the plasma have energy enough to create free radicals which recombination involves growth of a film, denoted plasma polymer film, which can be deposited on various substrates.

Correspondence to: Brigitte Mutel; e-mail: brigitte.mutel@univ-lille1.fr
Contract grant sponsor: Agence Nationale de la Recherche (ANR-MILLICAT); contract grant number: 06-BLAN-0126-01.
DOI 10.1002/pen.21899
Published online in Wiley Online Library (wileyonlinelibrary.com).

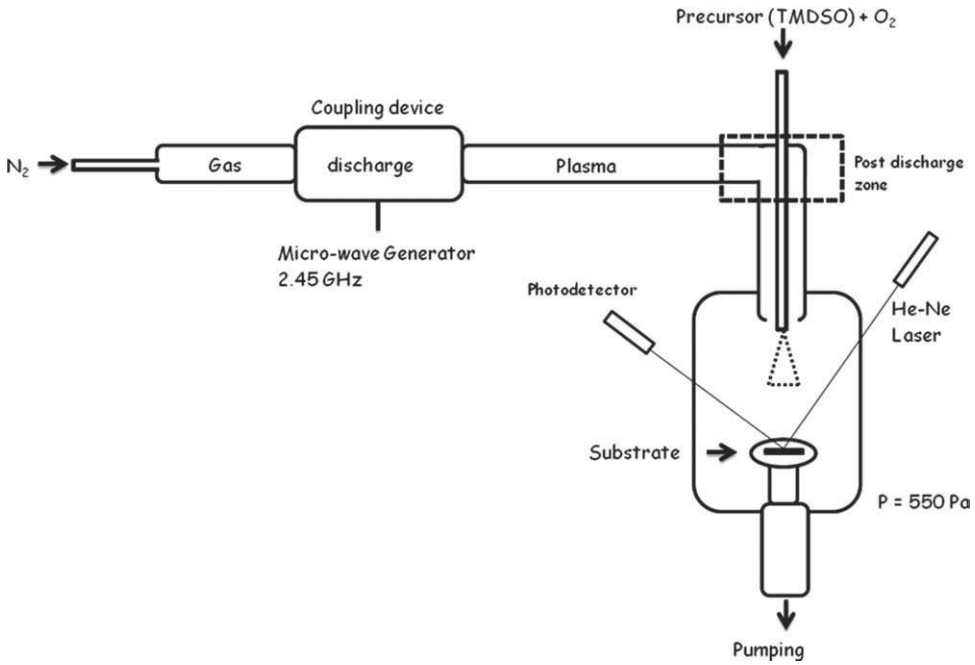

FIG. 1. Experimental setup.

When discharge plasma are involved the deposition rate is often low. Because such plasma are characterized by a high concentration of charged particles, there is a competition between deposition and etching induced by electrons and ions bombardment. The present work involves a cold remote nitrogen plasma (CRNP) located far from the discharge, the resulting mechanism is then free of charged particles, so the etching effect is very low and deposition rates reaching 100 times that obtained with discharge plasma can be obtained. The process is based on cold plasma assisted polymerization of TMDSO used in order to elaborate a silica-like layer on stainless steel substrate able to ensure the mechanical steadiness of the active phase [9–11], to play as a barrier effect against corrosion and Fe diffusion during catalyst reaction and also to act as a bonding layer for the deposition of the active phase. To reach this aim, a full mineralization of the deposited plasma polymer film—also called plasma polymer TMDSO (ppTMDSO) film—by thermal treatment is required.

In this article, the process was applied to two kinds of stainless steel substrates: laminated plates and foam, the aim being to ensure mechanical steadiness of active phase such as VO_x/TiO_2. The grafting of TiO_2 support is performed with the two substrates. Interest of metallic foam is to take advantage of their roughness and 3D dimension in order to increase useful surface area, a very important parameter for catalytic reactions.

EXPERIMENTAL

Plasma Polymerization Process

The experimental set up of the remote nitrogen plasma assisted polymerization reactors is shown in Fig. 1. The nitrogen (grade 99.99%) flow was excited by a microwave discharge (2450 MHz–200 W) in a fused silica tube. By a continuous pumping (roots pump Pfeiffer), the reactive species flow from the discharge to the deposition zone located 1 m from the discharge. The main reactive species in this zone, which is free of charged particles, are atomic nitrogen in the ground electronic state $N(^4S)$. The TMDSO monomer (Sigma Aldrich, grade 97%), premixed with oxygen (grade ≥99.5), was introduced in the CRNP through a coaxial injector. Flows of dinitrogen, dioxygen, and TMDSO at 1800, 25, 5 sccm (standard cubic centimeter per minute), respectively, were controlled at 550 Pa by means of MKS mass-flow controllers. The deposition rate was measured by in situ interferometry using He-Ne laser and a photodetector. The process included several steps: first, the substrate to be coated was pretreated by the single CRNP for 5 min to clean it and to desorb contaminants. Then the monomer/O_2 mixture was added without air exposure for the deposition step. Details about proposed reaction mechanism for decomposition of the monomer can be found in [12]. Finally the TMDSO coated substrate was post-treated in a N_2/1.5% O_2 plasma remote afterglow during 5 min.

Substrates

Stainless steel (AISI 316L) plates (50 mm × 20 mm × 0.5 mm) and foam (Porvair®, 40 ppi, density 5.4%) were used as substrates. Surface of stainless steel plates is shown in Fig. 2a. Figures 2b and c show pictures after cutting the foam in 1 cm × 1 cm × 0.7 cm blocks. Before use, the substrates were sonicated with ethanol (Sigma-Aldrich 99.9%) during 30 min to eliminate or-

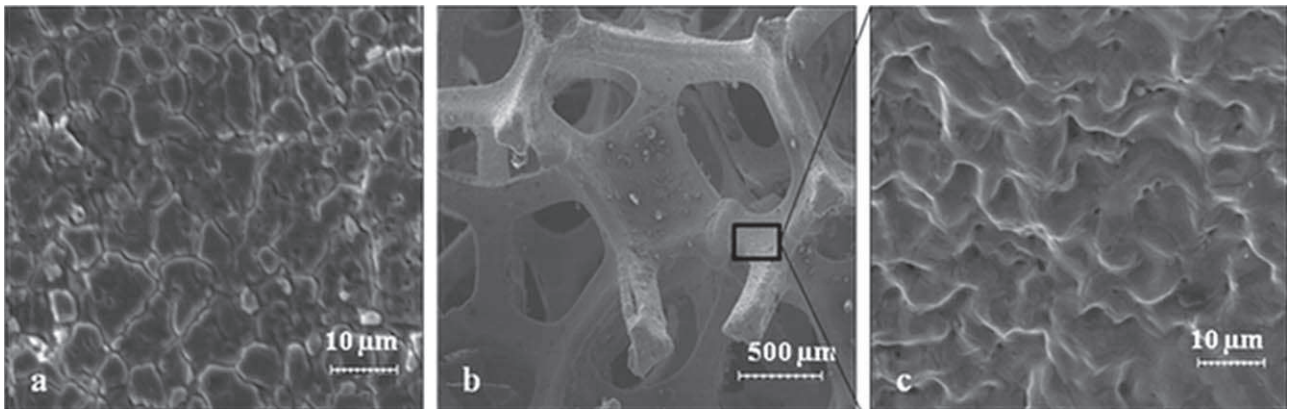

FIG. 2. SEM images of metallic (AISI 316) cross plates surface (a) and foam (b,c).

ganic traces, and then were sonicated two times in deionized water for 30 min before drying at 100°C for 3 h.

Mineralization Process

The ppTMDSO film was mineralized by a thermal treatment in air under forced convection in a Maton programmable furnace. The heating rate was controlled with a Nelotherm thermal regulator. To remove carbon remaining traces on the surface sample, a N_2/1.5% O_2 remote plasma treatment was finally applied during 5 min. The composition of the mineralized film can evolve to that of a material with high density of silanols after NaOH washing.

TiO_2 Coating

Substrates to be coated were dipped under stirring in an aqueous suspension containing 60 wt% TiO_2 particles during 5 min and withdrawn at 6 mm/s. TiO_2 was provided by Sigma-Aldrich (10 m^2/g, 99.8% anatase, and average particles size of 10 μm). After coating, the substrates were calcinated in air flow at 110°C during 1 h, and then at 700°C during 2 h (temperature ramp: 80°C/min).

CHARACTERIZATION METHODS

Fourier Transform Infrared and Raman Spectroscopy

The films were analyzed using a Fourier transform infrared (FTIR) Perkin-Elmer spectrometer. Spectra were recorded in specular reflexion mode in the spectral range 4000–400 cm^{-1} (resolution 4 cm^{-1}). Raman spectra (RS) were recorded on a LabRAM Infinity spectrometer (Jobin Yvon) equipped with a liquid nitrogen detector and a frequency-doubled Nd:YAG laser supplying the excitation line at 532 nm. The power applied on the sample was below 5 mW. The spectrometer was calibrated daily using the silicon line at 521 cm^{-1}.

X-Ray Photoelectron Spectroscopy Analysis

X-ray photoelectron spectroscopy (XPS) was carried out using Escalab 220 XL spectrometer from Vacuum Generators. A monochromatic Al Kα X-ray source was used and electron energies were measured in the constant analyzer energy mode. The pass energy was 100 eV for the survey spectra and 40 eV for the single element spectra. All XPS binding energies were referred to C 1s core level at 285 eV. The angle between the incident X-rays and the analyzer was 58°, photoelectrons being collected perpendicularly to the sample surface.

Electron Probe Micro Analysis

Before analysis, samples were embedded into epoxy resin, and polished with abrasive discs (2400 to 3 μm) granulometry. A Bal-Tec SCD005 sputter coated allowed depositing a thin carbon film. Elemental analysis were made using a wavelength dispersive X-ray spectrometer (Cameca SX-100 microprobe analyser) working at 15 kV and 15 nA for back scattered electron (BSE) images and at 15 kV and 49 nA for silicon, titanium, and iron X-ray profiles and mapping. Si, Fe, and Ti Kα X-rays were detected using TAP, LiF, and PET crystals, respectively.

Scanning Electron Microscopy

The Scanning Electron Microscope (SEM) Hitachi 4100 S was equipped with micro-analyzed (EDS) and a Field Emission Gun (FEG). The working voltage was 15 KeV. The analyzed volume was estimated to be approximately 1 μm $\times$ 1 μm deep and wide.

Laser Interferometry

The thickness of ppTMDSO film deposited on stainless steel plates was measured in situ by interferometry using a He-Ne laser (λ = 632.8 nm) and a photodetector.

 DOI 10.1002/pen

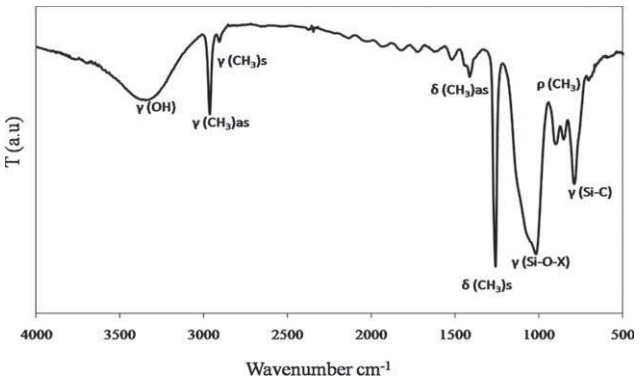

FIG. 3. FTIR-spectrum (specular reflexion) of ppTMDSO film.

Contact Angle Measurements

The wettability of the deposited layers was evaluated from contact angle with deionized water using a Krüss computer-controlled goniometer. The accuracy on measurement performed at room temperature was $\pm 1^{\circ}$.

RESULTS AND DISCUSSION

In a first approach, the process allowing to obtain a homogenous TiO_2 layer deposited by dip-coating on a mineralized ppTMDSO film was studied for SS-316L plates. Then the process was transposed for application on metallic foam.

Coating of Stainless Steel Plate

Depending on the thickness of the films, the deposition rate of ppTMDSO film was evaluated by two methods, interferometry measurements for thickness smaller than 12 μm and BSE images for thickness larger than 5 μm. Figure 3 shows an example of image obtained for a

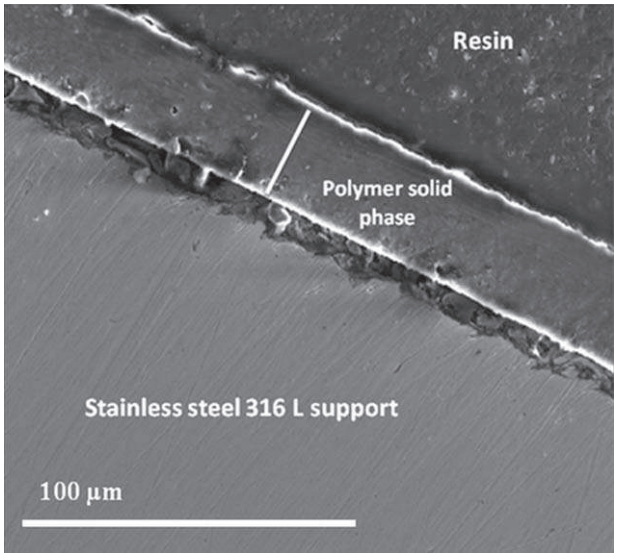

FIG. 4. EPMA image for pp TMDSO film deposited on SS.

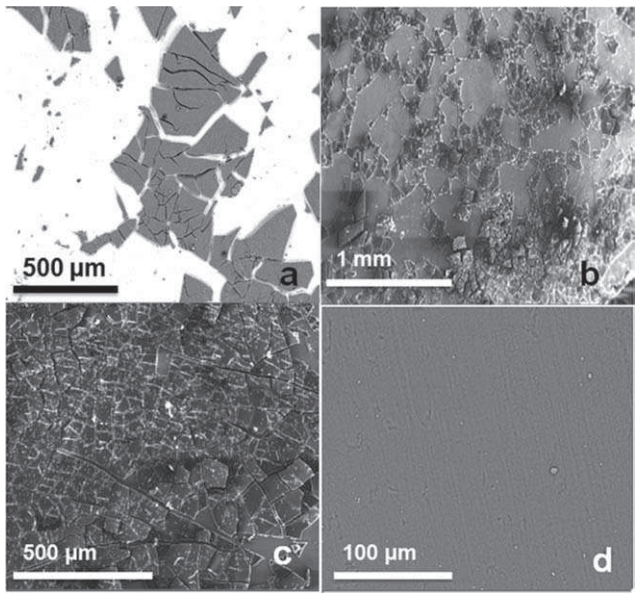

FIG. 5. EPMA images of ppTMDSO film deposited on SS and calcinated at 650°C during 1 h. (a) $t = 15$ μm, p-t = yes, t-r = 5°/min; (b) $t = 15$ μm, p-t = no, t-r = 1°/min; (c) $t = 5$ μm, p-t = yes, t-r = 1°/min; (d) $t = 5$ μm, p-t = no, t-r = 1°/min.

30-μm thick film. In the experimental conditions of this study, the deposit rate was 1.0 ± 0.1 μm/min with an excellent linearity for thicknesses ranging from 1 to 35 μm. Good agreement was obtained for the two methods. The ppTMDSO film was analyzed by FTIR spectroscopy to determine its chemical nature similar to that reported in previous studies [9–12]. The spectrum shows the decrease of the strong band at 2145 cm^{-1} (see Fig. 4) which is characteristic of the Si—H stretching bond in TMDSO [13], giving evidence of the H ablation by atomic nitrogen attack [12]. In the range 1200–1000 cm^{-1}, the enhancement of a double peak, which is characteristic of the asymmetrical elongation of the Si—O—Si bond in a polymeric conformation, is observed as well as the characteristic bands of Si—C.

Our aim was to find a protocol allowing conversion of a ppTMDSO film into an homogeneous fully mineralized film with an ex situ thermal treatment of ppTMDSO film in air. The 15-μm thick film post-treated during 5 min in N_2/O_2 plasma afterglow was submitted to a thermal treatment in air performed at 5°C/min heating rate up to 650°C. The final temperature was held during 1 h. This protocol led to a total burst of the layer as shown in Fig. 5a, which was also confirmed by the presence of the Fe2p photopeak at 710.68 eV detected by XPS. The layer could not resist to the physicochemical constraints induced by the chosen conditions. Therefore the influence of the film thickness (t), the post-treatment (p-t), and the temperature ramp (t-r), were studied in order to solve this problem. The response of each experiment was evaluated by BES images. As shown in Fig. 5a–d, the film thickness and the post-treatment are the most influent parameters. Best

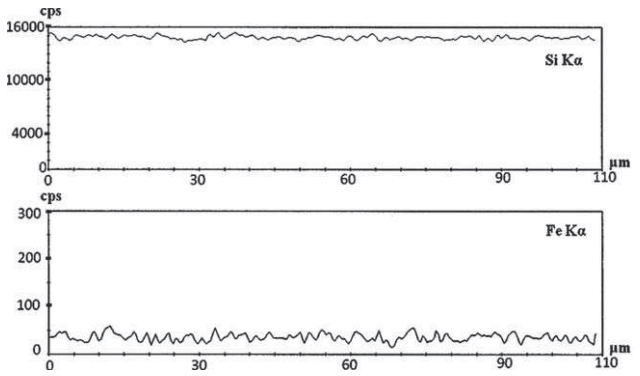

FIG. 6. EPMA analysis of ppTMDSO film calcinated in conditions of Fig. 5d: Si and Fe profiles on surface.

results are obtained for a thin film without post-treatment. It was previously shown [9, 14] that the plasma assisted post-treatment led to the formation of a quasi-two-layers material one being SiO_2 and the other being assimilated as an unmodified ppTMDSO layer. During the thermal treatment in air, the carbonyl groups of ppTMDSO react with oxygen leading to the formation of CO_2 and H_2O [15].

Good results were obtained for a 5-μm thick film with heating rate 1°C/min and no post-treatment. In these conditions, an homogeneous film was obtained (Fig. 5d), the SS plate being completely covered. Figure 6 shows the Si and Fe concentration profiles obtained from electron probe micro analysis (EPMA) analysis of the sample corresponding to this case. XPS analysis indicates a low carbon level, the stoechiometric composition being $SiC_{0.05}O_{1.8,}$ which is also evidenced by Raman spectroscopy (see Fig. 7). The remaining CH_3 traces which could be an inconvenient for further deposition of the active phase were efficiently removed by N_2/O_2 plasma afterglow performed during 5 min. After this post-treatment, the surface composition obtained by XPS was $SiO_{0.01}O_{1.82}$ (further called SiO_x). During the treatment the fully modified ppTMDSO film shrinked by $\approx$ 75%. To check the good adhesion and mechanical steadiness of the SiO_X layer, the sample was immersed into *n*-heptane ultrasonic bath during 1 min. No peel-off was observed. Before coating by TiO_2, the plate was immersed during 4 h in a basic solution (3 g NaOH, 4 mL ethanol, 3 mL water). After this treatment, the contact angle measured

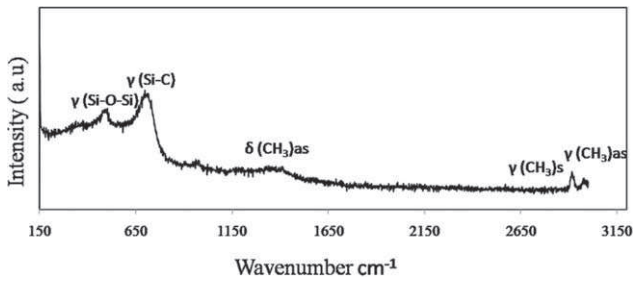

FIG. 7. Raman spectrum of ppTMDSO film calcinated in conditions of Fig. 5d.

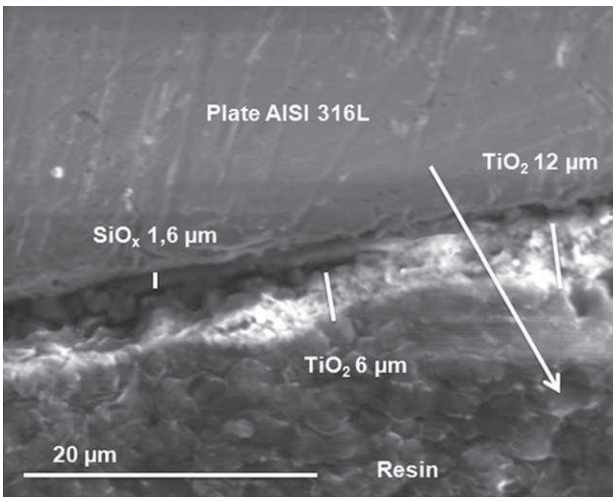

FIG. 8. EPMA image for TiO_2/SiO_x/SS deposited on plate.

with water was 29°. It was equal to 87° for the bare SS plate, 104° for ppTMDSO/SS and 34° for SiO_x/SS. Therefore, the combined treatment in N_2/O_2 plasma afterglow and basic washing improved the wettability of plates for the next TiO_2 coating step. Figure 8 shows a 12 μm thick coating of SiO_x/SS plate. The WDS profile of Si, Ti, and Fe shown in Fig. 9 gives evidence of the successive layers. This TiO_2/SiO_x/SS composite material remains quite stable, even after bathing in an *n*-heptane ultrasonic bath during 1 min, giving evidence of its good mechanical stability.

Coating of 316L Stainless Steel Foam

Owing to their large surface to volume ratio, foams present the advantages of increased mass and heat transfers which have to be controlled in catalytic exothermic reactions. To make an homogeneous coating of the foam with ppTMDSO, two configurations (A and B) of the sample holder were designed (see Fig. 10). In configuration A, the sample was just settled on the substrate holder, so the reactive gas flowed by diffusion through the foam, and was consumed before reaching the core of the sample. No more coating was observed (Fig. 11d) beyond 3.5 mm from the top surface of the sample. In

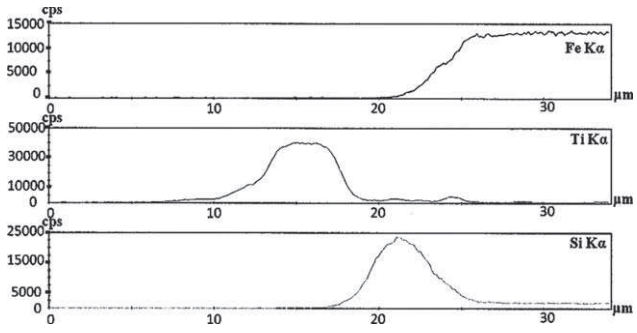

FIG. 9. EPMA analysis of TiO_2/SiO_x/SS: Fe, Ti, and Si profiles according to white arrow shown in Fig. 8.

 DOI 10.1002/pen

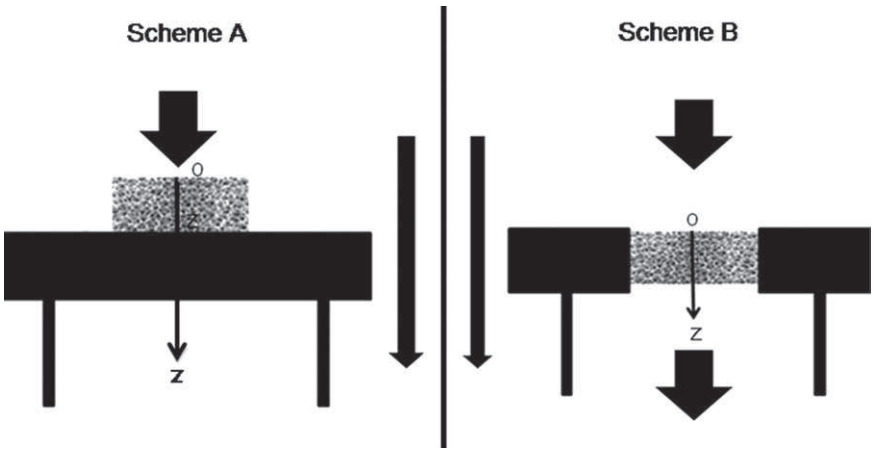

FIG. 10. The two schemes used to deposit ppTMDSO on metallic foams.

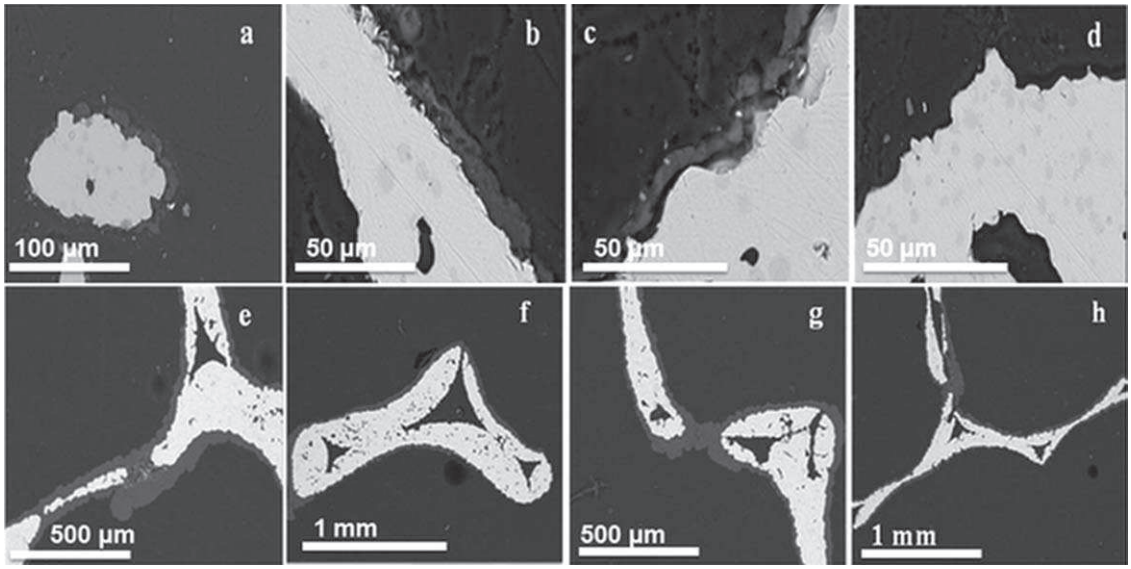

FIG. 11. Evolution of ppTMDSO film thickness versus the sample depth for the two experimental configurations. Scheme A: (a) $Z = 0$, $t = 12$ μm; (b) $Z = 1.0$ mm, $t = 11$ μm; (c) $Z \approx 1.8$ mm, $t = 6$ μm; (d) $Z = 3.5$ mm, $t = 0$ μm. Scheme B: (e) $Z = 0$; (f) $Z = 1.8$ mm; (g) $Z = 3.5$ mm; (h) $Z = 7.0$ mm. Whatever z, $t \approx 15$ μm.

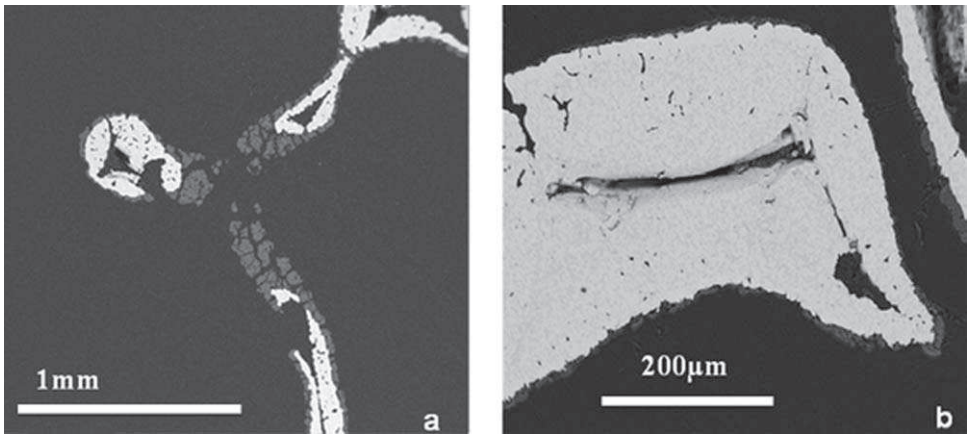

FIG. 12. EPMA image of calcinated ppTMDSO film versus thickness. (a) $t = 15$ μm; (b) $t = 7$ μm.

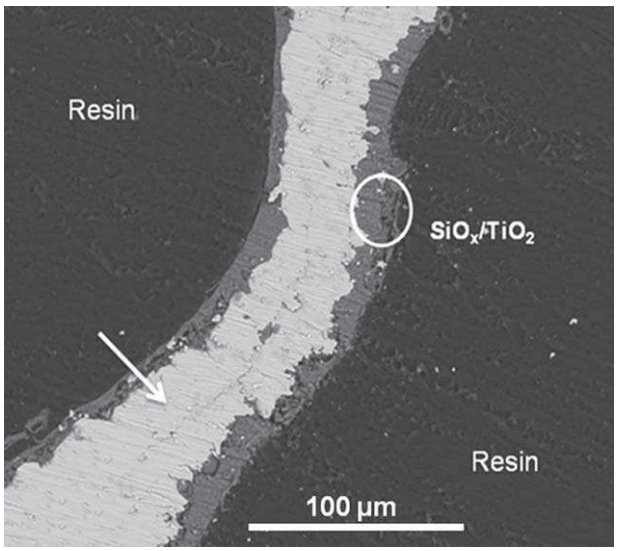

FIG. 13. EPMA image of TiO_2/SiO_x/SS deposited on foam.

configuration B, the reactive gas convectively flowed through the foam. The precursor transport was then ensured through the entire foam volume open to the flow. An homogeneous layer was observed through the whole foam with thicknesses higher or equal to 15 μm (Figs. 11e–h), as was evaluated by EPMA along z. To generate the SiO_x layer onto the metallic foam, the sample was calcinated in the conditions previously determined for plates (no post-treatment, 1°C/min heating rate, final temperature 650°C during 1 h). EPMA images show that it is possible to obtain an homogeneous calcined ppTMDSO only when the film thickness is lower than 7 μm (see Fig. 12). After plasma post-treatment step and chemical treatment in NaOH, the TiO_2 coating was performed as above. EPMA image (Fig. 13) and EPMA analysis (Fig. 14) as well as X-ray mapping (see Fig. 14) give evidence for the two successive layers.

CONCLUSION

For the first time in literature, a polymer plasma TMDSO film was deposited through the whole surface of a stainless steel foam by a plasma assisted polymerization process. The film could easily be converted into a stable, adhesive, and homogeneous SiO_x layer after calcination in air. This result is very interesting in the field of industrial application of heterogeneous catalysis. Indeed, SiO_x acts efficiently as a bonding layer for the deposition of oxide catalysts. The TiO_2 support onto which vanadium isopropoxide will be grafted was deposited by dip-coating in TiO_2-anatase aqueous suspension. SiO_x is expected to act both as a primer and as a barrier against poisoning of VO_x/TiO_2 catalyst by iron of the substrate. The catalytic experiments with such coated foams are in progress. Getting a success with these catalyst/structured reactors, the active phase of which is well-known for its application in chemical industry as well as in pollution abatment, could help to promote the use of new reactors with enhanced heat and mass transfers.

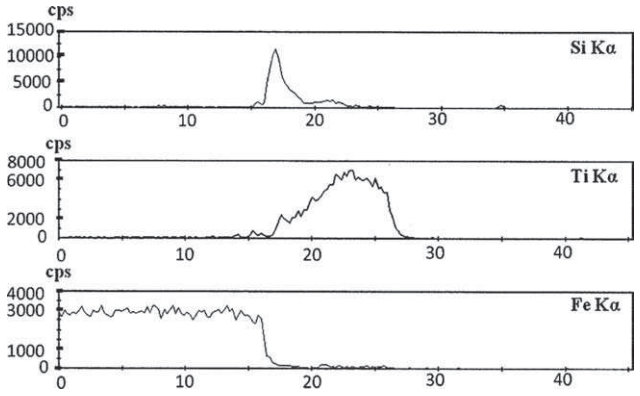

FIG. 14. EPMA analysis of TiO_2/SiO_x/SS: Fe, Ti, and Si profiles according to white arrow shown Fig. 13.

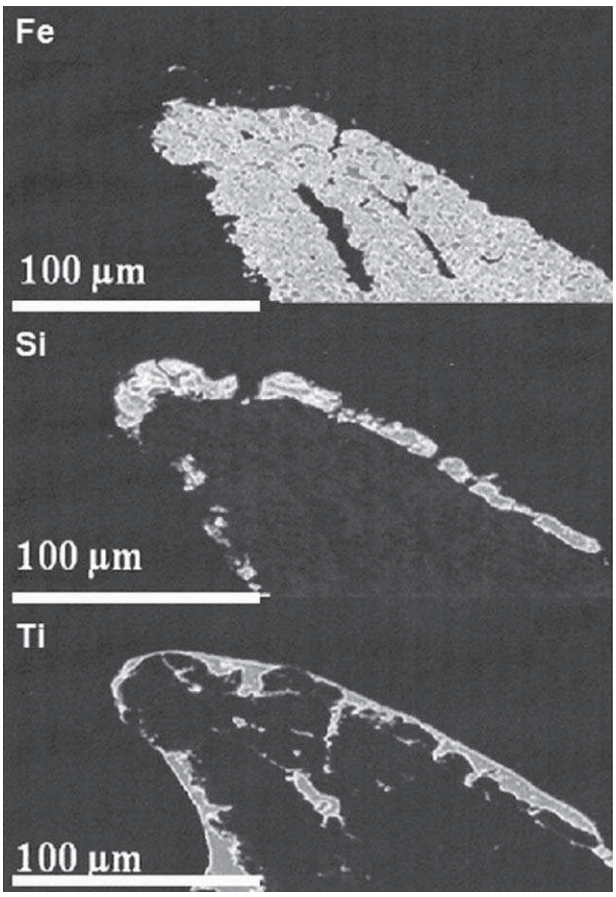

FIG. 15. X-ray mapping of the elements Ti, Si, and Fe on metallic foam.

ACKNOWLEDGMENTS

M. Frère and L. Gengembre are thanked for XPS measurements. S. Bellayer is thanked for EPMA analysis.

REFERENCES

1. H. Redlingshffer, O. Krfcher, W. Bfck, K. Huthmacher, and G. Emig, *Ind. Eng. Chem. Res.*, **41**, 1445 (2002).

2. G. Groppi, W. Ibashi, E. Tronconi, and P. Forzatti, *Catal. Today*, **69**, 399 (2001).
3. K.F. Jensen, *Chem. Eng. Sci.*, **56**, 293 (2001).
4. J.J. Lerou, M.P. Harold, J. Ashmead, T.C. O'Brien, M. Johnson, J. Perrotto, C.T. Blaisdell, T.A. Rensi, and J. Nyquist, in *Microsystem Technology for Chemical and Biological Microreactors, Dechema Monographs*, *Vol. 132*, W. Ehrfeld, Ed., Verlag Chemie, Weinheim, 51 (1996).
5. R.M. de Deugd, F. Kapteijnand, and J.A. Moulijn, *Top. Catal.*, **26**, 1 (2003).
6. T. Giornelli, A. Löfberg, and E. Bordes-Richard, *Thin Solid Films*, **479**, 64 (2005).
7. T. Giornelli, A. Löfberg, and E. Bordes-Richard, *Appl. Catal. A*, **305**, 197 (2006).
8. T. Giornelli, A. Löfberg, L. Guillou, S. Paul, V. Le Courtois, and E. Bordes-Richard, *Catal. Today*, **128**, 201 (2007).
9. L. Guillou, P. Supiot, and V. Le Courtois, *Surf. Coat. Technol.*, **202**, 4233 (2008).
10. L. Guillou, D. Balloy, P. Supiot, and V. Le Courtois, *Appl. Catal. A*, **324**, 42 (2007).
11. L. Guillou, V. Le Courtois, and P. Supiot, *Matér. Tech.*, **93**, 335 (2005).
12. F. Callebert, P. Supiot, K. Asfardjani, O. Dessaux, P. Dhamelincourt, and J. Laureyns, *J. Appl. Polym. Sci.*, **52**, 1595 (1994).
13. D.R. Anderson and A.L. Smith, Ed., *Analysis of Silicones*, Wiley, London (1974).
14. P. Supiot, C. Vivien, A. Granier, A. Bousquet, A. Mackova, F. Boufayed, D. Escaich, P. Raynaud, Z. Stryhal and J. Pavlik, *Plasma Processes Polym.*, **3**, 100 (2006).
15. A. Quéde, C. Jama, P. Supiot, M. Le Bras, R. Delobel, O. Dessaux, and P. Goudmand, *Surf. Coat. Technol.*, **151–152**, 424 (2002).

Chemical Engineering Journal 176–177 (2011) 49–56

Contents lists available at ScienceDirect

Chemical Engineering Journal

journal homepage: www.elsevier.com/locate/cej

Use of catalytic oxidation and dehydrogenation of hydrocarbons reactions to highlight improvement of heat transfer in catalytic metallic foams

A. Löfberg[a,b], A. Essakhi[a,b], S. Paul[a,c], Y. Swesi[d], M.-L. Zanota[d], V. Meille[d], I. Pitault[d], P. Supiot[a,e], B. Mutel[a,e], V. Le Courtois[a,c], E. Bordes-Richard[a,b,*]

[a] Université Lille Nord de France, F-59000 Lille, France
[b] CNRS UMR 8181, Unité de Catalyse et Chimie du Solide, UCCS, Université Lille 1, Sciences et Technologies, F-59655 Villeneuve d'Ascq, France
[c] Ecole Centrale de Lille, F-59655 Villeneuve d'Ascq, France
[d] Université de Lyon, Institut de Chimie de Lyon, Laboratoire de Génie des Procédés Catalytiques, CNRS UMR 2214, CPE-Lyon, F-69616 Villeurbanne, France
[e] Institut d'Electronique, de Microélectronique et de Nanotechnologies, CNRS UMR 8520, Université Lille 1, Sciences et Technologies, F-59655 Villeneuve d'Ascq, France

ARTICLE INFO

Article history:
Received 20 December 2010
Received in revised form 3 April 2011
Accepted 28 April 2011

Keywords:
Solid catalytic foams
Heat transfer
Oxidative dehydrogenation of propane
Dehydrogenation of methylcyclohexane
VO_x/TiO_2 coated foams
$Pt/\gamma\text{-}Al_2O_3$ coated foams

ABSTRACT

Two model reactions were used to show the influence of catalytic foams on improving heat transfer. The catalytic performances were compared to those observed when using the same reactors packed with catalytic powder or beads. One reaction was the exothermic oxidative dehydrogenation of propane which was investigated on $7\%V_2O_5/TiO_2$ coated on stainless steel foam. A silica layer was first deposited on the foam surface by Remote Plasma Enhanced Chemical Vapour Deposition to avoid poisoning of active phase by iron species, to favour the anchoring of TiO_2 support and to accommodate the difference of dilatation coefficients. When comparing catalytic foams with powders in the same reactor, the selectivity to propene at isoconversion was higher by 12–45 mol% for the same amount and composition ($7\%V_2O_5/TiO_2$) of the active phase and in the same operating conditions (contact time, C_3/O_2 ratio, temperature range). The other reaction was the endothermic dehydrogenation of methylcyclohexane on $2\%Pt/Al_2O_3$ directly coated on foams and on molecular sieve beads. To study the influence of heat and mass transfers, the material (FeCrAlloy or alumina) and porosity (81–97%) of foams were varied. It was found that, even for highly exothermic or endothermic reactions not limited by external transport, the coated foams significantly increased the effective conductivity of catalytic beds, the denser foam leading to higher effective conductivity.

1. Introduction

To increase the yield and selectivity of products in catalytic processes, one way is to improve the catalytic properties of the catalyst or to find a better one. The other way is to improve the efficiency of the gas/solid contacts and to diminish the thermal gradients in catalytic beds. In other words the goal is to increase the rates of heat and mass transfers and to improve the dispersions as well as the effective conductivities. Catalytic micro(milli)reactors or structured reactors offer a potential to conduct mass and/or heat transfer-demanding reactions under safer conditions while maintaining and/or increasing selectivity and productivity [1–3]. Structured inserts (packings) like honeycomb monoliths were first used in automotive exhaust pollution abatement, but others, like solid foams, in which the external mass transfer would increase while maintaining a low pressure drop, are now available. In a joint programme granted by the Agence Nationale de la Recherche we are currently studying how the structuration can help to enhance the catalytic reactor performance. Different methods with their advantages and drawbacks are available to evaluate the reactor performance improvement. One method is to carry out measurements of the transport phenomena (mass, heat and momentum) in the structures, followed by numerical simulations. It requires a perfect description of the structures in terms of characteristic parameters (diameter, tortuosity,. . .). These parameters are easy to measure or to estimate, in the case of e.g., fins in a heat exchanger, or spherical shaped catalysts. However, they are difficult to obtain in the case of foams that require a topological description due to their 3D-anisotropy. Moreover, a hydrodynamic study requires performing mass and heat transfer measurements in large enough pieces to obtain significant and measurable gradients. This way is chosen by several research teams because it is definitely useful to acquire the knowledge for the future design of industrial processes [4,5]. The second method is to perform catalytic experiments using a well known catalyst deposited onto the structure. It requires a

* Corresponding author at:Unite de Catalyse et Chimie du Solide, CNRS UMR 8181, Université Lille 1, Sciences et Technologies, F-59655 Villeneuve d'Ascq, France.
E-mail address: Elisabeth.Bordes@univ-lille1.fr (E. Bordes-Richard).

1385-8947/$ – see front matter © 2011 Elsevier B.V. All rights reserved.
doi:10.1016/j.cej.2011.04.064

perfect knowledge of the catalyst properties and of the kinetics of the reaction. To get the same catalyst density in reactors, it is also necessary to make sure that the catalyst is homogeneously distributed among the whole structure. An advantage of this way is also to allow the testing of small pieces of foam, wherein thermal gradients would be non-significant under low Reynolds as practised in academic laboratories. This method could seem to be less rigorous than the first one, but, first, it does not require onerous equipments such as X-ray tomograph, and, second, it considers the overall system (including the catalyst layer in working conditions) whereas most physical characterizations and modellings are made on bare, uncoated, foams. We have worked that way to show how highly exo or endothermic model reactions can be used for rapid evaluations of catalytic foam performance.

The two following model reactions were chosen because they are heat sensitive. The first one is the oxidative dehydrogenation of propane (ODP) to propene, the enthalpy of reaction of which is $\Delta_R H^\circ_{298} = -118\,kJ\,mol^{-1}$. Despite of many attempts and tries to find more efficient catalysts, the best yield using oxide catalysts in fixed bed reactors is currently less than ca. 40% [6,7], because the product (propene) is less stable than the reactant (propane) and very easily oxidized to CO_2. Obviously the combustion of propene is even more exothermic ($\Delta_R H^\circ_{298} = -1930\,kJ\,mol^{-1}$). Hot spots in packed bed reactors contribute to decrease the selectivity to propene as well as to deactivate the catalyst. The heat transfer control is therefore a key issue when dealing with such a selective oxidation reaction. Conversely, the selectivity to propene can be considered as an "indirect sensor" of the heat transfer efficiency. Very recently, a microstructured foam reactor was developed by Schwarz et al. [8] to conduct this reaction using VO_x/γ-Al_2O_3 catalyst. As in most kinetic studies on vanadium oxide based catalysts in packed bed reactors [9–11], the authors found that the selectivity to propene suffered from consecutive propene oxidation to CO and CO_2, but also from the accumulation of propene inside the particle pores leading to its degradation [8,12]. However the latter observation may be related to the use of porous γ-alumina as a support for VO_x species. In this concern, the textural properties (low surface area and little porosity) of TiO_2-anatase are more suitable. Moreover TiO_2-anatase exerts a structural influence on the supported vanadium species which is responsible for selectivity in reactions like, e.g., *o*-xylene oxidation to phthalic anhydride [13–16]. In former works [17–19] we studied several ways to coat aluminum and stainless steel plates by this catalyst. We examined their properties in ODP in a home—designed plate reactor, but the catalytic performances were not satisfying enough when compared to those obtained in a packed bed reactor, due, among other factors, to higher mean values of temperature in the plate reactor than in the packed bed reactor.

The other heat sensitive reaction is the dehydrogenation of methylcyclohexane (MCH) to toluene on Pt/γ-Al_2O_3. This reaction is often chosen among the many reactions that would be suitable to generate hydrogen for fuel-cell application. Roumanie et al. [20] operated the reaction in a silicon micro–structured reactor composed of microsized pillars. In another work [21], this endothermic reaction was coupled to the exothermic combustion of toluene in an autothermal heat-exchanger reactor. The dehydrogenation of MCH is endothermic ($\Delta_R H^\circ_{298} = 204\,kJ\,mol^{-1}$) and it requires temperatures higher than 300 °C to shift the thermodynamic equilibrium and to reach high conversions. However side reactions like cracking lead to undesired products above 400 °C. Though the rate of dehydrogenation is relatively slow, and no limitation due to external or internal mass transfer exists, significant thermal gradients occur in packed bed reactors filled with pellets, and the heat management has to be addressed.

The means chosen to study the influence of heat transfer was to deposit the respective catalysts on structured substrates known for their high thermal conductivity. Reticulated solid foams exhibit several interesting features like their large geometric areas, high void fractions leading to low pressure drop and high mechanical stability. Compared to straight channelled monoliths, one of their advantages is the 3D—open structure which is more suitable for the dispersion of the reacting gas phase and so for improving the external mass transfer [1,22–25].

Stainless steel and FeCrAlloy foams were coated by VO_x/TiO_2 and Pt/γ-Al_2O_3 catalysts, respectively. To assess the – expected – beneficial effect of reactor structuring, it was found necessary to compare the catalytic performance with that of the same active species, shaped as powders, beads or foams. Another difficulty stemmed, which was the fact that structured systems may require adapted preparation methods [26], but that, in turn, the preparation methods may affect the catalytic properties. This was found particularly true with VO_x species which are very sensitive to impurities [17,19]. To cope with these disagreements, a silica-like layer was deposited on plates by means of remote plasma enhanced vapour deposition (RPECVD), before coating by VO_x/TiO_2 catalyst [27]. Depositing such a silica primer on stainless steel or channelled plate was already attempted in the preparation of Co/SiO_2 catalyst for the Fischer–Tropsch synthesis of diesel cuts [28–30]. The successive Co/porous SiO_2/SiO_2-primer layers were proven to be stable in channelled and in single plate reactors, and the performance was enhanced as compared to that of Co/SiO_2 powders in packed bed. In the present paper the novelty is the adaptation to ASI316L foams of the coating technique elaborated for plates, to be further housed in a tube reactor and investigated in ODP reaction. A second interest is the direct comparison of foams differing by the material and porosity onto which Pt/γ-Al_2O_3 was deposited, in the endothermic reaction of dehydrogenation of methylcyclohexane. It is to be noticed that in these cases the stability of Pt/γ-Al_2O_3/foam was high enough, so that a silica interface was found unnecessary. During the methylcyclohexane dehydrogenation, the "sensor" was not the selectivity as in ODP, but the thermal gradients. They were measured thanks to several thermocouples loaded in an original foam reactor.

2. Experimental

2.1. Preparation of catalytic foams

2.1.1. VO_x/TiO_2/foam and VO_x/TiO_2 powder

Once cleaned by sonication in ethanol followed by washing in deionized water and drying at 110 °C for 3 h, the pieces of AISI 316L foam (Porvair®, 40 ppi, density 5.4%) were coated in three steps according to the method previously elaborated for plates [17,19]. A cylinder (⌀1.6 cm × 0.7 cm) of Fo (Fo for foam) was displayed on a specially designed sample holder in the RPECVD reactor to be coated by silica (step 1). Briefly, RPECVD consisted of the polymerisation of tetramethydisiloxane (TMDSO) (Aldrich, grade 97%, pre-mixed with oxygen) by means of the reactive nitrogen species (plasma) created in a remote area by a microwave discharge [31,32]. Details about the RPECVD reactor and operating conditions were reported in [27,33]. The deposition rate was *in situ* measured by laser interferometry. In the case of plates, the thickness of TMDSO polymer was found to increase linearly with time at 1 μm/min. No direct relationship could be obtained in the case of foams because of problems of laser focalisation. The TMDSO plasma polymer film deposited on plates or foams was further mineralised in a furnace by thermal treatment in air to obtain the SiO_2-like layer. That layer was amorphous to X-rays and had a quite glassy aspect in SEM pictures. Its mean composition was $SiC_{0.01}O_{1.82}$ according to XPS experiments carried out on plates [27,33].

Table 1
Characteristics of the four structure packings to be coated by 2% Pt/γ-Al_2O_3.

Ref	Structure	Size	Porosity (%)	m_{cata} (g)[b]
F1	FeCrAlY foam	33 ppi[a]	97	2.5
F2	FeCrAlY foam	33 ppi	81	2.0
F3	α-Al_2O_3 foam	37 ppi	87	2.6
B	Zeolite beads	⌀2 mm	40	2.5

[a] Pores per inch.
[b] Catalyst mass in the 19 cm long foam (vide supra).

The methods of coating by TiO_2 and VO_x species had already been elaborated to coat aluminum and AISI 316L stainless steel plates (thereafter abbreviated as SSt-Pl) [17,19]. SiO_2/SSt-Fo carriers were dip-coated in an aqueous suspension of TiO_2 (Aldrich) particles under stirring during 5 min, and withdrawn at 6 mm s^{-1}. The optimised concentration (60 wt% TiO_2) used for SiO_2/SSt-Pl led to the plugging of SiO_2/SSt-Fo open cells. The best compromise between the viscosity of TiO_2 suspension and the stability of the final TiO_2 coating was found for 37 wt% TiO_2 [34]. Like TiO_2/SiO_2/SSt-Pl, the TiO_2/SiO_2/SSt-Fo samples were calcined in air flow at 80 °C/min heating rate, up to 700 °C (2 h). Finally they were dip-coated in $VO(OiPr)_3$ in dry ethanol solution, yielding $VO_x/TiO_2/SiO_2$/SSt-Pl and $VO_x/TiO_2/SiO_2$/SSt-Fo after calcination (air flow, 450 °C for 4 h).

Powders with the same composition were prepared by conventional incipient-wetness impregnation [14,35]. TiO_2 (Aldrich) particles were impregnated with ammonium metavanadate in oxalic acid aqueous solution, dried at 110 °C and calcined in the same conditions than plates and foams.

2.1.2. Preparation of Pt/γ-alumina foams and beads

The catalyst was first prepared by wet impregnation of γ-alumina (SASOL, SBa-200) with a toluene solution of platinum acetylacetonate [20,21]. Foams (1.2 cm thick) differing by the material (FeCrAlloy or α-alumina) and the characteristics (Table 1) were cut into rectangular pieces of 4.9 cm × 19 cm. The foam pieces were washed with acetone to ensure a clean surface and then calcined at 500 °C prior to coating. They were dip-coated in an aqueous suspension containing the 2% Pt/γ-Al_2O_3 catalyst powder and nitric acid. After evacuation of the excess suspension, the coated foams were dried at room temperature and calcined at 500 °C. Molecular sieves (zeolite 4A, 8–12 meshed, Acros organics) were sieved to get the ⌀1.7–2.3 mm fraction. They were coated by incipient-wetness impregnation using the same Pt/γ-Al_2O_3 catalyst suspension. Alpha-alumina foam manufactured by CTTC (Center for Technology Transfers in Ceramics) at Limoges, France, was used as is. FeCrAl foams (Porvair) were calcined at 1100 °C in air during 15 min (heating rate 6 °C/min).

2.2. Physicochemical analyses

The structural and textural characteristics of VO_x/TiO_2 powders were reported in [16,17,27]. Most analyses of VO_x/TiO_2 coatings were carried out on plates because, except for Electron Probe Micro Analysis (EPMA) and Scanning Electron Microscopy (SEM) techniques (*vide infra*), the open cell geometry of foams makes them difficult to perform. In the case of plates which were analyzed at every stage of preparation, the thickness of TMDSO polymer film coating SSt-plates was measured by *in situ* interferometry, and the silica-like films were analyzed using a Fourier Transform Infrared Perkin-Elmer spectrometer to check the absence of C–H bonds. Laser Raman spectroscopy (LRS) (LabRAM Infinity–Jobin Yvon) and X-ray photoelectron spectroscopy (XPS) (VG-Escalab 220 XL) were used in steps 2 and 3. LRS experiments confirmed the presence of TiO_2-anatase (lines at 199, 397, 515, 645 cm^{-1}) on TiO_2/SiO_2/Pl and of mainly polyvanadates (very weak lines at 285, 996 and 1030 cm^{-1}) on both 2ML–$VO_x/TiO_2/SiO_2$/Pl after calcination and 2ML–VO_x/TiO_2 powders [17–19]. No iron (nor Fe or Fe^{3+}) was detected by XPS.

Electron Probe Micro Analysis (EPMA) was performed on coated plates and foams embedded into epoxy resin and polished with abrasive discs. A thin carbon film was deposited by means of a Bal-Tec SCD005 sputter. Elemental analysis was performed using a wavelength dispersive X-ray spectrometer (Cameca SX-100 microprobe analyser). Back scattered electron images and Si, Ti, FeKα X-ray profiles and mapping were obtained at 15 and 49 nA, respectively (15 kV). The Scanning Electron Microscope (SEM) Hitachi 4100 S was equipped with micro-analysis (EDS) and a field emission gun. The working voltage was 15 kV.

The mechanical stability of coatings on plates was examined by cross-cut-tape test. An ultrasonic *n*-heptane bath (during twice 1 min) was also used for foams and plates (both types of catalyst). A test of chemical stability (ageing) consisted of successive heat treatments (N_2 at 350 °C, 4 h, followed by air/steam 80/20 molar ratio, 8 h, and N_2/air/steam/acetic acid 79/10/10/1 molar ratio) for 5 h, followed by ultrasonic treatment [27,34].

2.3. Catalytic experiments

2.3.1. ODP of propane

The conventional test rig consisted of a continuous gas–solid reactor operated at atmospheric pressure with on-line analysis of reactants and products by gas chromatography (Varian 3800). Propane, oxygen, helium and argon were fed through mass flow controllers at 100 stpcm^3 min^{-1} (C_3H_8/O_2/He/Ar = 5/2.5/67.5/25, C_3H_8/O_2 = 2/1). The temperature was varied between 250 and 550 °C and measured outside but at the wall contact. The foam reactor (FR) could be loaded with four catalytic foam cylinders (⌀1.6 cm, length 0.7 cm for each foam), or with powder catalyst. It consisted of a stainless steel tube (i.d. ⌀1.6 cm, length 10 cm) with a frit. Silicon carbide granules (⌀250 μm) were packed below and above foam cylinders or powders to ensure an even distribution of gases. The powder catalyst (200 mg, grains ⌀ ca. 200 μm) loaded in the foam reactor was diluted with SiC in order to get the same catalytic bed volume and the same active phase loading (catalyst density) than for foams (5.6 cm^3 for 4 foam elements). The FR catalytic beds were 1.6 cm in diameter and 2.8 cm long. A small volume reactor (SVR) (stainless steel, i.d. ⌀1.2 cm, length 5 cm) was also used for powders. It was loaded with 200 mg of catalyst mixed with 1 g of SiC pellets (0.21 mm), the remaining volume on top of the powder being filled with SiC. The SVR catalytic bed was 1.2 cm in diameter and 0.88 cm long, leading to a 1 cm^3 volume. The catalyst density was 5.6 times higher in SVR than in FR. The main products were propene and carbon oxides. The amount of C_2 hydrocarbons and of acetaldehyde, acrolein, acetic and acrylic acids was below 1%. The catalytic activity was determined at the steady state, which was reached after 2 h at the temperature of reaction.

2.3.2. Dehydrogenation of MCH

The catalytic dehydrogenation of methylcyclohexane was performed in an original stainless steel rectangular reactor (4.9 cm × 39 cm × 1.2 cm internal dimensions) (Fig. 1) displayed in a conventional test rig. The inlet gases entering the reactor first flowed through an inactive (non coated) foam to ensure an uniform distribution and to reach the required temperature, and then through the catalytic packing (4.9 cm × 19 cm × 1.2 cm) (foam or beads) containing ca. 2.5 g catalyst. The thermocouple to control the temperature was located inside the coated packing at 6 cm from the beginning of the catalytic zone. Five thermocouples were displayed on the external surface of the reactive foam (T_{wall}) and nine at the center (T_{center}). The reactor was equipped with graphite gaskets

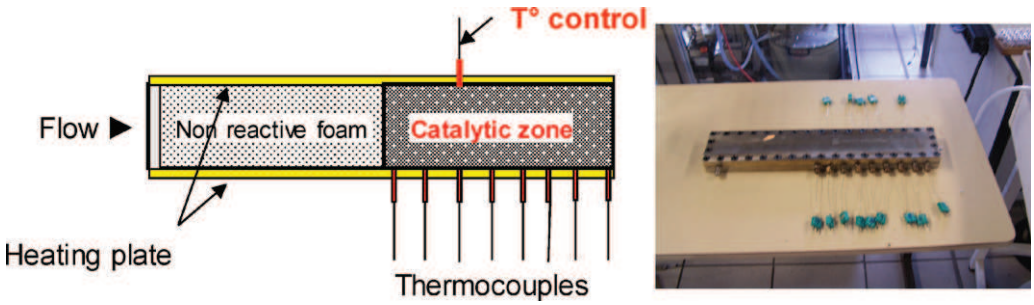

Fig. 1. Schematics of the parallelepipedic foam (i.d. 4.9 cm × 39.0 cm × 1.2 cm) reactor of dehydrogenation of methylcyclohexane, loaded with the non catalytic, gas dispersing, and the catalytic foams (from left to right), and equipped with thermocouples (one to control temperature, 5 and 9 to measure T_{wall} and T_{center}, respectively) (see text).

(DELTGRAP HT) designed to resist to high temperatures. The MCH flow was delivered with an ISMATEC pump in the range 1–9 g/min. MCH was then vaporised in a hot box (up to 250 °C) into which hydrogen was fed to limit the catalyst deactivation. The reactor was heated by means of two hot plates fixed at top and bottom of the reactor. The effluent passed through two condensers maintained at 0 °C, and was analyzed by GC. Experiments were performed at the same residence time W/F_{MCH} (from 2.6 to 15.4 kg_{cat} s mol^{-1}) for each structure by adjusting the inlet volumic flow rates of MCH and of H_2.

3. Results and discussion

3.1. Characterization of coated plates, foams and powders or beads

In the case of VO_x/TiO_2 catalyst to be deposited on silica/stainless steel it was necessary to first ensure the good mechanical and chemical holding of silica with the surface of the metal, which beared no chemical resemblance nor with silica or TiO_2 [17–19]. The influence of several parameters of synthesis of SiO_2-like layers (first step) and of coating by TiO_2 (second step) deposited on stainless steel plates was examined using experimental design. To summarize, the best results were obtained for a 5 μm-thick film of TMDSO polymer on plate, which was calcined at 1 °C/min heating rate, up to 650 °C (1 h). During calcination the film shrinked by ca. 70% and the final thickness of amorphous silica was ca. 1 μm. Once the parameters to get mechanically and chemically stable catalytic coatings of plates were optimised, they were supposed to be convenient for foam coating. However the design of the sample holder in the RPECVD reactor had to be modified in order to force the flow of the excited nitrogen reactive species (to which the TMDSO monomer and oxygen were added) to cross the whole volume of the foam cylinder. The thickness of the deposited layers of polymer was evaluated from SEM and EPMA pictures of the successively sliced pieces of foam. Typically, the thickness of TMDSO polymer was 5–50 μm (ca. 5 μm on struts and up to 50 μm in hollow parts) for 15 min long experiments. After optimisation of the time of deposition, 5–10 μm thick and stable SiO_2 layers after mineralisation (1 °C/min, 650 °C, 1 h) were obtained for 8 min of deposition of TMDSO polymer. As shown by measuring the contact angle in distilled water, the surface of silica-like layer on plates was slightly hydrophobic and the SiO_2/SSt-foams samples were further treated in a basic solution of NaOH + EtOH (Brown solution) [27,33].

For the second step to be optimised (dip-coating of SiO_2/SSt-Pl in TiO_2 suspension), the viscosity of TiO_2 anatase (Aldrich) particles suspended in deionised water was studied [34]. The optimal concentration to cover stainless steel foams was finally found for 37 wt% TiO_2 (Aldrich) in deionized water, instead of 60 wt% for plates. The same heating rate, maximum temperature and duration of plateau were used to obtain TiO_2/SiO_2/SSt-Fo. The cross section electron probe analysis (EPMA) across a strut clearly showed the two layers structure of the coatings on foam (Fig. 2, left) and plate (Fig. 2, right). The X-ray profile obtained by back-scattered electrons on foam showed the good covering by SiO_2 that should play its protective role, and by TiO_2, the support of the active polyvanadate VO_x species. As already mentioned, most methods of analysis of materials like X-ray diffraction, but also Raman spectroscopy or XPS, cannot be used for solid foams. The samples may be cut in pieces to be examined, but thus the contribution of iron can be very high and not representing the actual value. Therefore it was assumed that, for the third step as for the others, the surface active

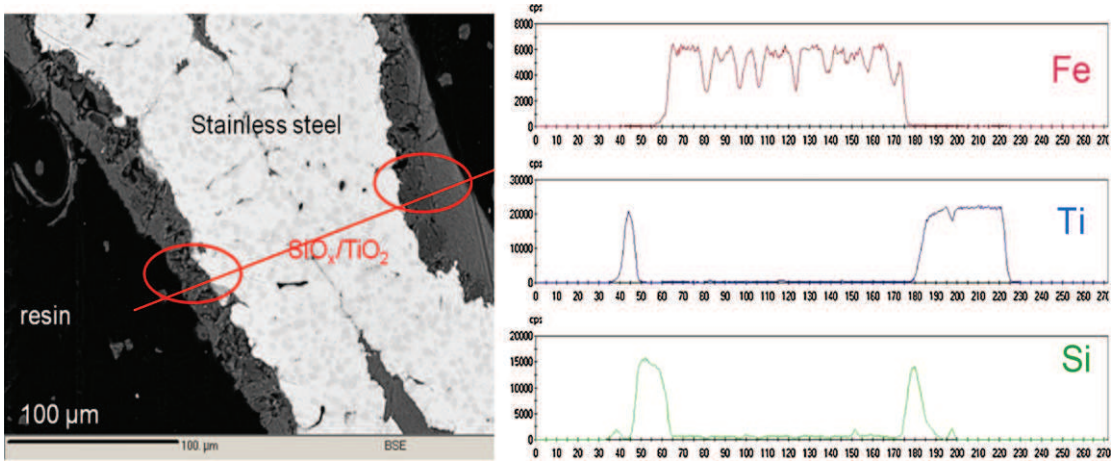

Fig. 2. Electron Probe Micro Analysis of a strut of stainless steel foam coated by TiO_2/SiO_2 after RPECVD and dip-coating steps (left), and X-ray BSE profiles of Fe, Ti, Si along the red line. (For interpretation of the references to color in this figure legend, the reader is referred to the web version of the article.)

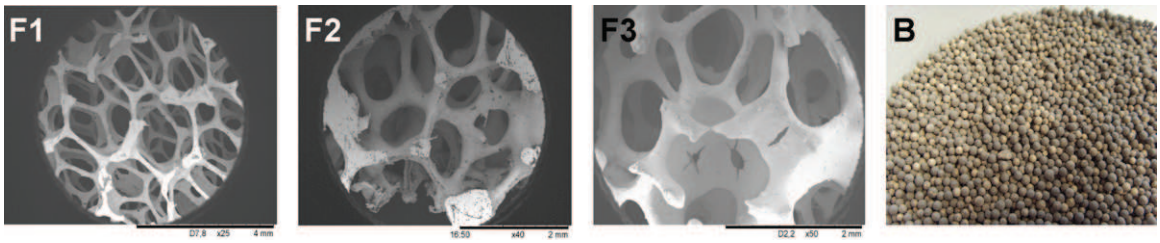

Fig. 3. DH of MCH. The four packings before coating by Pt/γ-Al_2O_3. From left to right: FeCrAlloy foams F1 (ε = 97%) and F2 (ε = 81%), alumina foam, molecular sieves beads.

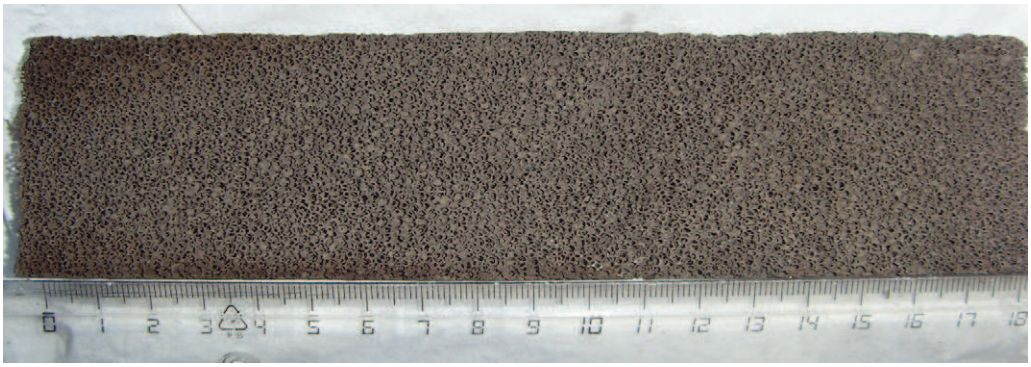

Fig. 4. DH of MCH. FeCrAlloy foam (19 cm × 4.9 cm) homogeneously coated by Pt/γ-Al_2O_3 catalyst.

VO_x species were the same on foams than on plates and powders for a given composition.

Stable coatings of foams and beads by Pt/γ-Al_2O_3 packings were easier to obtain. Molecular sieves were coated by incipient-wetness impregnation, in which case the amount of catalyst inside the pores was ascertained. In the case of foams, the mechanical but also the chemical compatibility between the material (alumina) and the catalyst were also ensured, including in the case of FeCrAlloy. Indeed alumina layers were formed during the thermal treatment of FeCrAlloy at 1100 °C in air [22,36,37]. The heat treatment was short to favour the formation of transition aluminas (close to the γ form) instead of the α form (corundum). The dispersion of Pt particles (63%) was measured by means of hydrogen chemisorption [21]. SEM pictures of the uncoated carriers and of the 19 cm long FeCrAlloy foam homogeneously coated by the Pt/γ-Al_2O_3 catalyst are presented Figs. 3 and 4, respectively.

3.2. Catalytic experiments

3.2.1. ODP on V_2O_5/TiO_2 foams and powders

The catalytic performance of foams and powders in the oxidative dehydrogenation of propane was compared for the same amount of active species (0.2 g of 2ML-VO_x/TiO_2) and in the same operating conditions. The same gaseous mixture composition, flowrate (6 stp L h^{-1}) and the same temperature range were used, with GHSV = 30 stpL h^{-1} g_{cat}^{-1}.

Fig. 5 presents the evolution of the conversions of propane (XC_3) and oxygen (XO_2), and of the selectivity to propene ($SC_3^=$) vs. temperature for 2ML-$VO_x/TiO_2/SiO_2$/SSt-Fo foam in FR. As it is usual in the oxidative dehydrogenation of alkanes, $SC_3^=$ decreased while selectivity to CO_2 and conversion increased upon increasing the temperature. To compare the catalytic properties of foams and powders, the selectivity to propene was plotted against the conversion of propane (Fig. 6). 2ML-VO_x/TiO_2 powder in the SVR exhibited the same behaviour than in literature and in our own work [19]. $SC_3^=$ decreased strongly when XC_3 increased, and at 500 °C the selectivity to carbon oxides was very high (86 mol%). When loaded in the FR, the same amount of active powder (0.2 g) led to both smaller oxygen conversion and selectivity to carbon oxides. The variation of selectivity $\Delta SC_3^=$ vs. the variation of conversion ΔXC_3 for the same range of temperature (100 °C) was taken as a rough indicator to compare the catalytic performance, but also to highlight the thermal gradients. For the two powder beds, the slope $\Delta SC_3^=/\Delta XC_3 = -4.2$ was steeper in SVR than in FR ($\Delta SC_3^=/\Delta XC_3 = -0.4$). In SVR, the catalyst bed density was 5.6 times higher than in FR. As GHSV was similar in both reactors, the difference of selectivity could not be related to the contact time. The gas velocity was higher in SVR (i.d. ⌀1.2 cm) than in FR (i.d. ⌀1.6 cm), leading to an increase of the global heat transfer coefficient (+30%). But this increase was not sufficient to balance the A_{FR}/A_{SVR} exchange area (A) ratio, which was about 4.2. Consequently, the ODH of propane being exothermic, the temperatures in the bed center in SVR were evidently higher than those in FR and the selectivity decreased. The lower $\Delta SC_3^=/\Delta XC_3$ slope could be directly linked to improved thermal gradients and heat transfer.

When comparing the selectivity to propene obtained with the catalytic foam and with the powders in FR, other parameters being equal (same catalyst loading at the same GHSV = 30 stpL h^{-1} g_{cat}^{-1}),

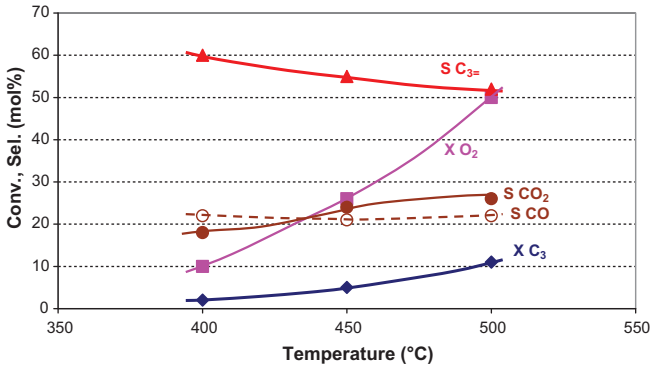

Fig. 5. ODP Conversion of reactants (XC_3 and XO_2) and selectivity (S) to products vs. temperature for 2ML-$VO_x/TiO_2/SiO_2$ foam.

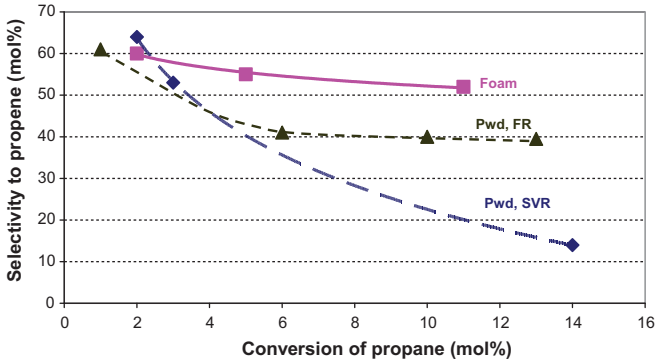

Fig. 6. ODP Comparison of 2ML-VO_x/TiO_2 powders and 2ML-$VO_x/TiO_2/SiO_2$ coated foam. Selectivity vs. conversion for powders in small volume reactor (pwd, SVR), in foam reactor (pwd, FR) and for foam in foam reactor.

$SC_3^=$ for the foam was much higher at any conversion, showing more efficient heat transfer in foam than in the packed bed. However, the void fraction being higher in the foam than in the packed bed, the actual residence time was higher, which thereby should have promoted the combustion of propene [9,11,12]. Moreover the gas velocity was lower in the foam than in the powder bed. Thus, if the heat transfer were due to gas convection only, it would be more favourable in powders than in foams. As a result, the temperature would be higher in the foam than in the powder bed, and as a consequence, the conversion of propane would be higher and the selectivity to propene would be lower. As the reverse situation (higher selectivity) was observed with the foam, it is assumed that the improved heat transfer was mostly due to conduction through the metallic substrate. Moreover, the external heat transfer between the reactor walls and the foam was probably good. Indeed it was very difficult to withdraw the foam from the reactor after reaction, without destroying it partially. However, these conclusions cannot be extrapolated to industrial reactors, due to the Reynolds range. In the previous experiments, Re values in packed bed in FR and in SVR were about 0.01, when in industrial reactors Re can be higher than 1000. The value of Re calculated using the mean diameter of struts in the foam was of the same order of magnitude. In conclusion, the contribution of the solid to the bed conductivities was higher for the foam than for the powder.

3.2.2. Dehydrogenation of MCH on Pt/alumina foams and beads

To confirm the beneficial effect of the structuration of the catalytic solid on the heat transfer, the dehydrogenation of MCH was studied in the second type of foam reactor (Fig. 1). The aim was to measure the temperature gradient, ΔT, between the reactor wall and the reactor center at different distances from the inlet, using the different packings during the reaction process. The effects due to the nature (metal, ceramic, molecular sieve) and geometry (beads or foams) of the structure on the temperature gradients in the reactor were studied. In the absence of reaction, a flat temperature profile was observed for all structures. In all experiments, no methylcyclohexane nor toluene decomposition, and no specific deactivation of uncoated metal, ceramic or molecular sieves were observed. We concluded that all substrates were inert in the reaction but also that they had no effect on the properties of Pt/γ-Al_2O_3 catalyst, and particularly on its catalytic activity (per g of Pt on alumina).

Fig. 7 presents the profiles of temperature at the center (T_{center}) and at the wall (T_{wall}) during the reaction at 300 °C and $W/F_{MCH} = 15.4\ kg_{cat}\ s\ mol^{-1}$. They were measured along the catalytic part of the reactor, from the inlet to the outlet (left to right in Fig. 1, respectively) through the two catalytic Pt/γ-Al_2O_3/FeCrAlloy

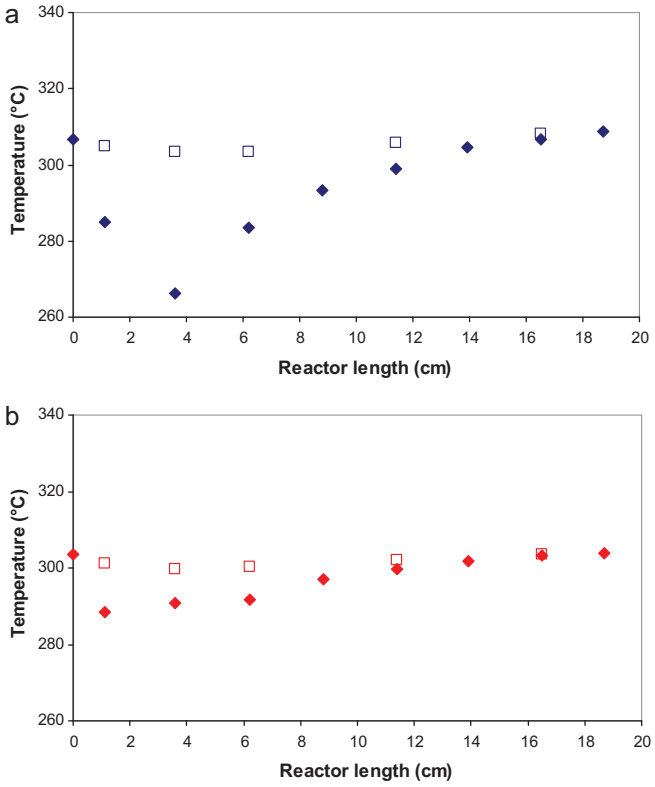

Fig. 7. DH of MCH. Variation of temperature vs. axial position. Central thermocouples (lozenges) and wall thermocouples (squares) in FeCrAl foams (a) F1: 33 ppi, $\varepsilon = 97\%$; (b) F2: 33 ppi, $\varepsilon = 81\%$.

foams. The temperature gradient ΔT showed a maximum which varied from ca. 10 to 35 °C by the only variation of the voidage, $\varepsilon = 81$ vs. 97%, respectively. The same type of experiment was repeated while varying W/F and temperature (Table 2). Pt/γ-Al_2O_3/corundum foam, as well as beads coated by Pt/γ-Al_2O_3, were also investigated. High maximum temperature gradients were observed at high W/F for beads and for the most porous of the metallic foams, but the MCH conversion (X_{MCH}) did not vary. The temperature gradient was the smallest with the denser foams (either ceramic or metallic) but X_{MCH} was lower for alumina at both W/F. The position of the control thermocouple, which laid at bed half-thickness (at 6 cm from the catalytic zone inlet), made it difficult to get exactly the same heat power, and thus to get the same wall temperature in each experiment. Moreover, the controlled temperature being near the cold point, the less conducting the bed, the higher was the temperature at wall. For example, let us compare F1 and F2 foams at low W/F ($2.6\ kg_{cat}\ s\ mol^{-1}$). The material with the lowest conductivity (F1) showed a large cold point in the center ($\Delta T = 42$, vs. 25° for F2), and thus a high T_{wall} which led to antagonist effects on the MCH conversion ($X_{MCH} = 40$ vs. 54 mol% for F2) (Table 2). For all experiments on catalytic beads, the

Table 2
Maximum temperature gradient (ΔT) and MCH conversion (X) for the three foams and for coated beads at two W/F contact times ($Q_{H_2} = 3.3 \times 10^{-4}\ mol\ s^{-1} = 3.3 \times 10^{-4}\ mol\ s^{-1}$; $T_{controller} = 300$ °C).

Packing	$W/F_{MCH} = 15.4\ kg_{cat}.s.mol^{-1}$		$W/F_{MCH} = 2.6\ kg_{cat}.s.mol^{-1}$	
	ΔT (°C)	X (%)	ΔT (°C)	X (%)
F1 (FeCrAlY)	38	98	42	40
F2 (FeCrAlY)	13	97	25	54
F3 (α-Al_2O_3)	13	78	30	40
B (zeolite)	37	97	66	54

values of Reynolds were comprised between 10 and 75. As the bead diameter were chosen to get the same pressure drop as for foams, the values of Re for foams and beads were of the same order. In the absence of a detailed modelling, which is in progress, it was difficult to correlate the MCH conversion with the conducting properties of foams. However, as a conclusion, even for highly endothermic reactions not limited by external transport, the catalytic foams seemed to significantly increase the effective conductivity of catalytic beds, the higher foam density leading to higher effective conductivity and to runs closer from being isothermal.

4. Conclusion

Using solid foams to carry catalysts is confirmed to be a good way to enhance heat and mass transfers, as shown in recent literature. The solid foam can improve the radial bed conductivity and decrease the thermal gradients. This was also demonstrated in this paper. Two different reactions, one exothermic and one endothermic, were operated with two different catalysts, and the catalytic performance of foams was compared to those of more usual catalyst shapings (powder or beads). For each reaction, experiments were performed with the same loading of active phase and in the same operating conditions. Using a catalytic stainless steel foam in the exothermic oxidative dehydrogenation of propane to propene was clearly responsible for increasing the yield of propene when compared to catalytic powder. It is assumed that hot spots were reduced, leading to more isothermal the operation. Some experiments (not shown here) were performed on unprotected (without SiO_2) 2ML-VO_x/TiO_2 foam. A similar activity was observed, in accordance with the fact that the same vanadate species were displayed on the same TiO_2 support, but the selectivity to propene was lower by ca. 10–15%. One of the beneficial effects of SiO_2 interlayer could therefore be due to a "chemical" effect. Indeed the metal was homogeneously covered by silica and the presence (or diffusion to the active surface) of iron or chromium cations, that would promote total oxidation, could be avoided. The very good mechanical stability of SiO_2/SSt plates and foams could be related to the small content of carbon in silica ($SiC_{0.01}O_{1.82}$). As most carbon was shown to be located inwards, close to stainless steel, a certain degree of plasticity could allow to accommodate the difference of dilatation coefficients between the oxidic support and the metallic substrate. Other parameters like W/F and C_2/O_2 ratio are currently varied to check the chemical regime and to increase the yield of propene as more as possible. The isothermicity due to more efficient heat transfer has to be confirmed by measuring the temperature gradient between the center of the foam and the wall of reactor, in the same way as done in MCH dehydrogenation experiments. Such temperature profiles could be obtained for this endothermic reaction in the original parallelepipedic reactor equipped with several thermocouples distributed along the bed length. The variation of temperature gradient between the reactor wall and the reactor center at different distances from the inlet was shown to depend more on the bed porosity than on the foam material. A nearly isothermal behaviour was shown with the denser foams. Though it would be risky to directly extrapolate our laboratory experiments (low Re) to larger reactors, the coating of catalysts on dense foams is a potential way to study the kinetics of highly endo or exothermic reactions at constant temperature and pressure.

Acknowledgements

The Agence nationale pour la Recherche (ANR-MILLICAT No. 06-BLAN-0216) is acknowledged for A. Essakhi and Y. Swesi grants and for financial support.

References

[1] A. Cybulski, J. Moulijn, Structured Catalysts and Reactors, Taylor & Francis, BocaRaton, USA, 2006.
[2] J.A. Moulijn, A. Stankiewicz, Structured catalysts and reactors, Catal. Today 69 (1–4) (2001).
[3] L. Kiwi-Minsker, A. Renken, Microstructured reactors for catalytic reactions, Catal. Today 110 (2005) 2–14.
[4] D. Edouard, T. Truong Huu, C. Pham Huu, F. Luck, D. Schweich, The effective thermal properties of solid foam beds: experimental and estimated temperature profiles, Int. J. Heat Mass Trans. 53 (2010) 3807–3816.
[5] G. Incera Garrido, B. Kraushaar-Czarnetzki, A general correlation for mass transfer in isotropic and anisotropic solid foams, Chem. Eng. Sci. 65 (2010) 2255–2257.
[6] F. Cavani, Catalytic selective oxidation: the forefront in the challenge for a more sustainable industrial chemistry, Catal. Today 156 (2010) 8–15.
[7] F. Cavani, N. Ballarini, A. Cericola, Oxidative dehydrogenation of ethane and propane: how far from commercial implementation? Catal. Today 127 (2007) 113–131.
[8] O. Schwarz, P.-Q. Duong, G. Schäfer, R. Schomäcker, Development of a microstructured reactor for heterogeneously catalyzed gas phase reactions: Part I. Reactor fabrication and catalytic coatings, Chem. Eng. J. 145 (2009) 420–428.
[9] R. Grabowski, S. Pietrzyk, J. Słoczynski, F. Genser, K. Wcisło, B. Grzybowska-Świerkosz, Kinetics of the propane oxidative dehydrogenation on vanadia/titania catalysts from steady-state and transient experiments, Appl. Catal. A: Gen. 232 (1–2) (2002) 277–288.
[10] A. Dinse, S. Khennache, B. Frank, C. Hess, R. Herbert, S. Wrabetz, R. Schlögl, R. Schomäcker, Oxidative dehydrogenation of propane on silica (SBA-15) supported vanadia catalysts: a kinetic investigation, J. Mol. Catal. A: Chem. 307 (1–2) (2009) 43–50.
[11] K. Routray, K.R.S.K. Reddy, G. Deo, Oxidative dehydrogenation of propane on V_2O_5/Al_2O_3 and V_2O_5/TiO_2 catalysts: understanding the effect of support by parameter estimation, Appl. Catal. A: Gen. 265 (1) (2004) 103–113.
[12] B. Frank, A. Dinse, O. Ovsitser, E.V. Kondratenko, R. Schomäcker, Mass and heat transfer effects on the oxidative dehydrogenation of propane over a low loaded VO_x/Al_2O_3 catalyst, Appl. Catal. A: Gen. 323 (2007) 66–76.
[13] G.C. Bond, P. König, The vanadium pentoxide–titanium dioxide system: Part 2. Oxidation of o-xylene on a monolayer catalyst, J. Catal. 77 (2) (1982) 309–322.
[14] G.C. Bond, Preparation and properties of vanadia/titania monolayer catalysts, Appl. Catal. A: Gen. 157 (1–2) (1997) 91–103.
[15] J.C. Védrine (Ed.), EUROCAT oxide, Catal. Today 20 (1) (1994).
[16] E. Bordes, Synergistic effects in selective oxidation catalysis: is phase cooperation resulting in site isolation? Top. Catal. 15 (2001) 131–137.
[17] T. Giornelli, A. Löfberg, E. Bordes-Richard, Grafting of VO_x/TiO_2 catalyst on anodized aluminum plates to be used in structured reactors, Thin Solid Films 479 (2005) 64–72.
[18] T. Giornelli, A. Löfberg, E. Bordes-Richard, Preparation and characterization of VO_x/TiO_2 catalytic coatings on stainless steel plates for structured catalytic reactors, Appl. Catal. A: Gen. 305 (2006) 197–203.
[19] A. Löfberg, T. Giornelli, S. Paul, E. Bordes-Richard, Catalytic coatings for structured supports and reactors: VO_x/TiO_2 catalyst coated on stainless steel for oxidative dehydrogenation of propane, Appl. Catal. A: Gen. 391 (1–2) (2011) 43–51.
[20] M. Roumanie, V. Meille, C. Pijolat, G. Tournier, C. de Bellefon, P. Pouteau, C. Delattre, Design and fabrication of a structured catalytic reactor at micrometer scale: example of methylcyclohexane dehydrogenation, Catal. Today 110 (2005) 164–170.
[21] P. Kerleau, Y. Swesi, V. Meille, I. Pitault, F. Heurtaux, Total catalytic oxidation of a side-product for an autothermal restoring hydrogen process, Catal. Today 157 (2010) 321–326.
[22] A. Shamsi, J.J. Spivey, Partial oxidation of methane on Ni–MgO catalysts supported on metal foams, Ind. Eng. Chem. Res. 44 (2005) 7298–7305.
[23] M. Maestri, A. Beretta, G. Groppi, E. Tronconi, P. Forzatti, Comparison among structured and packed-bed reactors for the catalytic partial oxidation of CH_4 at short contact times, Catal. Today 105 (2005) 709–717.
[24] V. Palma, E. Palo, P. Ciambelli, Structured catalytic substrates with radial configurations for the intensification of the WGS stage in H_2 production, Catal. Today 147S (2009) S107–S112.
[25] F.C. Moates, T.E. McMinn, J.T. Richardson, Radial reactor for trichloroethylene steam reforming, AIChE J. 45 (1999) 2411–2418.
[26] V. Meille, Review on methods to deposit catalysts on structured surfaces, Appl. Catal. A: Gen. 315 (2006) 1–17.
[27] A. Essakhi, A. Löfberg, Ph. Supiot, B. Mutel, S. Paul, V. Le Courtois, E. Bordes-Richard, Coating metallic foams and structured reactors by VOx/TiO2 oxidation catalyst: application of RPECVD, in: Proc. 10th International Symposium "Scientific Bases for the Preparation of Heterogeneous Catalysts", in: E.M. Gaigneaux, M. Devillers, S. Hermans, P. Jacobs, J. Martens, P. Ruiz (Eds.), Stud. Surf. Sci. Catal. 175 (2010) 17–24 (July 11–14).
[28] L. Guillou, D. Balloy, P. Supiot, V. Le Courtois, Preparation of a multilayered composite catalyst for Fischer–Tropsch synthesis in a micro-chamber reactor, Appl. Catal. A: Gen. 324 (2007) 42–51.
[29] T. Giornelli, A. Löfberg, L. Guillou, S. Paul, V. Le Courtois, E. Bordes-Richard, Catalytic wall reactor. Catalytic coatings of stainless steel by VO_x/TiO_2 and Co/SiO_2 catalysts, Catal. Today 128 (2007) 201–207.

[30] L. Guillou, S. Paul, V. Le Courtois, Investigation of H_2 staging effects on CO conversion and product distribution for Fischer–Tropsch synthesis in a structured microchannel reactor, Chem. Eng. J. 136 (2008) 66–76.
[31] P. Supiot, C. Vivien, A. Granier, A. Bousquet, A. Mackova, F. Boufayed, D. Escaich, P. Raynaud, Z. Stryhal, J. Pavlik, Growth and modification of organosilicon films in PECVD and PACVD reactors, Plasma Proc. Polym. 3 (2) (2006) 100–109.
[32] F. Callebert, P. Supiot, K. Asfardjani, O. Dessaux, P. Dhamelincourt, J. Laureyns, Cold remote nitrogen plasma polymerization from 1.1.3.3.tetramethyldisiloxane/oxygen mixture, J. Appl. Polym. Sci. 52 (1994) 1595–1606.
[33] A. Essakhi, A. Löfberg, P. Supiot, B. Mutel, S. Paul, V. Le Courtois, E. Bordes-Richard, Coating of structured reactors by plasma assisted polymerization of TMDSO, in: Proc. 6th Int. Symp. Polyimides and Other High Temperature/High Performance Polymers: Synthesis, Characterization and Applications, Melbourne, Florida, USA, November 9-11, Polym. Eng. Sci. 51 (2011) 940-947.
[34] A. Essakhi, A. Löfberg, S. Paul, B. Mutel, P. Supiot, V. Le Courtois, P. Rodriguez, V. Meille, E. Bordes-Richard, Materials chemistry for catalysis: coating of catalytic oxides on metallic foams, Microporous Mesoporous Mater. 140 (2011) 81–88.
[35] G.C. Bond, J. Perez Zurita, S. Flamerz, Structure and reactivity of titania-supported oxides. Part 2: Characterisation of various vanadium oxide on titania catalysts by X-ray photoelectron spectroscopy, Appl. Catal. 27 (2) (1986) 353–362.
[36] P.T. Moseley, K.R. Hyde, B.A. Bellamy, G. Tappin, The microstructure of the scale formed during the high temperature oxidation of a FeCrAlloy steel, Corros. Sci. 24 (6) (1984) 547–565.
[37] O. Sanz, F.J. Echave, M. Sánchez, A. Monzón, M. Montes, Aluminium foams as structured supports for volatile organic compounds (VOCs) oxidation, Appl. Catal. A: Gen. 340 (2008) 125–132.

Top Catal (2011) 54:698–707
DOI 10.1007/s11244-011-9676-z

ORIGINAL PAPER

From Materials Science to Catalysis: Influence of the Coating of 2D- and 3D-Inserts on the Catalytic Behaviour of VO_x/TiO_2 in Oxidative Dehydrogenation of Propane

A. Essakhi · A. Löfberg · S. Paul · P. Supiot · B. Mutel · V. Le Courtois · E. Bordes-Richard

Published online: 6 May 2011

Abstract The chemistry of the coating of stainless steel plates and foams with VO_x/TiO_2 catalyst to be utilised in the oxidative dehydrogenation of propane is described. A primer layer of SiO_2 was first deposited by RPECVD, to anchor the active phase, to accommodate the difference of dilatation coefficient with steel and to act as a barrier against diffusion of poisonous steel elements. The coated VO_x/TiO_2 foams were inserted in a tube that could also be loaded with VO_x/TiO_2 powders to compare their catalytic performance. Preliminary results showed that the selectivity to propene was higher by 10% on silica-protected (ca. 5 μm thick) VO_x/TiO_2 foam than in the absence of silica, and higher by more than 20% than VO_x/TiO_2 powders at any conversion. The better performance was attributed to enhanced heat and mass transfers due to turbulent flow regime and to the high conduction of metallic foam. Hot spots which generate over-oxidation of propene were avoided. The choice of the substrate material, of which depend the mechanical and chemical properties of the active phase coating, and of the reactor configurations vs. the efficiency of heat and mass transfers was also commented.

Keywords Catalytic foam · Coating of stainless steel foam · VO_x/TiO_2 catalyst · Oxidative dehydrogenation of propane · Catalytic foam reactor

A. Essakhi · A. Löfberg · S. Paul · V. Le Courtois · E. Bordes-Richard
Université Lille Nord de France, 59000 Lille, France

A. Essakhi · A. Löfberg
Unité de Catalyse et Chimie du Solide, CNRS—UMR8181, Université Lille 1, 59655 Villeneuve d'Ascq, France

S. Paul · V. Le Courtois
Ecole Centrale Lille, 59655 Villeneuve d'Ascq, France

P. Supiot · B. Mutel
Institut d'Electronique, de Microélectronique et de Nanotechnologie—UMR CNRS 8520, Université Lille 1, 59652 Villeneuve d'Ascq, France

E. Bordes-Richard (✉)
Unité de Catalyse et Chimie du Solide, CNRS—UMR8181, ENSCL-Université Lille 1, 59655 Villeneuve d'Ascq, France
e-mail: elisabeth.bordes@univ-lille1.fr

1 Introduction

A catalytic gas–solid reaction can a priori be performed in any type of reactor in which the catalyst is shaped as beads, powders, monolith, plate, membrane, etc. Industrially the overall economics of the process among which the reactor configuration determines the choice. Because of technical risks involved by disruptive innovations, other kinds of reactor are still poorly employed and packed and fluidized beds are the most commonly used reactors. Other solutions have often been chosen in the case of pollution abatement of mobile or stationary effluents. In particular, monolithic honeycomb catalysts are particularly interesting to operate combustion reactions owing to the specific constraints, among which the required high gas velocities. On the contrary, in the case of selective hydrocarbon oxidation reactions (a quarter of heterogeneous reactions of commercial interest), the goal is to suppress over-oxidation of the targetted product. Monolith honeycombs are not in use in this field but there are other possibilities to increase the yield of products. Because oxygen is usually co-fed with the hydrocarbon reactant it is partly responsible for the direct formation of carbon oxides. By decoupling the two steps of the redox mechanism one expects to increase the

selectivity and to decrease the carbon oxides production. Based on this redox decoupling concept, reactors designed to separate the oxidation of reactant from the reoxidation of the catalyst [1] were proposed. Among them, recirculating solids riser reactor (RSR) [2–4] and catalytic membrane reactors (CMR) [5–8] were experimented. *n*-Butane oxidation to maleic anhydride using VPO catalysts was studied using both RSR and CMR. Substantial increases of maleic anhydride yield were obtained which were due to the limited amount of co-fed O_2 in the RSR [2–4] and to staged distribution of O_2 in CMR [7, 8]. A modified version of CMR is the catalytic dense membrane reactor (CDMR) in which the membrane itself is an oxygen ion conductor, that can convey the O^{2-} oxygen specie known to be responsible for selectivity. Because of the difference of oxygen chemical potential between the reaction side and the air or oxygen side, the O^{2-} oxide ions which are formed by reduction of dioxygen migrate to the reaction side to react with hydrocarbons. CDMR were tried with success in steam reforming and partial oxidation of methane using e.g., nickel catalyst packed between dense membranes of perovskites, and in few other reactions [9–11]. Less success was met with CDMR when trying to oxidatively dehydrogenate C_2–C_3 alkanes on bismuth-based membranes like BIMEVOX [12–14]. The use of reactors similar to fuel cells where the flow of O^{2-} is assisted by electric power [11, 15] was proposed to selectively oxidize propene to acrolein on bismuth molybdate deposited on BIMEVOX membrane [16]. However, at the quite low (350–550 °C) temperature at which selective oxidation and oxidative dehydrogenations proceed (to avoid overoxidation of the product), both the oxide ion conductivity and the rate of O^{2-} diffusion are too slow. Even with BIMEVOX whose conductivity at 300 °C is about two orders of magnitude higher than that of yttria stabilized zirconia [17], the reaction with hydrocarbons was too fast as compared to the O^{2-} oxygen diffusion rate. It seems therefore that CDMR are more suitable for reactions at high temperatures like partial oxidation of alkanes to syngas.

Another way to decrease the amount of carbon oxides in selective oxidation is to manage with the strong exothermicity of reactions. Indeed the enhancement of heat transfer between catalyst and heating medium plays the most important role of the listed effects for heterogeneously catalysed processes [18]. Particularly in fixed bed reactors, it is difficult to guarantee isothermal conditions, and the presence of hot spots favours the over–oxidation of the product as well as the ageing of the catalyst. The structuration of reactor walls or the utilisation of structured inserts is a means to enhance both heat and mass transfers. Since two decades, microreaction technology offers a potential for intensifying gas-phase processes by minimizing transport distances [19]. It holds especially true for fast and exothermic reactions like partial oxidations where isothermal conditions should enhance selectivity [20]. Up to now there are few studies on mild oxidation of hydrocarbons which are processed on mixed oxides catalysts. Vanadium oxide supported on TiO_2 catalysts were deposited on mullite foam [21] or on stainless steel plates [22, 23] to be operated in *o*-xylene oxidation to phthalic anhydride, or in oxidative dehydrogenation of propane (ODP), respectively. Recently a VO_x/TiO_2 catalytic wall reactor was installed upstream to the conventional multitubular reactor in the oxidation of *o*-xylene to phthalic anhydride. Experimental details, among which the nature of substrate material and the reactor configuration were not available, but with an effective volume of only 20% of the total reactor unit the microstructured reactor removed 63% of the total heat [24]. The other reaction, ODP, is potentially interesting as an alternative to dehydrogenation of propane. However propene yields do not overcome 40% whatever the type of catalyst, from basic (alkaline earth oxides) to more acidic (VO_x/TiO_2, NiNbO) mixed oxides [25], because the olefinic product is more reactive than the reactant and easily oxidized to CO_2. Therefore ODP is particularly suitable a reaction to demonstrate the potentiality of microstructures, because it is fast, exothermic and (parallel-) consecutive reaction [26]. Any means allowing to operate isothermally is desirable, particularly to suppress hot spots as in fixed bed reactor in which the over-oxidation of propene to carbon dioxide is favoured. Moreover, mass transfer limitations can also occur in conventional reactor geometries [27].

As noticed by Klemm et al. [18], a successful use of microstructured reactors in heterogeneously catalysed processes makes high demands on the catalyst to be deposited. The catalyst coating must be mechanically stable, have a low thickness tolerance, an optimum porosity and obviously a high activity and selectivity. We can add that the chemical compatibility between the reactor material and the catalyst is also to be considered. In our first experiments carried out on VO_x/TiO_2/stainless steel plates in ODP up to 550 °C [22, 23] we noticed the presence of Fe^{3+} specie on the surface of VO_x/TiO_2, which thereby accounted for lower activity and selectivity as compared to those shown by VO_x/TiO_2 powders. To enhance the mechanical and chemical stabilities of the coated VO_x/TiO_2 plates a silica-like primer was deposited by RPECVD directly on stainless steel [28, 29]. Once the parameters of coating were optimized for plates, they were adapted with few modifications to coat stainless steel foams. Apart from electron probe microanalysis, most physicochemical analyses were carried out on VO_x/TiO_2 coated plates or powders because they were not suitable to analyse foams. Finally, preliminary catalytic results in the oxidative dehydrogenation of propane utilising foams and powders were compared.

2 Experimental

2.1 Preparation of $VO_x/TiO_2/SiO_2$/Foam

The method of coating foams was directly inspired from the coating of stainless steel plates [28–30], and it required four main steps (Fig. 1). AISI 316 L stainless steel foam (Porvair®, 40 pores per inch, porosity $\varepsilon = 81\%$, density 5.4%, mean weight 410 mg/cm^3) was cut as cylinders (∅ 1.6 × 0.7 cm height). First the foams were chemically cleaned by sonication in ethanol and then two times in deionized water (30 min each time), before drying in an oven at 100 °C for 3 h (step I).

The silica layer supported on foam (SiO_2/foam), was obtained by mineralisation of the organosilicate polymer (ppTMDSO) in a furnace in air flow at 5 °C/min up to 650 °C (1 h). The tetramethyldisiloxane (TMDSO) monomer was polymerized to ppTMDSO by Remote Plasma Enhanced Chemical Vapor Deposition (RPECVD) [31]. TMDSO (25 cm^3/min) was co-fed with O_2 (5 cm^3/min) at 550 Pa in the cold zone, far (at 1 m) from the microwave discharge, in the presence of plasmagenic atomic nitrogen species that flowed over the sample holder. The polymerization was performed for given times and the thickness of polymer deposits was measured by EPMA (Electron Probe Microanalysis). The SiO_2 surface was first treated in alkaline ethanolic solution (NaOH + EtOH, 4 h, drying at 100 °C for 1 h) to increase the hydrophilicity of the surface and favour further anchoring of TiO_2 particles (step II).

The treated SiO_2/foam samples were dipped in an aqueous suspension of TiO_2 anatase during 5 min at room temperature with stirring, and withdrawn at 6 mm s^{-1} after 5 min. After a study of rheology and stability of aqueous TiO_2 suspensions by zetametry [29], particles of TiO_2 Sigma-Aldrich (10 m^2/g, mean size of particles 0–250 μm) were chosen. The amount of TiO_2 was varied between 10 and 60 wt%. A 37 wt% TiO_2 suspension was found suitable to ensure an homogeneous coating throughout the foam volume. After withdrawing (6 mm s^{-1}), the TiO_2/SiO_2/foam was softly blown by air to suppress the excess of suspension and maintain open the pores, and further calcined in air flow at 80 °C/min heating rate, up to 700 °C (2 h) (step III).

Finally, the vanadium oxide specie were deposited on TiO_2/SiO_2/foam by grafting of $VO(OiPr)_3$ in ethanolic solution at various concentrations (up to 20 wt%) (step IV). The final calcination was carried out at 450 °C (2 h) to obtain $VO_x/TiO_2/SiO_2$/foam samples, where VO_x stands for polyvanadate species [30].

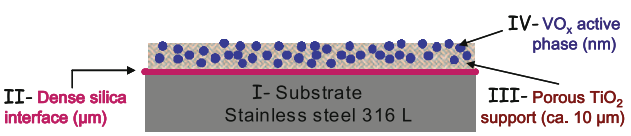

Fig. 1 Schematics of preparation steps (I–IV) to coat plates or foams; thickness in *brackets*

To evaluate its role, foam cylinders were also prepared without the silica interlayer. After cleaning, the foam was directly dip-coated in TiO_2 suspension and further grafted with the vanadium specie, in the same way than for silica-protected foams. The composition 7 wt%V_2O_5/TiO_2/foam was prepared, which corresponds to approximately 2 theoretical monolayers (2ML) of polyvanadates on TiO_2 10 m^2 g^{-1} [30, 32].

Powders with the same composition (2ML-VO_x/TiO_2 pwd) were prepared by conventional incipient-wetness impregnation. The same TiO_2 (Sigma-Aldrich) particles used for foams were impregnated with ammonium metavanadate in oxalic acid aqueous solution, dried at 110 °C and calcined in the same conditions than for foams [30].

2.2 Characterisation Methods

The main technique used to analyse the coated foams was EPMA (Electron Probe MicroAnalysis). The foam (or plate) samples were embedded into epoxy resin, and polished with abrasive discs (2400–3 μm granulometry) when the core of material had to be investigated. A thin carbon film was sputtered with Bal-Tec SCD005 sputter. The elemental analysis was made by wavelength dispersive X-ray spectrometry (WDS) utilising Cameca SX-100 microprobe analyser working at 15 kV and 15 nA for back scattered electron (BSE) images and at 15 kV and 49 nA for Si, Ti and Fe X-ray profiles and mapping. The Scanning Electron Microscope (SEM) Hitachi 4100 S was equipped with micro-analysis (Energy-Dispersive X-Ray Spectroscopy, EDS) and a field emission gun. The working voltage was 20 kV. Most analyses were performed on the coated plates (XPS, Raman spectroscopy) or on the scrapped off powder (BET). The equipment and methodology are classical and details can be found in [23, 29, 30]. Whereas scratch test (ASTMD3359-02) or loss of matter after sonication in heptane bath (twice 1 min) were used on plates, a test of both chemical and mechanical stability of the successive layers coated on foam was carried out. It consisted of measuring the weight of samples after successive heat treatments (N_2 at 350 °C during 4 h, followed by air/steam = 80/20 mol/mol during 8 h, and N_2/air/steam/acetic acid = 79/10/10/1 molar ratios for 5 h), followed by sonication in n-heptane (1 min) and drying in N_2 for 40 h [29].

2.3 Catalytic Experiments

The oxidative dehydrogenation of propane was carried out in a conventional test rig with on-line analysis of reactants

and products by gas chromatography (Varian 3800). Propane, oxygen, helium and argon were fed through mass flow controllers at 0.1 stpL min^{-1} ($C_3H_8/O_2/He/Ar = 5/2.5/67.5/25$, $C_3H_8/O_2 = 2/1$). The temperature was varied between 250 and 500 °C and measured outside, but at the contact of the reactor wall. The main products were propene and carbon oxides, other by-products amounting to less than below 1%. Carbon balance was close to 100%. The catalytic activity was determined at the steady state which was reached after 2 h at the temperature of reaction.

The foam cylinders (∅ 1.6, length 0.7 cm) were loaded in a "foam reactor" (FoR) which was a stainless steel tube (i.d.∅ 1.6, length 10 cm) displayed in an electrically heated furnace. The dead volume above the foam cylinders was filled with silicon carbide beads (∅ 250 μm) to preheat and ensure an even distribution of gases. Sieved powders (ca. 200 μm) were mixed with the silicon carbide beads and loaded in the same reactor than that used for foams (FoR). 200 mg of VO_x/TiO_2 catalyst, either deposited on foam (four foam elements) or as powder diluted in SiC, were loaded to obtain the same 5.6 cm^3 bed volume. Alternatively, the powders were diluted with SiC and loaded in a fixed bed reactor (FBR) (stainless steel tube, i.d. ∅ 1.2, length 5 cm, catalytic bed volume 1 cm^3).

3 Results

3.1 Comparison of Parameters to Coat Foams and Plates

The transformations of TMDSO to hydrophilic silica layer coating plates or foams are summarized Fig. 2. As shown by Raman spectra (Fig. 3), the amount of carbon on coated plates decreased during mineralisation and presented more silanols after NaOH washing. XPS measurements on coated plates showed that the mean stoichiometry was $SiC_{0.05}O_{1.8}$ after mineralisation. The carbon stoichiometry could be decreased down to 0.01 ($SiC_{0.01}O_{1.92}$) after a N_2/O_2 plasma afterglow post-treatment performed during 5 min [30], but, as stability tests and EPMA showed that the stability and integrity of coatings were not good, that post-treatment was abandoned. It was finally assumed that the $SiC_{0.05}O_{1.8}$ composition gives a certain degree of plasticity to the silica layer allowing to accommodate the difference of dilatation coefficient of stainless steel. During the mineralisation step, the carbonyl groups of ppTMDSO reacted with oxygen leading to the formation of CO_2 and H_2O that escaped from the forming silica-like layer. Therefore it is understandable that the integrity and stability of the coating depends on the heating rate (1°/min) and temperature plateau, but also on the initial thickness of ppTMDSO layer. To get an homogeneous layer of silica-like on plates the ppTMDSO layer was shown to necessarily be thinner than 9 μm, otherwise some parts of stainless steel could be uncovered as the result of shrinkage by ca. 70% [28, 29].

The open structure of foams makes very difficult the use of methods of analysis usually suitable for powders and, for some of them, for functionalised plates. This is particularly the case of techniques requiring the focalisation of a radiation beam (X-ray diffraction, Raman spectroscopy, XPS, etc.) that cannot be carried out without destruction of the sample. For this reason, the conditions leading to successful coatings of foams, that is to get homogeneously coated and stable layers, were optimized for plates and then adapted to foams.

To begin with the first step (Fig. 1), no pre-treatment (etching) of the foam in RPECVD reactor was necessary to create rugosity thanks to the microstructure, at variance with stainless steel plates [30]. A new sample holder had to be designed which allowed the flow of $TMDSO/O_2/N$ (N: atomic nitrogen specie) to cross the whole foam cylinder, instead of spreading like on plates [29]. The polymerisation was performed for given times and the thickness of polymer deposits was ex situ measured on EPMA micrographs. For the same time of deposition, the thickness of ppTMDSO was the same (15 μm) on foam struts than on plates, but it could be higher (up to 50 μm) in holes due to the configuration of cells (Fig. 4a). Indeed the deposition rate of ppTMDSO on plates (1 μm/min as observed by in situ interferometry with the used RPECVD conditions) could not be directly measured owing to problems of focalisation of the laser beam on the open structure of foam. However it was observed that the thickness of ppTMDSO layer must be less than 10 μm to avoid cracks after mineralisation (step II). An example of such a defective silica-like coating, where parts of stainless steel of ca. 5–15 μm look like uncovered, is presented Fig. 5.

The next step (step III) was the dip-coating of SiO_2/foam in TiO_2 suspension. The 37 wt% TiO_2 composition was found suitable to ensure both an homogeneous coating throughout the foam volume and a high mechanical stability of deposits. In the case of plates, it was necessary to use a higher loading (60 wt%) to get the same properties. EPMA pictures of TiO_2/SiO_2 coatings on plates and foams after calcination (Fig. 6) show that thicknesses of SiO_2 were quite regular (ca. 5–8 μm). The titania layer thickness varied between 25–30 μm for plates and 10–40 μm on foams. Finally (step IV), the vanadium oxide specie were identified by Raman spectroscopy of coated plates to be mainly polyvanadates for $7\%V_2O_5/TiO_2$ composition [30]. The presence of vanadium on foam was ascertained only by the yellowish tint which became greyish after reducing chemical treatment [33]. Vanadium could be quantitatively

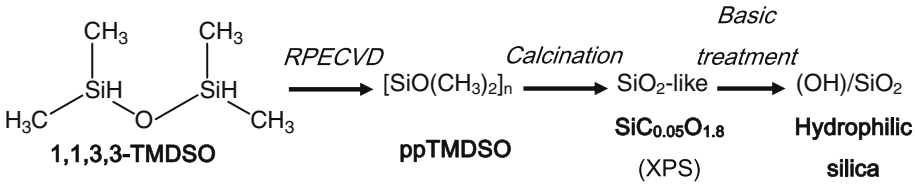

Fig. 2 Successive transformations of TMDSO to hydrophilic silica-like coating

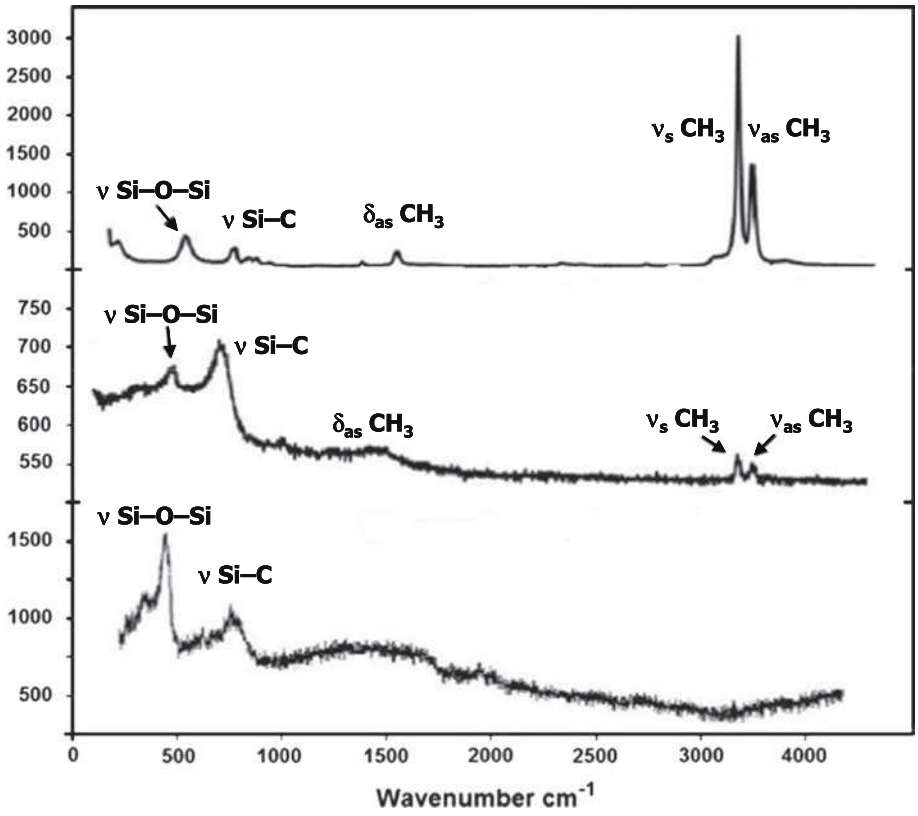

Fig. 3 Raman spectra of plates coated by ppTMDSO (*top*), after calcination (mineralisation) (*middle*), after basic surface treatment (*bottom*)

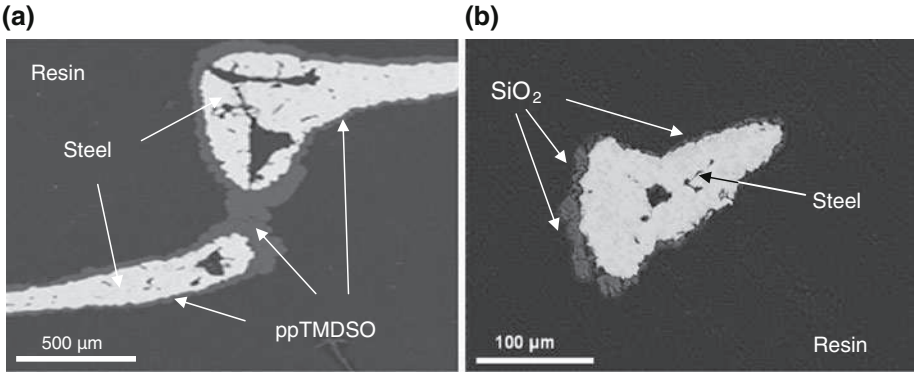

Fig. 4 EPMA pictures of foam: **a** coated by ppTMDSO after 15 min of RPECVD (*thickness* ca. 5 µm), **b** coated by silica-like after mineralisation of ppTMDSO

determined in the case of plates by XPS measurements, the V/Ti atomic ratio being linearly related to the concentration of $VO(OiPr)_3$ in ethanolic solution [30]. The test of mechanical stability showed that layers of SiO_2 (step II), TiO_2/SiO_2 (step III) and $VO_x/TiO_2/SiO_2$ (step IV) coating foams were firmly anchored, the variation of weight between each step being 0.4, 0.08 and 0.4%, respectively. The more drastic conditions of the combined ageing–mechanical test of stability led to 4.9, 5.0 and 3.9%, respectively.

EPMA was carried out on unprotected TiO_2/foam (without silica primer). Figure 7 gives an example of the thickness of TiO_2 deposits which varied largely as above, when a hole was filled or a strut was coated (BSE image), and the X-ray profile of O, Fe and Ti (along the dashed arrow) showing the thinner layers (<20 µm) on strut.

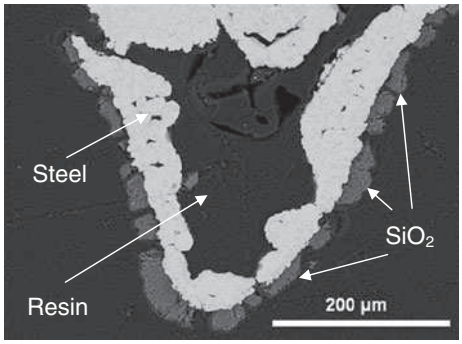

Fig. 5 Breakage of silica-like coating on foam after calcination of ppTMDSO layers with 10 µm initial *thickness*

3.2 Catalytic Results

Table 1 gathers the preliminary data in ODP obtained by varying temperature between 400 and 500 °C at constant contact time (GHSV = 30 stpL h^{-1} g_{cat}^{-1}). The conversion of propane and of oxygen (XC_3, XO_2) and the selectivity to propene, CO and CO_2 (mol.%) were measured for silica-protected and unprotected foams, as well as for powders diluted by silicon carbide granules (Fig. 8). For the validity of the comparison, care was taken to use the same amount (0.2 g) of the same 7%V_2O_5/TiO_2 composition. The catalytic properties of foams and powders were examined in the same "foam reactor" (FoR), with appropriate dilution of powders by SiC to obtain the same bed volume. The selectivity to propene on the silica-protected 7%V_2O_5/TiO_2/SiO_2 foam was higher by 10% at any conversion, when compared with the unprotected 7%V_2O_5/TiO_2 foam, whereas the conversion of propane did not change (Fig. 8). This means that, as expected because the preparation of VO_x/TiO_2 was the same, the same active species were supported on TiO_2 and the silica layer had no structural nor proper catalytic action. To get the most efficient heat transfer, the oxidic layers, whose thermal conductivity is lower by 10^2 than that of the metal, must be as thin as possible. Thus the selectivity should be higher for the unprotected TiO_2/stainless steel than for the multilayered silica-protected foam. The lower selectivity to propene could be due to a chemical effect, as observed with stainless steel plate reactor [22, 23]. The higher amount of CO_2 could be correlated to the higher conversion of O_2 upon increasing temperature (Table 1). The TiO_2 layer being less homogeneous and regular on the metallic foam as shown in Fig. 7, and the shiny parts observed by eye (vide infra) give evidence of uncovered parts of the metal, that could be like nanosized Fe_2O_3 layers. The upper surface of ASI 316L stainless steel was naturally covered by a thin layer of $(Cr,Fe)_2O_3$ which is responsible for the corrosion resistance, but after the calcination of TiO_2 deposit at 650 °C the chromium oxide escaped and Fe_2O_3 remained [23, 30]. Such Fe^{3+} specie could be responsible for combustion enhancement.

The comparison of the performance of the same catalytic powder when displayed in the two reactors, FoR and FBR, shows the effect of the dilution of VO_x/TiO_2 particles by SiC, a good thermal conductor (ca. 120 W m^{-1} K^{-1}). In the small FBR (V_{cat} = 1 cm^3), XC_3 did not vary much between 400 and 450 °C but it strongly increased (as well as XO_2 and S CO_2) at 500 °C, as if there was a kind of run-away or light-off due to the formation of hot spots. The same powder in the foam reactor did not behave the same. Upon increasing temperature the quite regular increase of XC_3 and XO_2 (Table 1) could be related to the higher dilution by SiC (ca. five times greater than in FBR). Both oxygen conversion and selectivity to carbon oxides were smaller. Thus trying to enhance the heat transfer between the catalyst particles and the reactor wall by means of SiC particles did result in increasing the selectivity to propene by decrease of CO_2.

Finally, the comparison of foams (silica-protected and unprotected) and powders when using the same reactor (FoR) at the same contact time shows that upon increasing temperature the conversions and the selectivity to propene varied regularly. At all XC_3 values the selectivity to propene on silica-protected foam was higher than for other catalysts. For example at 500 °C where XC_3 = 11–13 mol.%, the selectivity of propene decreased along the silica-protected foam (52%) > unprotected foam (44%) > powder (39%) series (Table 1).

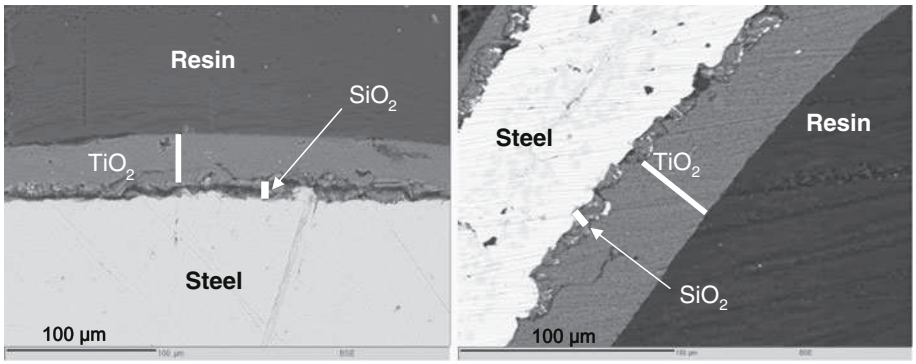

Fig. 6 TiO_2/SiO_2 coatings on plate (*left*) and foam strut (*right*) (EPMA)

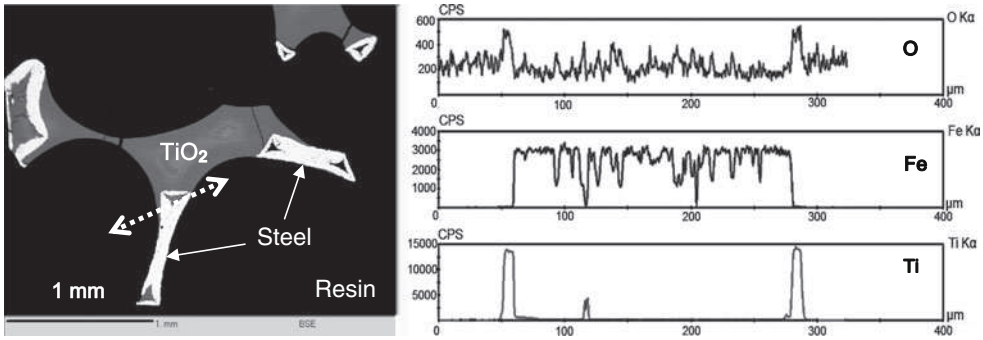

Fig. 7 EPMA of TiO_2/foam: BSE picture (*left*) and X-ray profile of O, Fe, Ti (*right*) along the *dashed arrow* (*left*)

Table 1 Catalytic experiments in oxidative dehydrogenation of propane on 7 wt%V_2O_5/TiO_2 functionalised foams and on 7 wt%V_2O_5/TiO_2 powders

VO_x/TiO_2 catalyst coating	Temp. (°C)	X C_3 (mol.%)	X O_2 (mol.%)	S $C_3^=$ (mol.%)	S CO (mol.%)	S CO_2 (mol.%)
SiO_2 protected foam (foam reactor)	400	2	10	60	22	18
	450	5	26	55	21	24
	500	11	50	52	22	26
Unprotected foam (foam reactor)	400	3	13	49	19	32
	450	7	36	45	15	41
	500	12	93	44	12	48
Powder (foam reactor)	400	6	13	61	17	42
	450	10	27	40	16	44
	500	13	42	39	19	40
Powder (fixed bed reactor)	400	2	5	64	11	25
	450	3	17	53	14	33
	500	14	71	14	20	66

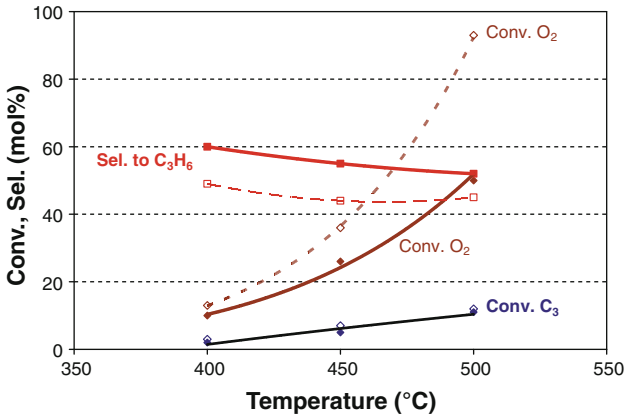

Fig. 8 Conversion of propane and oxygen and selectivity to propene for 2ML–$VO_x/TiO_2/SiO_2$ (*full symbols*, *plain lines*) and 2ML–VO_x/TiO_2 (*open symbols*, *dashed lines*) coated foams in foam reactor

4 Discussion and Conclusion

Even when millimeter, and not micrometer scale, catalytic reactors are concerned, there are three main factors which are of interest to be enhanced: The heat transfer (both internal and external with heating medium), the mass transfer which depends on turbulent or laminar flow, and the amount of loaded catalyst. Beginning by the latter factor, the thinner the layer, the higher is the rate of heat transfer, but such a requirement may be against a high catalytic performance. Indeed the manner in which the catalyst is coated may influence its intrinsic catalytic properties. However, the catalyst layer deposited on the substrate must be mechanically (good anchoring), thermally and chemically (good compatibility) stable. Whatever the shape of the substrate (honeycombs, fibers, foams, etc.), when coating ceramics like alumina, mullite, cordierite, etc., the mechanical anchoring is potentially good as due to the substrate porosity (Table 2). The similar dilatation coefficients of the oxidic support (e.g., of a metallic active phase), or of the active oxide phase itself are also favourable. The chemical compatibility between the ceramic constituents (Al, Mg, Si, …) and the oxidic support (alumina, silica, etc.) also is generally good. This is the reverse situation when using metallic substrates, the surface area being quite null, and the dilatation coefficient being very different when compared to those of oxides. To get a high mechanical stability of oxidic layers, a corrosion step is generally necessary. The interest of aluminium is its

Table 2 Relative properties of substrate (S) and/or catalyst (C)

Property of substrate S and/or Catalyst C[a]	Ceramic substrate	Metallic substrate
Mechanical anchoring of C	Easy	Difficult
Comparative dilatation coefficients	Similar	Different
Comparative chemical compatibility	Similar	Similar/different[b]
Thermal conductivity of S	Low	High

[a] Oxidic support or active phase; [b] see text

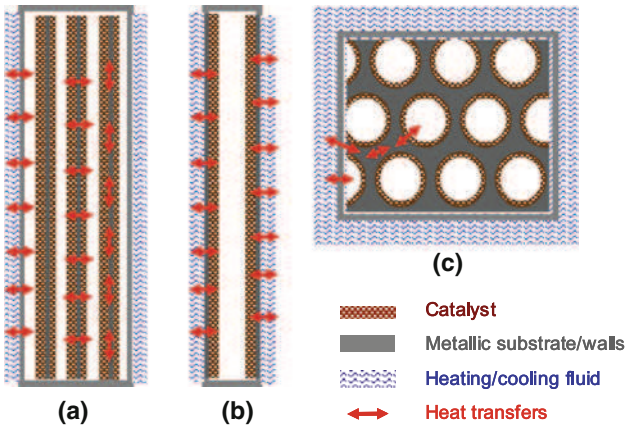

Fig. 9 Schematics of heat transfers in **a** multiplates reactor, **b** wall reactor, **c** monolith or foam inserts

high thermal conductivity (237 W m^{-1} K^{-1} for plain metal) compared to ceramics (ca. 40 W m^{-1} K^{-1} for dense α-alumina). In this case, the anodic oxidation of aluminium [34–36] or the thermal oxidation of fecralloy [36–38] results in the formation of alumina, and the chemical compatibility is good with layers of an alumina support. However the mechanical resistance of aluminium and its alloys is not very high at temperatures above 500 °C. An acidic treatment is required in the case of stainless steel (546 W m^{-1} K^{-1}), which is the cheapest metallic material of industrial reactors, by means of which the passive film of $(Fe,Cr)_2O_3$ laying under $Cr(OH)_3{\cdot}nH_2O$ (at room temperature) increases [23, 30, 39]. For most catalytic applications there are no elements common to both metal and oxidic catalyst unless special steels are used (e.g., titanium-containing steel to be further coated by TiO_2 layers), and so the chemical compatibility is not good. Moreover the surface area of the passive film is not high enough and it is necessary to add a primer, both to increase the surface area and to avoid migration and poisoning by steel elements [23, 30, 40]. One interest of the thin catalyst coatings is the absence of mass transfer limitations. However if numerous enough active sites have to be displayed, the layer must have an appropriate thickness. In this concern, structured inserts (Fig. 9c), either honeycombs or foams, are advantageous because their surface microstructure favours mechanical anchoring. A high amount of loaded catalyst may be obtained by using multiplates reactor, whereas wall rector reactor configuration is less favourable (unless its wall is microstructured) (Fig. 9a, b). Laminar flow may be suitable but only for very fast reactions like combustion. In mild oxidation and for thin layers of catalyst a turbulent flow is preferable, like in foam insert reactor. It is well-known that the heat is transferred by convection and by radiation particularly in the reacting gas phase, and by conduction inside the catalyst pellets or coated layers, as well as inside the reactor walls. The heat transfer by conduction though the external heating medium is prominent in reactions at medium temperatures (<500 °C), and its efficiency is thought to be maximum in the catalytic wall reactor configuration (Fig. 9b) [18, 20, 24].

Foam inserts combine several advantages because they allow high loading of catalyst, high mass transfer due to turbulent flow, and high internal and external heat transfers, provided that their material is metallic. In a forthcoming paper [41] the endothermic catalytic dehydrogenation of methylcyclohexane was performed in a stainless steel reactor containing foams (or beads) coated by Pt/γ-Al_2O_3. Several thermocouples were displayed on the external surface and at the center of the foam (or beads). The temperature profile was determined during reaction at 300 °C and at the same residence time on foams differing by the material (alumina and fecralloy), porosity (33–37 ppi) and density (81–97%), but coated by the same amount of catalyst. The results showed that the temperature gradient was the smallest (5 °C) with denser foams, due to higher effective conductivity. A similar reactor would be interesting to use for studying the temperature profile during ODP on VO_x/TiO_2/stainless steel foam.

We are currently studying the catalytic properties by varying the active phase loading as well as the operating parameters in a wider range. As incomplete as they are today, the results confirm that metallic foams are interesting devices to operate mild oxidation reactions, and particularly the oxidative dehydrogenation of propane. Recently Schwartz et al. [42] deposited pre-prepared VO_x/Al_2O_3 catalysts by spray coating on microchannels carved in stainless steel. Organic or organometallic binders were used to ensure the adhesion of the catalyst after etching of stainless steel. It was shown that the catalytic performance

was systematically less good when, e.g., tetraethylorthosilicate, was used, as compared with organic binders which were more easily eliminated during calcination. It may be that the active VO_x/Al_2O_3 specie were detrimentally modified by this treatment. The hydrolysis and calcination steps of the VO_x/Al_2O_3-binder/stainless steel did not lead to the same layered system as the one we made by using RPECVD to transform TMDSO to silica. Moreover Schwartz et al. found that powders in fixed bed were more selective at isoconversion than in the coated reactor [42]. We had the same observation when carrying ODP in our catalytic multiplates reactor and comparing with powders [23]. Chemical reasons, which were the poisoning by elements of stainless steel, and/or the nature of active specie on powders which was not similar to those on plates, were invoked.

Therefore, notwithstanding the difficulties when one wants to cope with the differences of heat and mass transfers due to different reactor configurations, the activity and selectivity exhibited by the active specie is to be enhanced. Indeed, an alternative explanation to the above observations is that a catalyst designed to be efficient in a fixed bed reactor, and thus to stand hot spots, may have to be designed especially to work, e.g., as a thin layer on a higly heat conducting material. This was already noticed, for example in the case of VPO catalyst for n-butane oxidation. The value of P/V ratio, which is the prominent parameter ruling the catalytic properties because it is responsible for the mean oxidation state of vanadium and the occurrence of special V^{5+} phases [43], varies between 1.00 (recirculating solid reactor) [2, 3, 44] and 1.20 (fixed and fluidised bed reactors). It means that chemistry has still a long future and that success in utilising (micro)structured reactor walls will not be met by improving technology only.

Acknowledgments The authors gratefully acknowledge the support of the Agence Nationale pour la Recherche (ANR-06-BLAN-0126 “Millicat”).

References

1. Di Cosimo R, Burrington JD, Grasselli R (1986) J Catal 102:234
2. Contractor RM, Ebner J, Mummey MJ (1990) Stud Surf Sci Catal 55:553
3. Contractor RM, Garnett DI, Horowitz HS, Bergna HE, Patience GS, Schwartz JT, Sisler GM (1994) Stud Surf Sci Catal 82:233
4. Patience GS, Bockrath RE (2010) Appl Catal A Gen 376:4
5. Dalmon J-A, Cruz-López A, Farrusseng D, Guilhaume N, Iojoiu E, Jalibert J–C, Miachon S, Mirodatos C, Pantazidis A, Rebeilleau-Dassonneville M, Schuurman Y, van Veen AC (2007) Appl Catal A Gen 325:198
6. Julbe A, Farrusseng D, Guizard C (2001) J Membr Sci 181:3
7. Mallada R, Menéndez M, Santamaría J (2000) Catal Today 56:191
8. Xue E, Ross J (2000) Catal Today 61:3
9. Lu Y, Dixon AG, Moser WR, Hua Maa Y, Balachandran U (2000) J Membr Sci 170:27
10. Akin FT, Lin YS (2002) J Membr Sci 209:457
11. Park S, Gorte RJ, Vohs JM (2000) Appl Catal A Gen 200:55
12. Löfberg A, Bodet H, Pirovano C, Steil MC, Vannier R-N, Bordes-Richard E (2006) Top Catal 38:169
13. Löfberg A, Boujmiai S, Capoen E, Steil MC, Pirovano C, Vannier RN, Mairesse G, Bordes-Richard E (2004) Catal Today 91–92C:81
14. Löfberg A, Bodet H, Pirovano C, Steil C, Vannier R-N, Bordes-Richard E (2006) Catal Today 117:168
15. Sundmacher K, Rihko-Struckmann LK, Galvita V (2005) Catal Today 104:185
16. Bodet H, Löfberg A, Pirovano C, Steil MC, Vannier RN, Bordes-Richard E (2009) Catal Today 141:260
17. Abraham F, Debreuille-Gresse MF, Mairesse G, Nowogrocki G (1988) Solid State Ion 28–30:529
18. Klemm E, Döring H, Geisselmann A, Schirrmeisterds S (2007) Chem Eng Technol 30(12):1615
19. Stankiewicz A, Moulijn JA (2004) Re-engineering the chemical processing plant: process intensification. Marcel Dekker Inc, New York
20. Gavriilidis A, Angeli P, Cao E, Yeong KK, Wan YSS (2002) Chem Eng Res Des 80:3
21. Schimmoeller B, Schulz H, Pratsinis SE, Bareiss A, Reitzmann A, Kraushaar-Czarnetzki B (2006) J Catal 243:82
22. Giornelli T, Löfberg A, Guillou L, Paul S, Le Courtois V, Bordes-Richard E (2007) Catal Today 128:201
23. Giornelli T, Löfberg A, Paul S, Bordes-Richard E (2011) Appl Catal A Gen 391:43
24. Becht S, Franke R, Geißelmann A, Hahn H (2009) Chem Eng Proc 48:329
25. Cavani F (2010) Catal Today 156:8
26. Grabowski R, Pietrzyk S, Słoczyłski J, Genser F, Wcisło K, Grzybowska–Świerkosz B (2002) Appl Catal A Gen 232:277
27. Frank B, Dinse A, Ovsitser O, Kondratenko EV, Schomäcker R (2007) Appl Catal A Gen 323:66
28. Essakhi A, Löfberg A, Supiot P, Mutel B, Paul S, Le Courtois V, Meille V, Pitault I, Bordes-Richard E (2011) Polym Eng Sci 51:940
29. Essakhi A, Löfberg A, Supiot Ph, Mutel B, Paul S, Le Courtois V, Bordes-Richard E (2010) In: Gaigneaux EM, Devillers M, Hermans S, Jacobs P, Martens J, Ruiz P (eds) Proceedings of 10th international symposium “scientific bases for the preparation of heterogeneous catalysts”, vol 175. Studies in Surface Science and Catalysis, p 17, 11–14 July 2010
30. Giornelli T, Löfberg A, Bordes-Richard E (2006) Appl Catal A Gen 305:197
31. Supiot P, Vivien C, Granier A, Bousquet A, Mackova A, Boufayed F, Escaich D, Raynaud P, Stryhal Z, Pavlik J (2006) Plasma Proc Polym 3:100
32. Bond GC (1997) Appl Catal A Gen 157:91
33. Essakhi A, Löfberg A, Paul S, Mutel B, Supiot P, Le Courtois V, Rodriguez P, Meille V, Bordes-Richard E (2011) Microporous Mesoporous Mater 140:81
34. Hönicke D (1983) Appl Catal 5:179
35. Giornelli T, Löfberg A, Bordes-Richard E (2005) Thin Solid Films 479:64
36. Meille V (2006) Appl Catal A Gen 315:1
37. Heck RM, Gulati S, Farrauto RJ (2001) Chem Eng J 82:149
38. Sanz O, Echave FJ, Sánchez M, Monzón A, Montes M (2008) Appl Catal A Gen 340:125
39. Gerisher H (1986) Corros Sci 26:191
40. Guillou L, Balloy D, Supiot Ph, Le Courtois V (2007) Appl Catal A Gen 324:42

41. Löfberg A, Essakhi A, Swesi Y, Meille V, Pitault I, Zanota M-L, Paul S, Supiot P, Mutel B, Le Courtois V, Bordes-Richard E Chem Eng J (submitted)
42. Schwarz O, Duong P-Q, Schäfer G, Schomäcker R (2009) Chem Eng J 145:420
43. Cavani F, De Santi D, Luciani S, Löfberg A, Bordes-Richard E, Cortelli C, Leanza R (2010) Appl Catal A Gen 376:66
44. Bordes E, Contractor R (1996) Topics Catal 3:365

Microporous and Mesoporous Materials 140 (2011) 81–88

Contents lists available at ScienceDirect

Microporous and Mesoporous Materials

journal homepage: www.elsevier.com/locate/micromeso

Materials chemistry for catalysis: Coating of catalytic oxides on metallic foams

A. Essakhi [a,b], A. Löfberg [a,b], S. Paul [b,c], B. Mutel [a,d], P. Supiot [a,d], V. Le Courtois [b,c], P. Rodriguez [e], V. Meille [e], E. Bordes-Richard [a,b,*]

[a] Université Lille Nord de France, F-59000, Lille, France
[b] UMR CNRS 8181, Unité de Catalyse et Chimie du Solide, Université Lille 1, F-59655 Villeneuve d'Ascq, France
[c] Ecole Centrale Lille, F-59655 Villeneuve d'Ascq, France
[d] Institut d'Electronique, de Micro électronique et de Nano technologie - UMR CNRS 8520, Université Lille 1, F-59652 Villeneuve d'Ascq, France
[e] Université de Lyon, Institut de Chimie de Lyon, Laboratoire de Génie des Procédés Catalytiques, UMR CNRS 2214, CPE-Lyon, F-69616 Villeurbanne, France

ARTICLE INFO

Article history:
Received 30 June 2010
Received in revised form 13 October 2010
Accepted 13 October 2010
Available online 29 October 2010

Keywords:
Metallic foam
RPECVD
TiO_2-anatase coating
VO_x/TiO_2 catalyst coating
Structured reactors

ABSTRACT

Catalytic structured reactors are designed to improve both heat and mass transfers during reactions in the presence of catalytic layers. The know-how acquired in the coating of stainless steel walls by catalytic layers of VO_x/TiO_2, active in the abatement of volatile organic compounds and in the production of chemical intermediates, was extended to metallic foams. The preferred and original way was to first make a deposit of a silica-like primer by cold plasma assisted polymerization of tetramethyldisiloxane in the presence of oxygen. After mineralisation, this layer was supposed to act as a barrier against poisoning by elements of the metallic substrate, as well as a stabilizer of the catalyst layers. The cells of the foam were homogeneously covered by a 5 μm-thick polysiloxane film ending in ca. 1 μm thick silica after calcination. After studying the textural properties and zeta potential of aqueous suspensions of TiO_2 particles, the silica-coated foams were dipped in a 37 wt.% aqueous suspension of TiO_2-anatase. The final $VO_x/TiO_2/SiO_2$/foams were obtained by grafting polyvanadate specie in sol–gel medium. At every step of coating, the multilayer materials were studied mainly by X-ray Photoelectron Spectroscopy and Electron Probe Micro-Analysis. Moreover the mechanical and chemical stability of the successive coatings was checked.

1. Introduction

There are two main ways to increase the yield of products obtained by catalytic reaction, improving the properties of the catalytic material or optimizing the catalytic process. In the first case it is necessary to improve both activity and selectivity of catalysts. Oxidic materials are used either as supports (alumina, silica, zeolites,...) or as active phases (mostly transition metal mixed oxides) in the very numerous reactions for synthesis of chemical commodities from, e.g., hydrocarbons, including alkanes, environmental issues ($deNO_x$, VOC abatement,...), energetics (anodes for fuel cell) and the like. As in the case of anchored metal organic complexes, oxide particles can be inserted or oxidic species can be grafted in zeotypes. More recently several methods of preparation to obtain nanosized particles of oxides, and even special techniques to manufacture nanostructured catalysts were developed [1]. The second way is to optimize the process itself, beginning by the improvement of the contact efficiency between the catalyst and the molecules to be transformed.

Since more than a decade the concept of process intensification has boosted research on structured (micro)reactors, the microscale (1–100 μm) being related to safer, cleaner, and above all more efficient heat and mass transfers [2]. One way of implementing reaction technology is in the form of a catalytic wall reactor, the walls being engraved by channels in the sub-millimetre range inside which is attached a solid catalyst. Another way is to coat the catalyst onto structured inserts like monoliths, ending in monolithic reactors. This is not so new since that technology was chosen in the 1970's to solve environmental problems due to mobile or stationary installations. For example three-way catalysts for automotive engine exhausts are made of noble metals on alumina deposited in channels of monoliths, while NO_x effluents are treated on monoliths made with vanadium–tungsten–titanium mixed oxides. In the case of exhaust pipes, metallic honeycombs were considered for a while because of their high thermal conductivity but finally they were abandoned at the profit of cordierite monoliths which could better stand the very high temperatures due to combustion reactions. The problem to solve is not so different when seeking for chemical products like acrolein, maleic anhydride, phthalic anhydride, etc., manufactured by mild oxidation

* Corresponding author at: UMR CNRS 8181, Unité de Catalyse et Chimie du Solide, Université Lille 1, F-59655 Villeneuve d'Ascq, France. Tel.: +33 320434526; fax: +33 320436561.
E-mail address: elisabeth.bordes@univ-lille1.fr (E. Bordes-Richard).

1387-1811/$ - see front matter © 2010 Elsevier Inc. All rights reserved.
doi:10.1016/j.micromeso.2010.10.018

of hydrocarbons. Most reactions are consecutive and to be obtained the targetted product must be "kinetically" quenched at the expense of carbon oxides. For example, propylene obtained by oxidative dehydrogenation (ODH) of propane ($\Delta_R H_{298}$ = -118 kJ mol^{-1}) is very easily converted to carbon dioxide ($\Delta_R H_{298}$ = -1926 kJ mol^{-1}) because it is more reactive than the reactant. Several catalytic formulas have been tried with little success, as up to now yields of propylene hardly overcome 40%. To get rid of hot spots which are unavoidable in packed bed reactors and which are (partly) responsible for the formation of carbon oxides, a solution would be to structure metallic wall reactors or to use metallic substrates like honeycombs, foams, wires, and the like, as inserts. Indeed modifying the contact between the gas phase and the catalyst, and particularly increasing the heat transfer between them, should lead to an increase of yields of propene. This has just been demonstrated by Schwarz et al. [3] who deposited a VO_x/γ-Al_2O_3 catalyst on micro-channels carved in stainless steel walls. They found that isothermal reaction conditions over a wide range of concentrations and temperatures could lead to substantial increase of the propylene productivity.

Some years ago we have undertaken studies about the coating of metallic (anodized aluminum, stainless steel) plates by VO_x/TiO_2 anatase layers. The properties of VO_x/TiO_2 catalyst are well documented for several reactions, including the ODH of propane [4–6]. The sol–gel method was used to graft TiO_2 and the active vanadia phase in successive layers onto plates, because it presents several advantages among which the easy control of composition, the low processing temperature, as well as the possibility of large area coatings at low equipment cost [7]. Another method for TiO_2 deposits, more simple as the textural properties of the powder (surface area, porous volume, etc.) are retained after drying, consisted of dip-coating the plates in an aqueous suspension of titania [8,9].

Foams have several interesting features thanks to their large geometric areas, high void fractions, high mechanical stability and low pressure drop, and the formation of hot spots should be avoided if the material is metallic due to its high thermal conductivity [10–12]. The amount and dispersion of the active phase can be controlled by changing the thickness of the coating, which is important because the performance of the catalyst is determined by the synthesis procedure, morphology and stability of the film [13].

The know-how that we acquired on the coating of stainless steel plates by VO_x/TiO_2 [7–9] was extended to the coating of metallic foams that we propose for the first time in the literature. The stainless steel foams were covered by three successive layers. First a primer constituted by silica was deposited by remote plasma enhanced chemical vapor deposition. The SiO_2/foam was dipped in titania aqueous suspension, and after calcination polyvanadates were grafted on TiO_2/SiO_2/foam by sol–gel method. The textural properties were studied and most analyses were performed mainly by electron probe micro analysis and X-ray photoelectron spectroscopy. Attention was paid to the mechanical and chemical stability of the successive layers.

2. Experimental

2.1. Preparation of samples

Plates and foams were coated in a three-step procedure (method A), consisting of (i), deposition of a silica film by polymerization of tetramethyldisiloxane (TMDSO) by remote plasma enhanced chemical vapor deposition (RPECVD, vide infra) [14], (ii), dip-coating of SiO_2/substrate in an aqueous suspension of TiO_2 while stirring (5 min) followed by calcination, (iii), grafting of vanadium oxide species on calcined TiO_2/SiO_2/substrate. The amount of TiO_2 particles in water was adapted to coat plates or foams (vide infra). After calcination vanadium oxide specie were grafted as in (iii). In (ii) and (iii) steps plates or foams were withdrawn at constant rate (6 mm s^{-1}) after dipping. Solutions containing different amounts (C = 1.0, 1.8, 3.5, 7.5 wt.% in dry ethanol) of $VO(OPr)_3$ were prepared. A final calcination was carried out at 450 °C (2 h). ASI 316L stainless steel was chosen for the metallic substrates plates ($50 \times 20 \times 0.5$ mm) and foams (Porvair®, 40 ppi, density 5.4%, porosity ε = 81%). Foams were cut as cylinders ($\varnothing 1.6 \times 0.7$ cm height) or parallelepipeds ($1.0 \times 1.0 \times 0.7$ cm). The mean weight was 410 mg/cm^3. Before use, the substrates were sonicated, first with ethanol (30 min) to eliminate organic traces, and then twice in deionized water (30 min) before drying at 100 °C for 3 h.

To compare with materials without silica primer, an alternative procedure (method B) consisted first of superficial corrosion of the metal in 30 wt.% H_2SO_4 aqueous solution at room temperature during 3 h, and followed by washing with water in ultrasonic bath (30 min) to eliminate impurities present in H_2SO_4 (e.g. K^+). The (ii) step was the same as above, the corroded substrate being dipped 5 min in aqueous suspension of TiO_2 powder while stirring. After calcination vanadium oxide specie were grafted as in (iii).

2.2. Remote plasma enhanced chemical vapor deposition (RPECVD)

The principle of the remote nitrogen plasma assisted polymerization [15] and details about the plasma reactor can be found in [16–18]. The nitrogen (1.8 L min^{-1} STP) flowing in the reactor was excited by a microwave discharge (2450 MHz–200 W) in a fused silica tube. By continuous pumping, the reactive atomic *N* species flowed from the discharge zone to the deposition zone located far (at 1 m) from the discharge (called CRNP, cold remote nitrogen plasma). In this way, the resulting flow was free of charged particles, so the etching effect was very low and deposition rates reaching 100 times that obtained with discharge plasma could be obtained. Tetramethyldisiloxane (TMDSO) monomer and oxygen (25 and 5 cm^3 min^{-1} STP respectively) were flowed at 550 Pa by means of MKS mass-flow controllers in the CRNP through a coaxial injector. The deposition rate of the polymer (here called ppTMDSO) on plates was *in situ* measured by interferometry using He–Ne laser and a photodetector. The ppTMDSO film was further mineralized by thermal treatment at 650 °C for 1 h (5 °C/min heating rate) in air under forced convection in a furnace. As traces of carbon remained, a N_2/1.5% O_2 remote plasma treatment could be finally applied during 5 min.

2.3. Characterization methods

Several methods of analysis as well as tests of stability were conducted after each step of preparation of the coated plates, and on foams for some of them.

X-ray diffraction patterns were obtained on powders or on scrapped layer from the substrate when possible using Huber D5000 diffractometer (CuKα radiation). X-ray photoelectron spectroscopy (XPS) was carried out using Escalab 220 XL spectrometer (Vacuum Generators). A monochromatic Al Kα X-ray source was used and electron energies were measured in the constant analyzer energy mode. The pass energy was 100 eV for the survey spectra and 40 eV for the single element spectra. All XPS binding energies were referred to C*1s* core level at 285 eV. The angle between the incident X-rays and the analyzer was 58°, photoelectrons being collected perpendicularly to the sample surface.

To be examined by Electron Probe Micro-Analysis (EPMA), samples were embedded into epoxy resin, and successively polished with abrasive discs (2400 to 3 μm granulometry) when the core of material had to be investigated. A Bal-Tec SCD005 sputter coated allowed depositing a thin carbon film. The elemental analysis was made by wavelength dispersive X-ray spectrometry (WDS) using Cameca SX-100 microprobe analyser working at 15 kV and 15 nA

for back scattered electron (BSE) images and at 15 kV and 49 nA for Si, Ti and Fe X-ray profiles and mapping. Si, Fe and Ti Kα X-rays were detected using TAP, LiF and PET crystals respectively. The Scanning Electron Microscope (SEM) Hitachi 4100 S was equipped with micro-analysis (Energy-Dispersive X-ray Spectroscopy, EDS) and a field emission gun. The working voltage was 20 kV.

Nitrogen adsorption measurements were carried out with Micromeritics ASAP2010 on scrap recovered catalyst powders. Results were analyzed in terms of specific area and total pore volume by B.E.T. method. The size and particle size distributions of powder particles of TiO_2 were analysed by laser scattering with a granulometer (LS Coulter). The rheological behaviour of suspensions was measured with a Gemini HRnano rheometer (Bohlin Instruments). All measurements were performed at the same temperature (25 °C) using a spiral bob mobile which avoids particle settling. The electrostatic stability of suspensions was studied using a zeta potential analyser (Zetasizer Nano ZS, Malvern Instruments).

The mechanical stability of the coated layers was evaluated by the scratch test method (ASTMD3359–02). Obviously this test was not possible on foams and it was replaced by the use of an ultrasonic bath. The foam was weighted before and after being placed in *n*-heptane in a beaker and submitted to ultrasounds for twice 1 min. A combined test of mechanical and chemical stability was also performed. The coated sample was first weighted (m_1) after a heat treatment in N_2 at 350 °C (4 h). At 400 °C the sample was contacted with air/steam (80/20) for 8 h followed by N_2/air/steam/acetic acid (79/10/10/1) for 5 h (total flow rate 1.4 L min^{-1}). After drying in N_2 at 200 °C (40 h) the m_2 mass was obtained. Finally samples were sonicated in *n*-heptane (1 min) and weighted again (m_3) after drying in N_2 for 40 h.

3. Results

3.1. Silica layer coating as a primer (Method A)

The way to obtain an homogenous silica layer was first studied on ASI316L plates [14,16,18] and then applied to coat ASI316L foams with some modifications. The rate of deposition of ppTMDSO film on ASI316L plates was 1.0 ± 0.1 μm min^{-1}. The film was mineralized by ex situ calcination (5 °C/min, 650 °C, 1 h). The final stoichiometric composition was $SiC_{0.05}O_{1.82}$ (further called SiO_2) according to XPS experiments (Table 1). A post-treatment in N_2/1.5%O_2 plasma remote afterglow during 5 min was usually applied after calcination [15,17] but the layer on ASI316L was completely burst when the thickness of the film was 15 μm [14]. XPS experiments showed that both iron and Fe^{3+} were detected, in addition to $SiC_{0.01}O_{1.82}$ (Table 1). Finally the most homogeneous and stable silica layer was obtained for a 5 μm-thick film of polymer calcined at 1 °C/min heating rate and not plasma post-treated. During calcination the film shrinked by ca. 70%. The good adhesion to ASI316L and the mechanical steadiness of the SiO_2 layer was checked by the ultrasonic bath test which revealed no loss of weight at less than 0.1%.

Once optimized for plates, the same protocol was applied to coat ASI316L foam cylinders, with some modifications. The microstructure of the foam allowing a good mechanical holding (Fig. 1), the plasma or acidic treatments to increase roughness after cleaning was found unnecessary. The design of the sample holder used for plates had to be modified in order to force the reactive flow to cross the whole volume of the foam, otherwise there was no ppTMDSO coating beyond 3.5 mm from the top surface of the sample [14]. This way, the deposit of ppTMDSO was found homogeneous throughout the foam. The deposition rate could not be *in situ* measured by interferometry because the laser beam could not be focalised on this 3D open structure. After 15 min deposition, the mean thickness was ca. 15 μm on foam struts, the walls of which were quite straight, like on plates for the same time. However the deposit was thicker when filling "holes" depending on the geometry of the cells (Fig. 2a). The ppTMDSO/ASI316L foam was further calcined as above (Fig. 2b) and post-treated in N_2/1.5% O_2 remote plasma (5 min). As in the case of plates, the layers were partly burst (Fig. 2c). An homogeneous calcined film of SiO_2 could be obtained without the post-treatment, provided the thickness of ppTMDSO film was smaller than 7 μm. Consequently this thickness was targetted and the post-treatment step was suppressed. The combined test of stability carried out on SiO_2/ASI316L foams showed that the weight losses during mechanical (0.4%) and chemical (5%) stresses were small (Table 2).

3.2. Coating of SiO_2/ASI316L foams by TiO_2

The textural properties of commercial samples of TiO_2-anatase and of TiO_2 particles obtained by sol–gel method were examined with the aim of preparing suspensions to coat ASI316L plates and foams. Indeed the suspension used in dip-coating process is often prepared just before coating, but it is worthwhile to know about its stability. For such dispersions, the electrostatic stability of particles within the liquid is a key parameter for avoiding fast flocculation. Meille et al. [19,20] addressed this point, particularly in the case of TiO_2-P25 (Degussa). We did not choose that sample because of its high amount of rutile (>10%) which is not welcome as a support for VO_x species in the reaction we deal with. It is well known that the pH of aqueous medium has a strong influence on the stability of aqueous dispersion of oxide particles. The zeta po-

Table 1
Binding energy of elements in 15-thick ppTMDSO film (left columns) and in bursted SiO_x (right columns) coatings of stainless steel plates (XPS).

Elements in ppTMDSO/ASI316L	BE (eV)	Elements in bursted SiO_x/ASI316L plate	BE (eV)
Carbon[a]	285	O(–Fe^{3+})	529.8
C(–O)	288.6	Iron	710
O(–Si)[b]	533	Fe^{3+}(–O)[c]	725
Silicon	154.7	Si(–O)	158.7
Si(–O)	158.7	–	–

[a] Contamination.
[b] O-chemisorbed: BE = 536.9 eV.
[c] Small amount of Fe^{2+}.

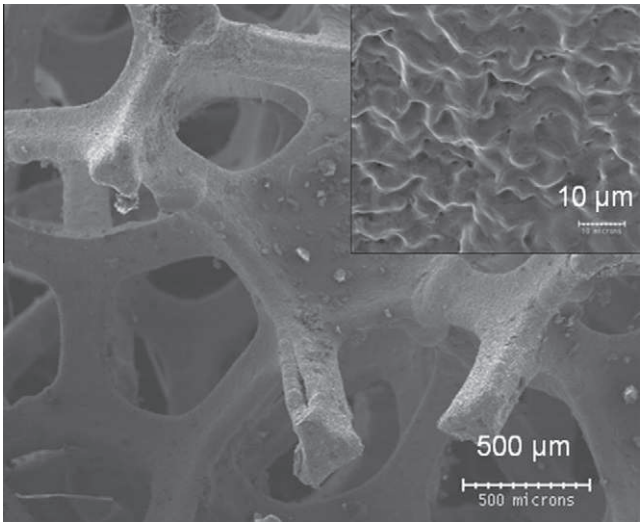

Fig. 1. SEM pictures of a cut piece of stainless steel foam and its microstructure (inset).

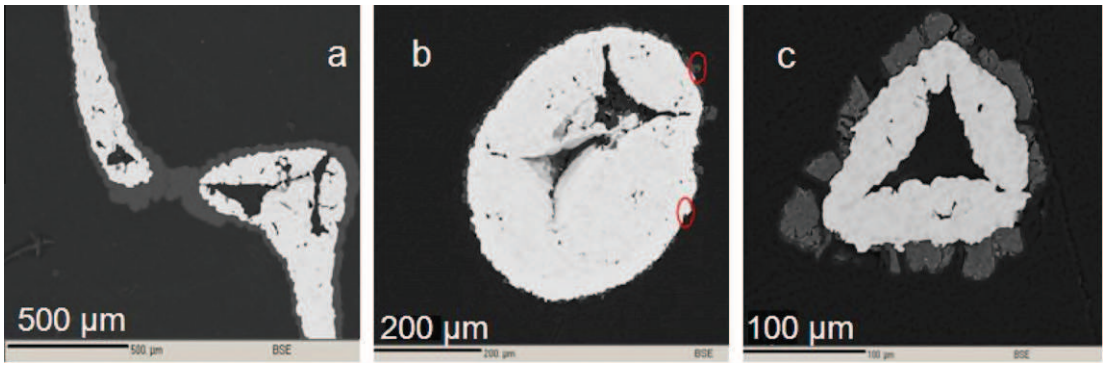

Fig. 2. EPMA of a branch section of ASI316L foam after (a) coating by ppTMDSO, (b) calcination, (c) cold plasma post-treatment (1–10 µm thickness).

Table 2
Weight losses after the two steps of the combined mechanical and chemical stability procedure for $VO_x/TiO_2/SiO_2$/ASI316L foam (see text); Weight of uncoated foam: $m_0 = 287 \pm 15$ mg.

Coated layer	m_1 (mg)	m_2[a] (mg)	m_3[b](mg)	$\Delta m_{12}/\Delta m_{10}$[c] (%)	$\Delta m_{13}/\Delta m_{10}$ (%)
SiO_2	368.3	368.0	364.0	0.37	5.29
TiO_2/SiO_2	415.5	415.4	408.9	0.08	5.14
$VO_x/TiO_2/SiO_2$	498.2	497.2	490.0	0.47	3.88

[a] Mechanical test.
[b] Chemical test.
[c] $\Delta m_{12}=m_1-m_2$; $\Delta m_{10}=m_1-m_0$; $\Delta m_{13}=m_1-m_3$.

tential of suspensions is related to the electrostatic stability of particles and determines the trend of particles to flocculate or not. A negative sign means that H^+ ions are released out of the surface and OH^- ions are adsorbed (and the reverse if the sign is positive), and the higher the absolute value of zeta potential, the lower the trend of particles to flocculate. After discarding Hombicat sample (50 m^2/g, mean size of particles 50 µm) whose particles flocculated in the beaker, the influence of the distribution of particles size, of addition of acid or base on the zeta potential and of the rheology of aqueous suspensions of TiO_2 was examined. Particles of Eurotitania-1 (1–60 wt.%) (45 m^2/g, prepared by Tioxide International for EUROCAT [5]) were added to nitric acid 0.01 M. At a shear stress of 1 Pa, the viscosity slightly increased from 3.3 (1 wt.%) to 4.8 mPa s (60 wt.%). However, these suspensions were not very stable because the zeta potential was close to the point of zero charge (PZC = 5.4). When particles were added to NH_4OH 0.01 M, the zeta potential became negative (−34 mV). A sol–gel prepared according to [7,9] from $Ti(OBu)_4$ and diethanolamine in ethanol was shown to form colloids after hydrolysis with water. Using the zetameter, colloids of 8.7 nm were formed after 3 h and grew by Ostwald ripening to 13.4 and 16.2 nm after 20 and 40 h, respectively. The rheological behaviour of this suspension was Newtonian with a viscosity of 2.5 mPa s. As the particle size distribution of TiO_2-Aldrich (10 m^2/g) was narrower (size range 0–250 µm) than that of TiO_2-Alfa-Aesar (52 m^2/g, 0–1500 µm), the former sample was studied. Whichever these titania samples, the rheological behaviour was almost identical. The suspensions exhibited a Newtonian behaviour like for TiO_2-P25 (Degussa) suspensions which were shown to be the most stable at high (basic) pH [20]. The zeta potential of TiO_2 Aldrich aqueous suspension was found to be negative in deionised water (−4.0 mV) as well as upon addition of HNO_3 0,01 M (−18.7 mV) or NH_4OH 0.01 M (−35.6 mV).

At variance with the case of alumina or of TiO_2 primer coatings [7,9] the silica coating after RPECVD was quite hydrophobic, as shown by measuring the contact angle with deionized water on SiO_2/ASI316L plates [14]. To make them more hydrophilic, they were dipped in a basic solution of NaOH + EtOH (Brown solution) for 4 h, withdrawn at 6 mm s^{-1} and further dried at 100 °C during 1 h, before dip-coating in TiO_2 suspension. EPMA image and WDS profile of Fe, Ti, Si and O elements (Fig. 3) give evidence for the two successive layers SiO_2 and TiO_2 on the ASI316L plate. The same Brown treatment was applied to SiO_2/ASI316L foams, before step (ii) which had to be adapted. Different concentrations of TiO_2 suspension from 10 to 60 wt.% were tried. After withdrawing, the foam was softly blown in air to suppress the excess of suspension and keep the pores open. The thickness, homogeneity and stability of the TiO_2 coating were examined by EPMA and stability tests. High concentration like 60 wt.% TiO_2 Aldrich used in the case of plates led to a non homogeneous distribution throughout the foam with plugging of the external surface cells. Low concentration resulted in surfaces not fully covered. As shown in Figs. 4 and 5 which present the cross section of a strut and WDS profiles and X-ray mapping of Fe, Si, Ti, respectively, the thickness of the TiO_2/SiO_2 coating (after calcination) was quite the same (ca. 14 µm) on both sides of the strut when concentration was 37%. Moreover the combined test of stability carried out on these TiO_2/SiO_2/ASI316L foams showed that the mechanical stability was very high (0.08%), and that the chemical stability (5%) remained the same as compared to SiO_2/ASI316L foams (Table 2).

3.3. Direct coating of stainless steel foam by TiO_2 layer

As an alternative to silica or TiO_2 primer attempted by Giornelli et al. [9], experiments were carried out to directly coat stainless steel plates and foams by TiO_2. The acidic pretreatment which was necessary for a good holding of TiO_2 layers on plates was not required for foams owing to their microstructure that mechanically favours adhesion. The direct deposition of TiO_2 was successful using suspensions of TiO_2 Aldrich (60 wt.% and 37% wt.% for coating plates and foams, respectively). The calcination was performed at 650 °C. A regular coating with the same thickness was easily obtained on plates but less easily when foams were used (Figs. 6 and 7). Few metallic brightnesses revealed at first glance that some parts of the foam were not covered.

3.4. Grafting of VO_x onto TiO_2/SiO_2/ASI316L and TiO_2/ASI316L foams

Two theoretical monolayers (ML) of VO_x were grafted onto TiO_2/SiO_2/ASI316L and TiO_2/ASI316L foams using vanadium(V)-oxytripropoxide, followed by calcination at 450 °C. The change of colour, which became yellowish as formerly observed on plates, was the only means to be sure that vanadium was present in the upper layer of foams [9]. The mechanical stability remained quite high (0.4%) (Table 2). The second (ageing) step led to higher losses

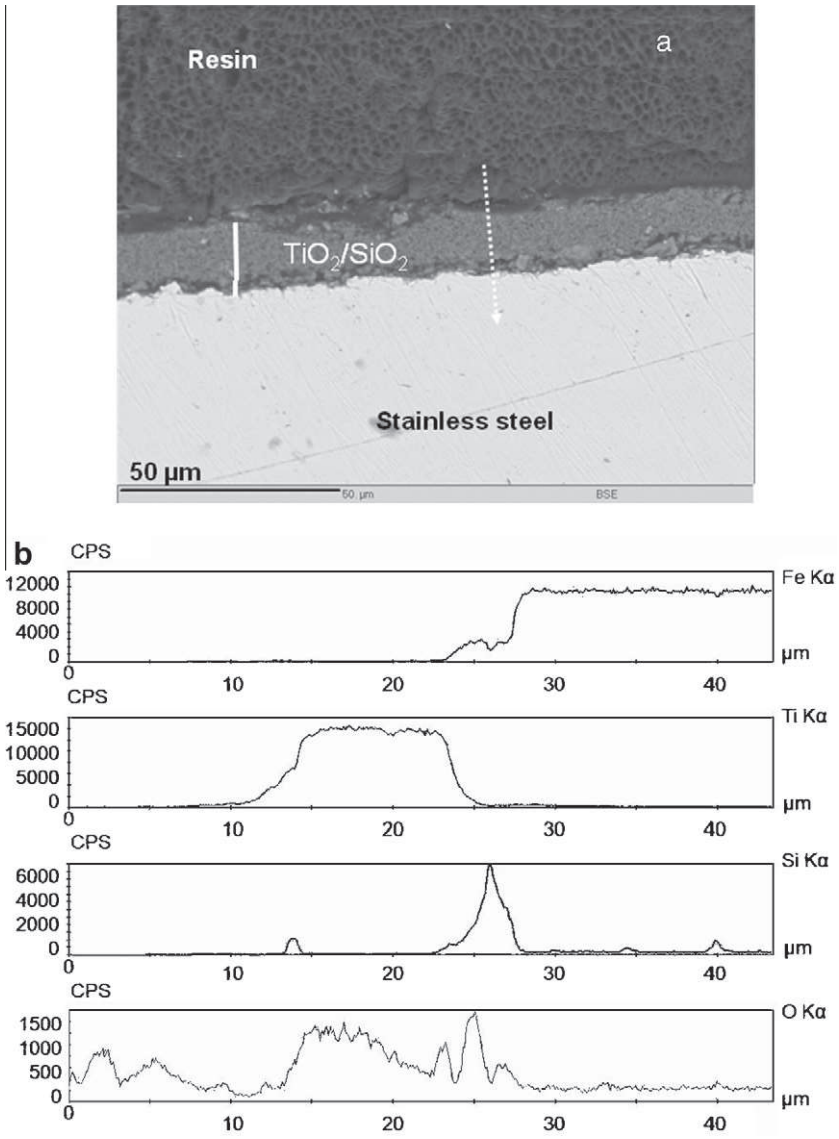

Fig. 3. Stainless steel plate coated by TiO_2/SiO_2 (thickness of TiO_2 layer 20 µm): (a) EPMA (black: resin; white: stainless steel; grey: deposit); (b) WDS profiles of Fe, Ti, Si and O elements along the white dashed arrow on (a).

(3.9%). Moreover the colour turned light grey, which probably meant that part of vanadium was reduced from V^{5+} to V^{4+} state. The polyvanadate specie are certainly more sensitive to the presence of steam (air/steam = 80/20) and acetic acid than TiO_2 and SiO_2, and a given amount of vanadium may have been leached out. Analyses of the samples after these treatments are in progress.

4. Discussion

The coating of substrates bearing some chemical compatibility with the support of the active phase is quite easy, like, e.g., the coating of aluminium or FeCrAlloy by γ-alumina, the usual support of precious metals. Indeed alumina layers could be formed on the surface of these substrates by means of anodisation or simply by calcination of the substrates at high temperature [21,22]. When the oxidizing treatment was short enough, the formation of transition aluminas (close to the gamma form) was obtained instead of the α form (corindon), thereby facilitating the anchoring of the porous layer of γ-alumina during dip-coating. At variance, getting stable coatings of stainless steel by oxides like silica or titania is more difficult. We found suitable to add an intermediate layer that could favour anchoring of oxides and act as a barrier against the diffusion of metallic elements. In order to increase both surface area and strong anchoring of TiO_2 support, Giornelli et al. [9] grafted TiO_2 layers (<1 µm thick) obtained by controlled hydrolysis of tetrabutylorthotitanate onto stainless steel. To ensure the good adhesion of this micronic layer onto stainless steel the calcination was carried out 900 °C for 2 h. XPS showed that the Ti/Fe surface ratio was ca. 15%. To the X-ray diffraction pattern of the austenitic phase of stainless steel were superimposed lines of α-Fe_2O_3, and of pseudobrookite Fe_2TiO_5 in very small amount. Despite the high temperature of calcination, most TiO_2 remained in the anatase form as shown by XRD, the rutile formed during calcination amounting to less than 3%. Unfortunately the catalytic properties in ODH of propane were not as good as expected, mainly because iron diffused from stainless steel as Fe^{3+} which poisoned the active vanadia phase [23]. To by-pass these difficulties we have chosen to deposit the intermediate silica-like layer by RPECVD. Among others, one advantage of RPECVD is the possibility to clean and to pre-treat the substrates just before depositing the polymer. Thus the surface roughness as well as the concentration of surface OH groups is increased, which allows a better anchoring of the titania

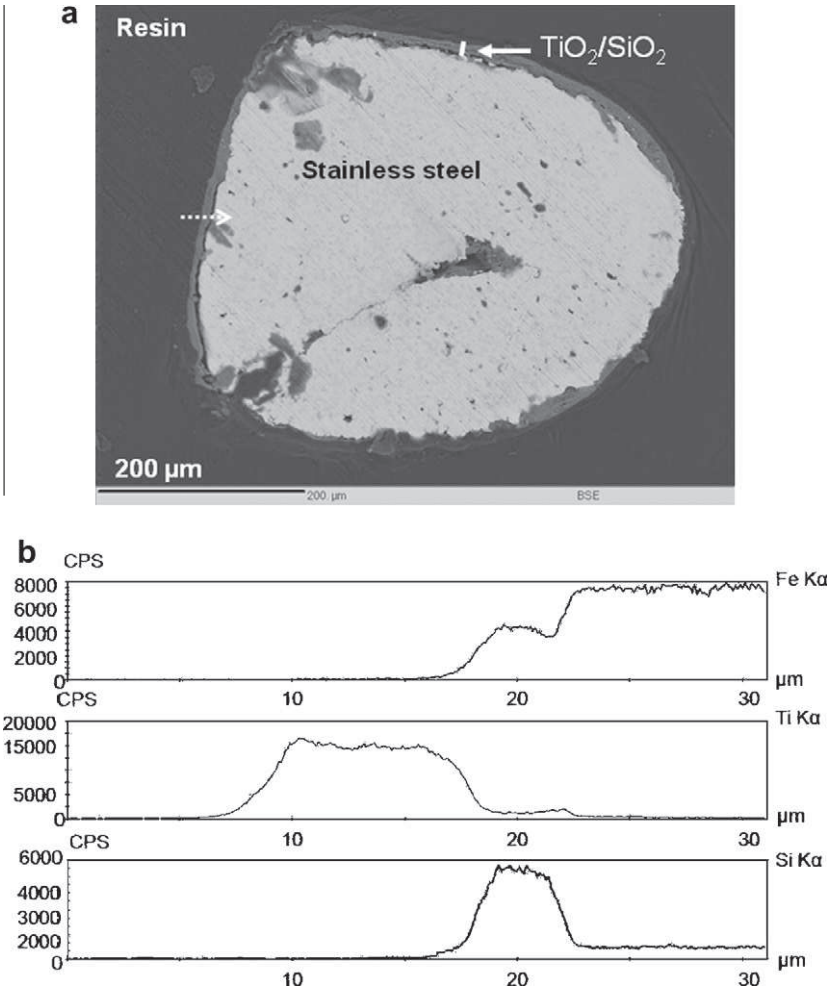

Fig. 4. Branch section of stainless steel foam coated by TiO_2/SiO_2 (thickness of TiO_2 layer 14 µm): (a) EPMA (black: resin; white: stainless steel; grey: deposit); (b) WDS profiles (along the white dashed arrow) of Fe, Ti, Si and O elements.

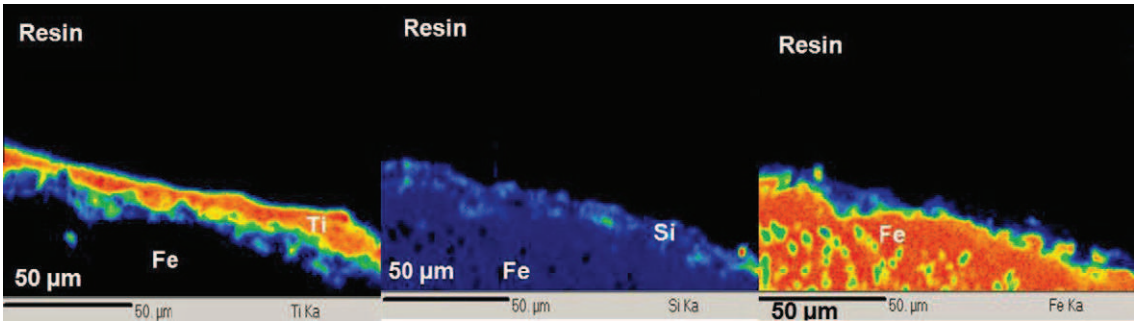

Fig. 5. X-ray mapping of Fe, Si, Ti on coated TiO_2/SiO_2/ASI316L foam.

deposit. As presented above, the technique developed for plates was applied to coat stainless steel foams. As also shown, it was not interesting for the integrity of the silica-like coating to apply the post-treatment by $N_2/1.5\%O_2$ plasma remote afterglow to eliminate the remaining traces of carbon. Indeed analyses showed that the amorphous silica was a quasi two-layers material, one being SiO_2 and the other close to unmodified ppTMDSO [15,17]. Probably this composition gives a certain degree of plasticity to silica, which helps to accommodate the difference of dilatation coefficients between the silica primer film and the metallic substrate. The stability tests are in favour of this hypothesis. As the anchoring of TiO_2 was strong enough, the calcination of TiO_2/SiO_2/foam could be performed at 650 °C only (instead of 900 °C in the case of TiO_2 primer), so that the diffusion of iron in the layers was expected to be hindered. However a drawback of the silica-like layer was the surface hydrophobicity which obliged us to add a step to facilitate further anchoring of the TiO_2 layer.

There are other difficulties when working with foams. One concerns the loading of vanadium specie onto TiO_2 support. The amount of vanadium on TiO_2/ASI316L plate could be related to XPS results, which showed that, in all cases, the variation of V/Ti ratio depended on the concentration of the VO_x precursor [7,9].

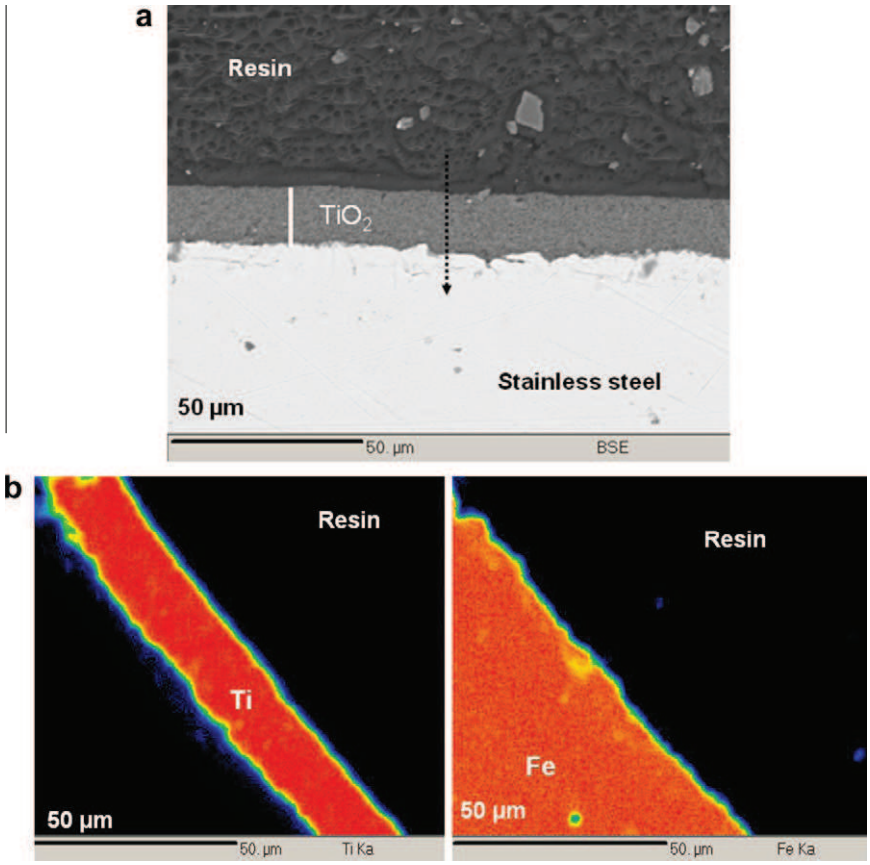

Fig. 6. (a) EPMA of stainless steel plate coated by TiO_2 after calcination (thickness of TiO_2 layer 18 µm) (black: resin; white: stainless steel; grey: deposit); (b) X-ray mapping of Fe, Ti.

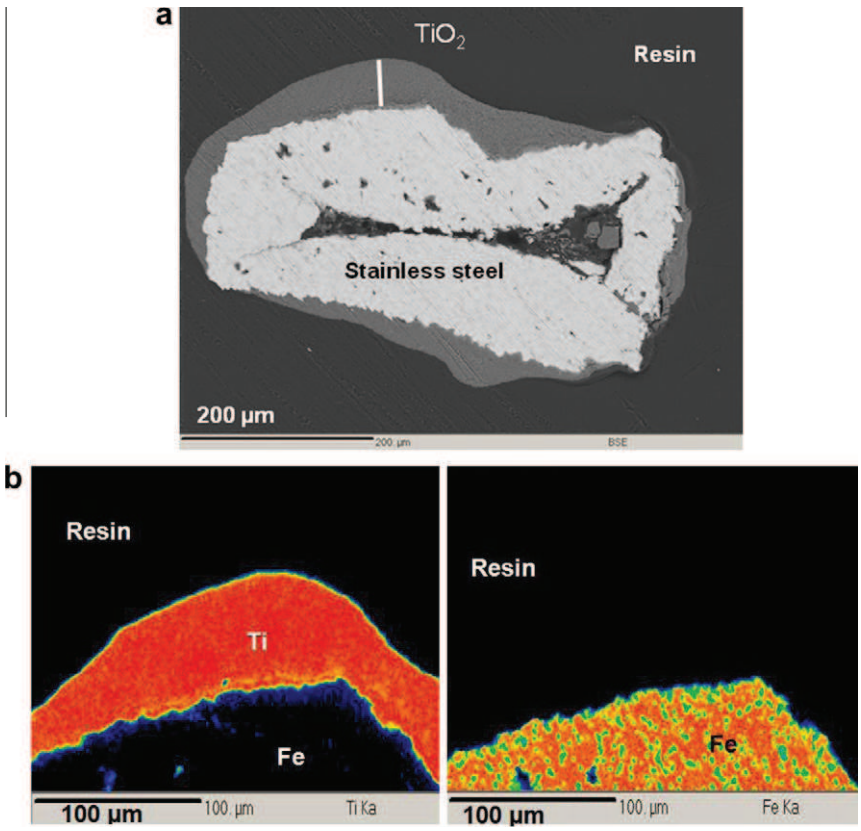

Fig. 7. (a) EPMA of a branch section of stainless steel foam coated by TiO_2 after calcination (thickness of TiO_2 layer <40 µm) (black: resin; white: stainless steel; grey: deposit); (b) X-ray mapping of Fe, Ti.

V/Ti increased linearly with concentration and reached a plateau at V/Ti = 0.2 corresponding to the formation of a "monolayer", exactly like in the case of VO_x/TiO_2 powders [4–6]. However we found that, up to now, this technique could not be applied to analyze foams, the main difficulty being the focusing of X-rays (as in the case of X-ray diffraction) on the sample. EPMA also could not give results precise enough because the vanadium loading was too low. For obvious reasons, the wettability of SiO_2 deposited on foams could not be measured. Therefore, most methods of analysis of materials cannot be used for solid foams without destroying them. The samples may be cut in pieces to be examined, as we did for EPMA and SEM-EDX experiments, but every time values of concentration are required, the error due to the contribution of exposed Fe or Fe^{3+} may be very high. Therefore it was assumed that, for the third step (VO_x deposition) as for the others, the surface active VO_x species were the same on foams and on plates for a given composition which was chosen here 1.4 wt.% V_2O_5 (≈2 monolayers of VO_x) onto TiO_2-Aldrich (10 m^2/g) powders [9,23]. The same assumption was made in the case of the unprotected VO_x/TiO_2 foam with the same composition.

Preliminary catalytic results in ODH of propane on the silica-protected and unprotected VO_x/TiO_2 foams were obtained. The catalytic experiments were carried out in a same reactor constituted by a tube filled partly with the same volume of foams (5.40 cm^3), in the same operating conditions (T = 400–500 °C, total flowrate 0.1 stpL h^{-1} of $C_3H_8/O_2/He/Ar$ = 5/2.5/67.5/25 and GHSV = 30 stpL h^{-1} g_{cat}^{-1}) and for the same loading of active specie (≈2 ML) [24]. The same activity of oxidation of propane was observed since the conversion of propane varied from 2 to 11 ± 0.5 mol% between 400 and 500 °C. This result could be expected because of the same loading of vanadium on TiO_2. On the contrary the selectivity to propene was higher by 10% at every conversion for the silica protected foam. The lower selectivity to propene observed with unprotected foam was related with the conversion of oxygen which reached 100% at 500 °C and the concomitant production of CO_x. The main reason could be the presence of iron in the parts of foam uncovered by the catalytic layer.

5. Conclusion

For the first time in literature we have demonstrated that VO_x/TiO_2 catalyst could be successfully deposited on stainless steel foams, coated or not by an intermediate, silica-like, primer. The mechanical and chemical stabilities were quite high. Using the same procedure than for plates but with a specially designed sample holder, RPECVD was applied to the coating of a metallic foam. The modelling of the polymer flow through the foam is in progress and it should help to ensure a more regular thickness of layers in the foam cells. The thin layer of silica-like film had two functions, stabilizing the titania support and acting as a barrier against the diffusion of elements that could diffuse outwards and poison the active phase. The preliminary catalytic experiments which are currently carried out showed that the higher productivity of propylene resulted from protecting the steel by the silica coating.

Acknowledgements

This work was granted by "Agence Nationale de la Recherche" (ANR-MILLICAT 06-BLAN-0126-01). S. Pallier (LGPC) is thanked for rheological and zeta potential measurements and S. Bellayer (Ecole Nationale Supérieure de Chimie de Lille) is thanked for performing EPMA.

References

[1] G. Centi, S. Perathoner, Catal. Today 79–80 (2003) 3.
[2] A. Gavriilidis, Trans. I. ChemE, Part A 80 (2003) 709.
[3] O. Schwarz, P.-Q. Duong, G. Schäfer, R. Schomäcker, Chem. Eng. J. 145 (2009) 420. ibid, 429.
[4] B. Grzybowska-Świerkosz, Appl. Catal. A: General 157 (1997) 263.
[5] J.C. Vedrine (Ed.), "Eurocat Oxide", Catal. Today, 20 (1994), and papers therein.
[6] G.C. Bond, Appl. Catal. A: General 157 (1997) 91.
[7] T. Giornelli, A. Löfberg, E. Bordes-Richard, Thin Solid Films 479 (2005) 64.
[8] T. Giornelli, A. Löfberg, L. Guillou, S. Paul, V. Le Courtois, E. Bordes-Richard, Catal. Today 128 (2007) 201.
[9] T. Giornelli, A. Löfberg, E. Bordes-Richard, Appl. Catal. A: General 305 (2006) 197.
[10] A. Cybulski, J.A. Moulijn (Eds.), 'Structured Catalysts and Reactors', CRC Taylor & Francis, Boca Raton (USA), 2005.
[11] A. Shamsi, J.J. Spivey, Ind. Eng. Chem. Res. 44 (2005) 7298.
[12] M. Maestri, A. Beretta, G. Groppi, E. Tronconi, P. Forzatti, Catal. Today 105 (2005) 709.
[13] V. Meille, Appl. Catal. A: General 315 (2006) 1.
[14] A. Essakhi, A. Löfberg, P. Supiot, B. Mutel, S. Paul, V. Le Courtois, V. Meille, I. Pitault, E. Bordes-Richard, Polym. Eng. Sci. J. accepted (2010). doi:21899.
[15] F. Callebert, P. Supiot, K. Asfardjani, O. Dessaux, P. Dhamelincourt, J. Laureyns, J. App. Polym. Sci. 52 (1994) 1595.
[16] P. Supiot, C. Vivien, A. Granier, A. Bousquet, A. Mackova, F. Boufayed, D. Escaich, P. Raynaud, Z. Stryhal, J. Pavlik, Plasma Proc. Polym. 3 (2006) 100.
[17] L. Guillou, P. Supiot, V. Le Courtois, Surf. Coat. Technol. 202 (2008) 4233.
[18] L. Guillou, D. Balloy, P. Supiot, V. Le Courtois, Appl. Catal. A: General 324 (2007) 42.
[19] P. Rodriguez, V. Meille, S. Pallier, M.A. Al Sawah, Appl. Catal. A: General 360 (2009) 154.
[20] V. Meille, S. Pallier, G.V. Santa Cruz Bustamante, M. Roumanie, J.-P. Reymond, Appl. Catal. A: General 286 (2005) 232.
[21] O. Sanz, F.J. Echave, M. Sánchez, A. Monzón, M. Montes, Appl. Catal. A: General 340 (2008) 125–132.
[22] P. Kerleau, Y. Swesi, V. Meille, I. Pitault, F. Heurtaux, Catal. Today 157 (2010) 321.
[23] T. Giornelli, A. Löfberg, S. Paul, E. Bordes-Richard, Appl. Catal. A: General, "Recent Developments in Model Catalysis - Closing the Gap to Technical Applications", G. Mestl (Ed.). in press; doi.org/10.1016/j.apcata.2010.09.002.
[24] A. Löfberg, A. Essakhi, Y. Swesi, V. Meille, I. Pitault, M.-L. Zanota, S. Paul, P. Supiot, B. Mutel, V. Le Courtois, E. Bordes-Richard, Chem. Eng. J., submitted.

Chemical Engineering Journal 176–177 (2011) 49–56

Contents lists available at ScienceDirect

Chemical Engineering Journal

journal homepage: www.elsevier.com/locate/cej

Use of catalytic oxidation and dehydrogenation of hydrocarbons reactions to highlight improvement of heat transfer in catalytic metallic foams

A. Löfberg[a,b], A. Essakhi[a,b], S. Paul[a,c], Y. Swesi[d], M.-L. Zanota[d], V. Meille[d], I. Pitault[d], P. Supiot[a,e], B. Mutel[a,e], V. Le Courtois[a,c], E. Bordes-Richard[a,b,*]

[a] Université Lille Nord de France, F-59000 Lille, France
[b] CNRS UMR 8181, Unité de Catalyse et Chimie du Solide, UCCS, Université Lille 1, Sciences et Technologies, F-59655 Villeneuve d'Ascq, France
[c] Ecole Centrale de Lille, F-59655 Villeneuve d'Ascq, France
[d] Université de Lyon, Institut de Chimie de Lyon, Laboratoire de Génie des Procédés Catalytiques, CNRS UMR 2214, CPE-Lyon, F-69616 Villeurbanne, France
[e] Institut d'Electronique, de Microélectronique et de Nanotechnologies, CNRS UMR 8520, Université Lille 1, Sciences et Technologies, F-59655 Villeneuve d'Ascq, France

ARTICLE INFO

Article history:
Received 20 December 2010
Received in revised form 3 April 2011
Accepted 28 April 2011

Keywords:
Solid catalytic foams
Heat transfer
Oxidative dehydrogenation of propane
Dehydrogenation of methylcyclohexane
VO_x/TiO_2 coated foams
$Pt/\gamma\text{-}Al_2O_3$ coated foams

ABSTRACT

Two model reactions were used to show the influence of catalytic foams on improving heat transfer. The catalytic performances were compared to those observed when using the same reactors packed with catalytic powder or beads. One reaction was the exothermic oxidative dehydrogenation of propane which was investigated on $7\%V_2O_5/TiO_2$ coated on stainless steel foam. A silica layer was first deposited on the foam surface by Remote Plasma Enhanced Chemical Vapour Deposition to avoid poisoning of active phase by iron species, to favour the anchoring of TiO_2 support and to accommodate the difference of dilatation coefficients. When comparing catalytic foams with powders in the same reactor, the selectivity to propene at isoconversion was higher by 12–45 mol% for the same amount and composition ($7\%V_2O_5/TiO_2$) of the active phase and in the same operating conditions (contact time, C_3/O_2 ratio, temperature range). The other reaction was the endothermic dehydrogenation of methylcyclohexane on $2\%Pt/Al_2O_3$ directly coated on foams and on molecular sieve beads. To study the influence of heat and mass transfers, the material (FeCrAlloy or alumina) and porosity (81–97%) of foams were varied. It was found that, even for highly exothermic or endothermic reactions not limited by external transport, the coated foams significantly increased the effective conductivity of catalytic beds, the denser foam leading to higher effective conductivity.

1. Introduction

To increase the yield and selectivity of products in catalytic processes, one way is to improve the catalytic properties of the catalyst or to find a better one. The other way is to improve the efficiency of the gas/solid contacts and to diminish the thermal gradients in catalytic beds. In other words the goal is to increase the rates of heat and mass transfers and to improve the dispersions as well as the effective conductivities. Catalytic micro(milli)reactors or structured reactors offer a potential to conduct mass and/or heat transfer-demanding reactions under safer conditions while maintaining and/or increasing selectivity and productivity [1–3]. Structured inserts (packings) like honeycomb monoliths were first used in automotive exhaust pollution abatement, but others, like solid foams, in which the external mass transfer would increase while maintaining a low pressure drop, are now available. In a joint programme granted by the Agence Nationale de la Recherche we are currently studying how the structuration can help to enhance the catalytic reactor performance. Different methods with their advantages and drawbacks are available to evaluate the reactor performance improvement. One method is to carry out measurements of the transport phenomena (mass, heat and momentum) in the structures, followed by numerical simulations. It requires a perfect description of the structures in terms of characteristic parameters (diameter, tortuosity,. . .). These parameters are easy to measure or to estimate, in the case of e.g., fins in a heat exchanger, or spherical shaped catalysts. However, they are difficult to obtain in the case of foams that require a topological description due to their 3D-anisotropy. Moreover, a hydrodynamic study requires performing mass and heat transfer measurements in large enough pieces to obtain significant and measurable gradients. This way is chosen by several research teams because it is definitely useful to acquire the knowledge for the future design of industrial processes [4,5]. The second method is to perform catalytic experiments using a well known catalyst deposited onto the structure. It requires a

* Corresponding author at:Unite de Catalyse et Chimie du Solide, CNRS UMR 8181, Université Lille 1, Sciences et Technologies, F-59655 Villeneuve d'Ascq, France.
E-mail address: Elisabeth.Bordes@univ-lille1.fr (E. Bordes-Richard).

1385-8947/$ – see front matter © 2011 Elsevier B.V. All rights reserved.
doi:10.1016/j.cej.2011.04.064

perfect knowledge of the catalyst properties and of the kinetics of the reaction. To get the same catalyst density in reactors, it is also necessary to make sure that the catalyst is homogeneously distributed among the whole structure. An advantage of this way is also to allow the testing of small pieces of foam, wherein thermal gradients would be non-significant under low Reynolds as practised in academic laboratories. This method could seem to be less rigorous than the first one, but, first, it does not require onerous equipments such as X-ray tomograph, and, second, it considers the overall system (including the catalyst layer in working conditions) whereas most physical characterizations and modellings are made on bare, uncoated, foams. We have worked that way to show how highly exo or endothermic model reactions can be used for rapid evaluations of catalytic foam performance.

The two following model reactions were chosen because they are heat sensitive. The first one is the oxidative dehydrogenation of propane (ODP) to propene, the enthalpy of reaction of which is $\Delta_R H^\circ_{298} = -118\,kJ\,mol^{-1}$. Despite of many attempts and tries to find more efficient catalysts, the best yield using oxide catalysts in fixed bed reactors is currently less than ca. 40% [6,7], because the product (propene) is less stable than the reactant (propane) and very easily oxidized to CO_2. Obviously the combustion of propene is even more exothermic ($\Delta_R H^\circ_{298} = -1930\,kJ\,mol^{-1}$). Hot spots in packed bed reactors contribute to decrease the selectivity to propene as well as to deactivate the catalyst. The heat transfer control is therefore a key issue when dealing with such a selective oxidation reaction. Conversely, the selectivity to propene can be considered as an "indirect sensor" of the heat transfer efficiency. Very recently, a microstructured foam reactor was developed by Schwarz et al. [8] to conduct this reaction using VO_x/γ-Al_2O_3 catalyst. As in most kinetic studies on vanadium oxide based catalysts in packed bed reactors [9–11], the authors found that the selectivity to propene suffered from consecutive propene oxidation to CO and CO_2, but also from the accumulation of propene inside the particle pores leading to its degradation [8,12]. However the latter observation may be related to the use of porous γ-alumina as a support for VO_x species. In this concern, the textural properties (low surface area and little porosity) of TiO_2-anatase are more suitable. Moreover TiO_2-anatase exerts a structural influence on the supported vanadium species which is responsible for selectivity in reactions like, e.g., *o*-xylene oxidation to phthalic anhydride [13–16]. In former works [17–19] we studied several ways to coat aluminum and stainless steel plates by this catalyst. We examined their properties in ODP in a home—designed plate reactor, but the catalytic performances were not satisfying enough when compared to those obtained in a packed bed reactor, due, among other factors, to higher mean values of temperature in the plate reactor than in the packed bed reactor.

The other heat sensitive reaction is the dehydrogenation of methylcyclohexane (MCH) to toluene on Pt/γ-Al_2O_3. This reaction is often chosen among the many reactions that would be suitable to generate hydrogen for fuel-cell application. Roumanie et al. [20] operated the reaction in a silicon micro–structured reactor composed of microsized pillars. In another work [21], this endothermic reaction was coupled to the exothermic combustion of toluene in an autothermal heat-exchanger reactor. The dehydrogenation of MCH is endothermic ($\Delta_R H^\circ_{298} = 204\,kJ\,mol^{-1}$) and it requires temperatures higher than 300 °C to shift the thermodynamic equilibrium and to reach high conversions. However side reactions like cracking lead to undesired products above 400 °C. Though the rate of dehydrogenation is relatively slow, and no limitation due to external or internal mass transfer exists, significant thermal gradients occur in packed bed reactors filled with pellets, and the heat management has to be addressed.

The means chosen to study the influence of heat transfer was to deposit the respective catalysts on structured substrates known for their high thermal conductivity. Reticulated solid foams exhibit several interesting features like their large geometric areas, high void fractions leading to low pressure drop and high mechanical stability. Compared to straight channelled monoliths, one of their advantages is the 3D—open structure which is more suitable for the dispersion of the reacting gas phase and so for improving the external mass transfer [1,22–25].

Stainless steel and FeCrAlloy foams were coated by VO_x/TiO_2 and Pt/γ-Al_2O_3 catalysts, respectively. To assess the – expected – beneficial effect of reactor structuring, it was found necessary to compare the catalytic performance with that of the same active species, shaped as powders, beads or foams. Another difficulty stemmed, which was the fact that structured systems may require adapted preparation methods [26], but that, in turn, the preparation methods may affect the catalytic properties. This was found particularly true with VO_x species which are very sensitive to impurities [17,19]. To cope with these disagreements, a silica-like layer was deposited on plates by means of remote plasma enhanced vapour deposition (RPECVD), before coating by VO_x/TiO_2 catalyst [27]. Depositing such a silica primer on stainless steel or channelled plate was already attempted in the preparation of Co/SiO_2 catalyst for the Fischer–Tropsch synthesis of diesel cuts [28–30]. The successive Co/porous SiO_2/SiO_2-primer layers were proven to be stable in channelled and in single plate reactors, and the performance was enhanced as compared to that of Co/SiO_2 powders in packed bed. In the present paper the novelty is the adaptation to ASI316L foams of the coating technique elaborated for plates, to be further housed in a tube reactor and investigated in ODP reaction. A second interest is the direct comparison of foams differing by the material and porosity onto which Pt/γ-Al_2O_3 was deposited, in the endothermic reaction of dehydrogenation of methylcyclohexane. It is to be noticed that in these cases the stability of Pt/γ-Al_2O_3/foam was high enough, so that a silica interface was found unnecessary. During the methylcyclohexane dehydrogenation, the "sensor" was not the selectivity as in ODP, but the thermal gradients. They were measured thanks to several thermocouples loaded in an original foam reactor.

2. Experimental

2.1. Preparation of catalytic foams

2.1.1. VO_x/TiO_2/foam and VO_x/TiO_2 powder

Once cleaned by sonication in ethanol followed by washing in deionized water and drying at 110 °C for 3 h, the pieces of AISI 316L foam (Porvair®, 40 ppi, density 5.4%) were coated in three steps according to the method previously elaborated for plates [17,19]. A cylinder (⌀1.6 cm × 0.7 cm) of Fo (Fo for foam) was displayed on a specially designed sample holder in the RPECVD reactor to be coated by silica (step 1). Briefly, RPECVD consisted of the polymerisation of tetramethydisiloxane (TMDSO) (Aldrich, grade 97%, pre-mixed with oxygen) by means of the reactive nitrogen species (plasma) created in a remote area by a microwave discharge [31,32]. Details about the RPECVD reactor and operating conditions were reported in [27,33]. The deposition rate was *in situ* measured by laser interferometry. In the case of plates, the thickness of TMDSO polymer was found to increase linearly with time at 1 μm/min. No direct relationship could be obtained in the case of foams because of problems of laser focalisation. The TMDSO plasma polymer film deposited on plates or foams was further mineralised in a furnace by thermal treatment in air to obtain the SiO_2-like layer. That layer was amorphous to X-rays and had a quite glassy aspect in SEM pictures. Its mean composition was $SiC_{0.01}O_{1.82}$ according to XPS experiments carried out on plates [27,33].

Table 1
Characteristics of the four structure packings to be coated by 2% Pt/γ-Al_2O_3.

Ref	Structure	Size	Porosity (%)	m_{cata} (g)[b]
F1	FeCrAlY foam	33 ppi[a]	97	2.5
F2	FeCrAlY foam	33 ppi	81	2.0
F3	α-Al_2O_3 foam	37 ppi	87	2.6
B	Zeolite beads	⌀2 mm	40	2.5

[a] Pores per inch.
[b] Catalyst mass in the 19 cm long foam (vide supra).

The methods of coating by TiO_2 and VO_x species had already been elaborated to coat aluminum and AISI 316L stainless steel plates (thereafter abbreviated as SSt-Pl) [17,19]. SiO_2/SSt-Fo carriers were dip-coated in an aqueous suspension of TiO_2 (Aldrich) particles under stirring during 5 min, and withdrawn at 6 mm s^{-1}. The optimised concentration (60 wt% TiO_2) used for SiO_2/SSt-Pl led to the plugging of SiO_2/SSt-Fo open cells. The best compromise between the viscosity of TiO_2 suspension and the stability of the final TiO_2 coating was found for 37 wt% TiO_2 [34]. Like TiO_2/SiO_2/SSt-Pl, the TiO_2/SiO_2/SSt-Fo samples were calcined in air flow at 80 °C/min heating rate, up to 700 °C (2 h). Finally they were dip-coated in $VO(OiPr)_3$ in dry ethanol solution, yielding $VO_x/TiO_2/SiO_2$/SSt-Pl and $VO_x/TiO_2/SiO_2$/SSt-Fo after calcination (air flow, 450 °C for 4 h).

Powders with the same composition were prepared by conventional incipient-wetness impregnation [14,35]. TiO_2 (Aldrich) particles were impregnated with ammonium metavanadate in oxalic acid aqueous solution, dried at 110 °C and calcined in the same conditions than plates and foams.

2.1.2. Preparation of Pt/γ-alumina foams and beads

The catalyst was first prepared by wet impregnation of γ-alumina (SASOL, SBa-200) with a toluene solution of platinum acetylacetonate [20,21]. Foams (1.2 cm thick) differing by the material (FeCrAlloy or α-alumina) and the characteristics (Table 1) were cut into rectangular pieces of 4.9 cm × 19 cm. The foam pieces were washed with acetone to ensure a clean surface and then calcined at 500 °C prior to coating. They were dip-coated in an aqueous suspension containing the 2% Pt/γ-Al_2O_3 catalyst powder and nitric acid. After evacuation of the excess suspension, the coated foams were dried at room temperature and calcined at 500 °C. Molecular sieves (zeolite 4A, 8–12 meshed, Acros organics) were sieved to get the ⌀1.7–2.3 mm fraction. They were coated by incipient-wetness impregnation using the same Pt/γ-Al_2O_3 catalyst suspension. Alpha-alumina foam manufactured by CTTC (Center for Technology Transfers in Ceramics) at Limoges, France, was used as is. FeCrAl foams (Porvair) were calcined at 1100 °C in air during 15 min (heating rate 6 °C/min).

2.2. Physicochemical analyses

The structural and textural characteristics of VO_x/TiO_2 powders were reported in [16,17,27]. Most analyses of VO_x/TiO_2 coatings were carried out on plates because, except for Electron Probe Micro Analysis (EPMA) and Scanning Electron Microscopy (SEM) techniques (*vide infra*), the open cell geometry of foams makes them difficult to perform. In the case of plates which were analyzed at every stage of preparation, the thickness of TMDSO polymer film coating SSt-plates was measured by *in situ* interferometry, and the silica-like films were analyzed using a Fourier Transform Infrared Perkin-Elmer spectrometer to check the absence of C–H bonds. Laser Raman spectroscopy (LRS) (LabRAM Infinity–Jobin Yvon) and X-ray photoelectron spectroscopy (XPS) (VG-Escalab 220 XL) were used in steps 2 and 3. LRS experiments confirmed the presence of TiO_2-anatase (lines at 199, 397, 515, 645 cm^{-1}) on TiO_2/SiO_2/Pl and of mainly polyvanadates (very weak lines at 285, 996 and 1030 cm^{-1}) on both 2ML–$VO_x/TiO_2/SiO_2$/Pl after calcination and 2ML–VO_x/TiO_2 powders [17–19]. No iron (nor Fe or Fe^{3+}) was detected by XPS.

Electron Probe Micro Analysis (EPMA) was performed on coated plates and foams embedded into epoxy resin and polished with abrasive discs. A thin carbon film was deposited by means of a Bal-Tec SCD005 sputter. Elemental analysis was performed using a wavelength dispersive X-ray spectrometer (Cameca SX-100 microprobe analyser). Back scattered electron images and Si, Ti, FeKα X-ray profiles and mapping were obtained at 15 and 49 nA, respectively (15 kV). The Scanning Electron Microscope (SEM) Hitachi 4100 S was equipped with micro-analysis (EDS) and a field emission gun. The working voltage was 15 kV.

The mechanical stability of coatings on plates was examined by cross-cut-tape test. An ultrasonic *n*-heptane bath (during twice 1 min) was also used for foams and plates (both types of catalyst). A test of chemical stability (ageing) consisted of successive heat treatments (N_2 at 350 °C, 4 h, followed by air/steam 80/20 molar ratio, 8 h, and N_2/air/steam/acetic acid 79/10/10/1 molar ratio) for 5 h, followed by ultrasonic treatment [27,34].

2.3. Catalytic experiments

2.3.1. ODP of propane

The conventional test rig consisted of a continuous gas–solid reactor operated at atmospheric pressure with on-line analysis of reactants and products by gas chromatography (Varian 3800). Propane, oxygen, helium and argon were fed through mass flow controllers at 100 stpcm^3 min^{-1} (C_3H_8/O_2/He/Ar = 5/2.5/67.5/25, C_3H_8/O_2 = 2/1). The temperature was varied between 250 and 550 °C and measured outside but at the wall contact. The foam reactor (FR) could be loaded with four catalytic foam cylinders (⌀1.6 cm, length 0.7 cm for each foam), or with powder catalyst. It consisted of a stainless steel tube (i.d. ⌀1.6 cm, length 10 cm) with a frit. Silicon carbide granules (⌀250 μm) were packed below and above foam cylinders or powders to ensure an even distribution of gases. The powder catalyst (200 mg, grains ⌀ ca. 200 μm) loaded in the foam reactor was diluted with SiC in order to get the same catalytic bed volume and the same active phase loading (catalyst density) than for foams (5.6 cm^3 for 4 foam elements). The FR catalytic beds were 1.6 cm in diameter and 2.8 cm long. A small volume reactor (SVR) (stainless steel, i.d. ⌀1.2 cm, length 5 cm) was also used for powders. It was loaded with 200 mg of catalyst mixed with 1 g of SiC pellets (0.21 mm), the remaining volume on top of the powder being filled with SiC. The SVR catalytic bed was 1.2 cm in diameter and 0.88 cm long, leading to a 1 cm^3 volume. The catalyst density was 5.6 times higher in SVR than in FR. The main products were propene and carbon oxides. The amount of C_2 hydrocarbons and of acetaldehyde, acrolein, acetic and acrylic acids was below 1%. The catalytic activity was determined at the steady state, which was reached after 2 h at the temperature of reaction.

2.3.2. Dehydrogenation of MCH

The catalytic dehydrogenation of methylcyclohexane was performed in an original stainless steel rectangular reactor (4.9 cm × 39 cm × 1.2 cm internal dimensions) (Fig. 1) displayed in a conventional test rig. The inlet gases entering the reactor first flowed through an inactive (non coated) foam to ensure an uniform distribution and to reach the required temperature, and then through the catalytic packing (4.9 cm × 19 cm × 1.2 cm) (foam or beads) containing ca. 2.5 g catalyst. The thermocouple to control the temperature was located inside the coated packing at 6 cm from the beginning of the catalytic zone. Five thermocouples were displayed on the external surface of the reactive foam (T_{wall}) and nine at the center (T_{center}). The reactor was equipped with graphite gaskets

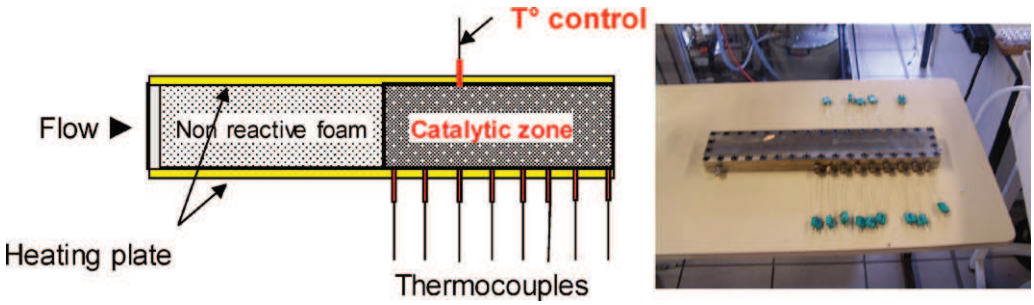

Fig. 1. Schematics of the parallelepipedic foam (i.d. 4.9 cm × 39.0 cm × 1.2 cm) reactor of dehydrogenation of methylcyclohexane, loaded with the non catalytic, gas dispersing, and the catalytic foams (from left to right), and equipped with thermocouples (one to control temperature, 5 and 9 to measure T_{wall} and T_{center}, respectively) (see text).

(DELTGRAP HT) designed to resist to high temperatures. The MCH flow was delivered with an ISMATEC pump in the range 1–9 g/min. MCH was then vaporised in a hot box (up to 250 °C) into which hydrogen was fed to limit the catalyst deactivation. The reactor was heated by means of two hot plates fixed at top and bottom of the reactor. The effluent passed through two condensers maintained at 0 °C, and was analyzed by GC. Experiments were performed at the same residence time W/F_{MCH} (from 2.6 to 15.4 kg_{cat} s mol^{-1}) for each structure by adjusting the inlet volumic flow rates of MCH and of H_2.

3. Results and discussion

3.1. Characterization of coated plates, foams and powders or beads

In the case of VO_x/TiO_2 catalyst to be deposited on silica/stainless steel it was necessary to first ensure the good mechanical and chemical holding of silica with the surface of the metal, which beared no chemical resemblance nor with silica or TiO_2 [17–19]. The influence of several parameters of synthesis of SiO_2-like layers (first step) and of coating by TiO_2 (second step) deposited on stainless steel plates was examined using experimental design. To summarize, the best results were obtained for a 5 μm-thick film of TMDSO polymer on plate, which was calcined at 1 °C/min heating rate, up to 650 °C (1 h). During calcination the film shrinked by ca. 70% and the final thickness of amorphous silica was ca. 1 μm. Once the parameters to get mechanically and chemically stable catalytic coatings of plates were optimised, they were supposed to be convenient for foam coating. However the design of the sample holder in the RPECVD reactor had to be modified in order to force the flow of the excited nitrogen reactive species (to which the TMDSO monomer and oxygen were added) to cross the whole volume of the foam cylinder. The thickness of the deposited layers of polymer was evaluated from SEM and EPMA pictures of the successively sliced pieces of foam. Typically, the thickness of TMDSO polymer was 5–50 μm (ca. 5 μm on struts and up to 50 μm in hollow parts) for 15 min long experiments. After optimisation of the time of deposition, 5–10 μm thick and stable SiO_2 layers after mineralisation (1 °C/min, 650 °C, 1 h) were obtained for 8 min of deposition of TMDSO polymer. As shown by measuring the contact angle in distilled water, the surface of silica-like layer on plates was slightly hydrophobic and the SiO_2/SSt-foams samples were further treated in a basic solution of NaOH + EtOH (Brown solution) [27,33].

For the second step to be optimised (dip-coating of SiO_2/SSt-Pl in TiO_2 suspension), the viscosity of TiO_2 anatase (Aldrich) particles suspended in deionised water was studied [34]. The optimal concentration to cover stainless steel foams was finally found for 37 wt% TiO_2 (Aldrich) in deionized water, instead of 60 wt% for plates. The same heating rate, maximum temperature and duration of plateau were used to obtain TiO_2/SiO_2/SSt-Fo. The cross section electron probe analysis (EPMA) across a strut clearly showed the two layers structure of the coatings on foam (Fig. 2, left) and plate (Fig. 2, right). The X-ray profile obtained by back-scattered electrons on foam showed the good covering by SiO_2 that should play its protective role, and by TiO_2, the support of the active polyvanadate VO_x species. As already mentioned, most methods of analysis of materials like X-ray diffraction, but also Raman spectroscopy or XPS, cannot be used for solid foams. The samples may be cut in pieces to be examined, but thus the contribution of iron can be very high and not representing the actual value. Therefore it was assumed that, for the third step as for the others, the surface active

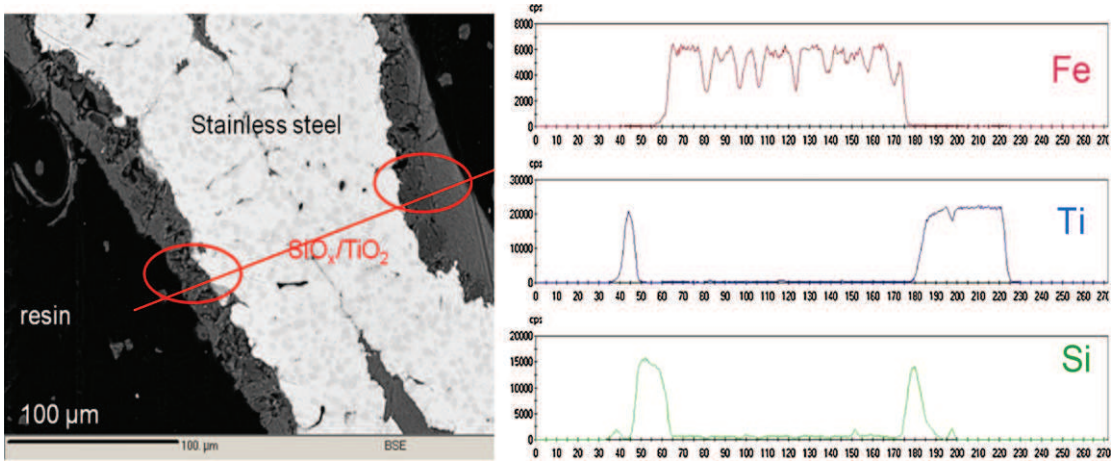

Fig. 2. Electron Probe Micro Analysis of a strut of stainless steel foam coated by TiO_2/SiO_2 after RPECVD and dip-coating steps (left), and X-ray BSE profiles of Fe, Ti, Si along the red line. (For interpretation of the references to color in this figure legend, the reader is referred to the web version of the article.)

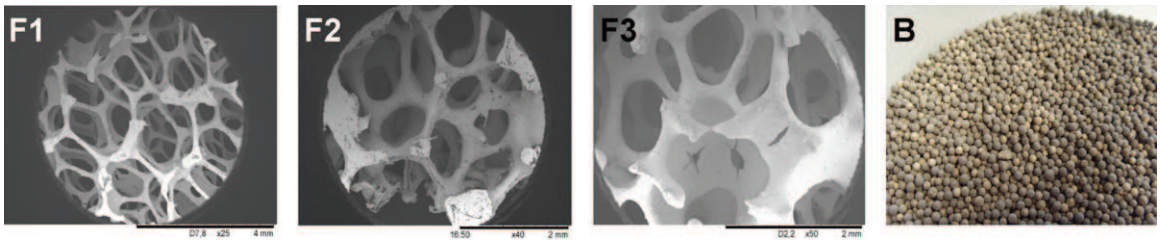

Fig. 3. DH of MCH. The four packings before coating by Pt/γ-Al_2O_3. From left to right: FeCrAlloy foams F1 (ε = 97%) and F2 (ε = 81%), alumina foam, molecular sieves beads.

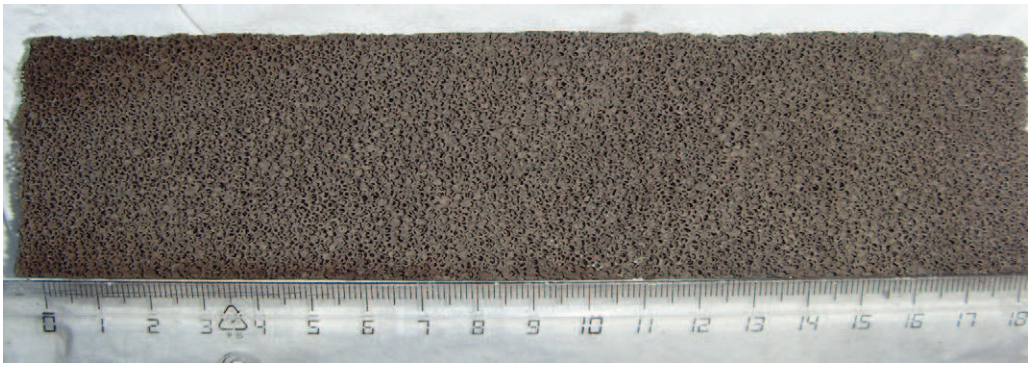

Fig. 4. DH of MCH. FeCrAlloy foam (19 cm × 4.9 cm) homogeneously coated by Pt/γ-Al_2O_3 catalyst.

VO_x species were the same on foams than on plates and powders for a given composition.

Stable coatings of foams and beads by Pt/γ-Al_2O_3 packings were easier to obtain. Molecular sieves were coated by incipient-wetness impregnation, in which case the amount of catalyst inside the pores was ascertained. In the case of foams, the mechanical but also the chemical compatibility between the material (alumina) and the catalyst were also ensured, including in the case of FeCrAlloy. Indeed alumina layers were formed during the thermal treatment of FeCrAlloy at 1100 °C in air [22,36,37]. The heat treatment was short to favour the formation of transition aluminas (close to the γ form) instead of the α form (corundum). The dispersion of Pt particles (63%) was measured by means of hydrogen chemisorption [21]. SEM pictures of the uncoated carriers and of the 19 cm long FeCrAlloy foam homogeneously coated by the Pt/γ-Al_2O_3 catalyst are presented Figs. 3 and 4, respectively.

3.2. Catalytic experiments

3.2.1. ODP on V_2O_5/TiO_2 foams and powders

The catalytic performance of foams and powders in the oxidative dehydrogenation of propane was compared for the same amount of active species (0.2 g of 2ML-VO_x/TiO_2) and in the same operating conditions. The same gaseous mixture composition, flowrate (6 stp L h^{-1}) and the same temperature range were used, with GHSV = 30 stpL h^{-1} g_{cat}^{-1}.

Fig. 5 presents the evolution of the conversions of propane (XC_3) and oxygen (XO_2), and of the selectivity to propene ($SC_3^=$) vs. temperature for 2ML-$VO_x/TiO_2/SiO_2$/SSt-Fo foam in FR. As it is usual in the oxidative dehydrogenation of alkanes, $SC_3^=$ decreased while selectivity to CO_2 and conversion increased upon increasing the temperature. To compare the catalytic properties of foams and powders, the selectivity to propene was plotted against the conversion of propane (Fig. 6). 2ML-VO_x/TiO_2 powder in the SVR exhibited the same behaviour than in literature and in our own work [19]. $SC_3^=$ decreased strongly when XC_3 increased, and at 500 °C the selectivity to carbon oxides was very high (86 mol%). When loaded in the FR, the same amount of active powder (0.2 g) led to both smaller oxygen conversion and selectivity to carbon oxides. The variation of selectivity $\Delta SC_3^=$ vs. the variation of conversion ΔXC_3 for the same range of temperature (100 °C) was taken as a rough indicator to compare the catalytic performance, but also to highlight the thermal gradients. For the two powder beds, the slope $\Delta SC_3^=/\Delta XC_3 = -4.2$ was steeper in SVR than in FR ($\Delta SC_3^=/\Delta XC_3 = -0.4$). In SVR, the catalyst bed density was 5.6 times higher than in FR. As GHSV was similar in both reactors, the difference of selectivity could not be related to the contact time. The gas velocity was higher in SVR (i.d. ⌀1.2 cm) than in FR (i.d. ⌀1.6 cm), leading to an increase of the global heat transfer coefficient (+30%). But this increase was not sufficient to balance the A_{FR}/A_{SVR} exchange area (A) ratio, which was about 4.2. Consequently, the ODH of propane being exothermic, the temperatures in the bed center in SVR were evidently higher than those in FR and the selectivity decreased. The lower $\Delta SC_3^=/\Delta XC_3$ slope could be directly linked to improved thermal gradients and heat transfer.

When comparing the selectivity to propene obtained with the catalytic foam and with the powders in FR, other parameters being equal (same catalyst loading at the same GHSV = 30 stpL h^{-1} g_{cat}^{-1}),

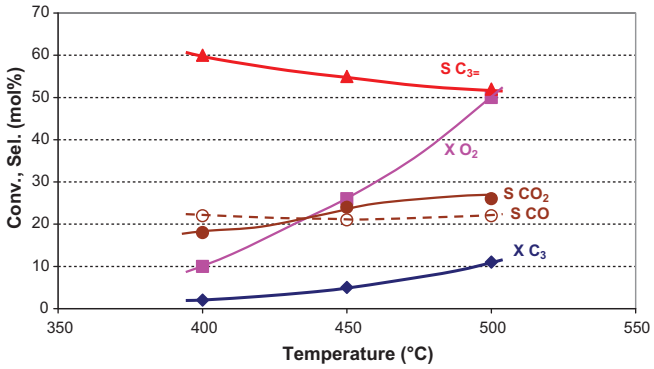

Fig. 5. ODP Conversion of reactants (XC_3 and XO_2) and selectivity (S) to products vs. temperature for 2ML-$VO_x/TiO_2/SiO_2$ foam.

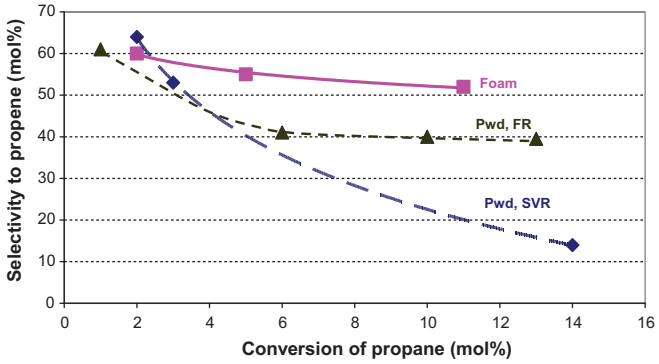

Fig. 6. ODP Comparison of 2ML-VO_x/TiO_2 powders and 2ML-$VO_x/TiO_2/SiO_2$ coated foam. Selectivity vs. conversion for powders in small volume reactor (pwd, SVR), in foam reactor (pwd, FR) and for foam in foam reactor.

$SC_3^=$ for the foam was much higher at any conversion, showing more efficient heat transfer in foam than in the packed bed. However, the void fraction being higher in the foam than in the packed bed, the actual residence time was higher, which thereby should have promoted the combustion of propene [9,11,12]. Moreover the gas velocity was lower in the foam than in the powder bed. Thus, if the heat transfer were due to gas convection only, it would be more favourable in powders than in foams. As a result, the temperature would be higher in the foam than in the powder bed, and as a consequence, the conversion of propane would be higher and the selectivity to propene would be lower. As the reverse situation (higher selectivity) was observed with the foam, it is assumed that the improved heat transfer was mostly due to conduction through the metallic substrate. Moreover, the external heat transfer between the reactor walls and the foam was probably good. Indeed it was very difficult to withdraw the foam from the reactor after reaction, without destroying it partially. However, these conclusions cannot be extrapolated to industrial reactors, due to the Reynolds range. In the previous experiments, Re values in packed bed in FR and in SVR were about 0.01, when in industrial reactors Re can be higher than 1000. The value of Re calculated using the mean diameter of struts in the foam was of the same order of magnitude. In conclusion, the contribution of the solid to the bed conductivities was higher for the foam than for the powder.

3.2.2. Dehydrogenation of MCH on Pt/alumina foams and beads

To confirm the beneficial effect of the structuration of the catalytic solid on the heat transfer, the dehydrogenation of MCH was studied in the second type of foam reactor (Fig. 1). The aim was to measure the temperature gradient, ΔT, between the reactor wall and the reactor center at different distances from the inlet, using the different packings during the reaction process. The effects due to the nature (metal, ceramic, molecular sieve) and geometry (beads or foams) of the structure on the temperature gradients in the reactor were studied. In the absence of reaction, a flat temperature profile was observed for all structures. In all experiments, no methylcyclohexane nor toluene decomposition, and no specific deactivation of uncoated metal, ceramic or molecular sieves were observed. We concluded that all substrates were inert in the reaction but also that they had no effect on the properties of Pt/γ-Al_2O_3 catalyst, and particularly on its catalytic activity (per g of Pt on alumina).

Fig. 7 presents the profiles of temperature at the center (T_{center}) and at the wall (T_{wall}) during the reaction at 300 °C and $W/F_{MCH} = 15.4\ kg_{cat}\ s\ mol^{-1}$. They were measured along the catalytic part of the reactor, from the inlet to the outlet (left to right in Fig. 1, respectively) through the two catalytic Pt/γ-Al_2O_3/FeCrAlloy

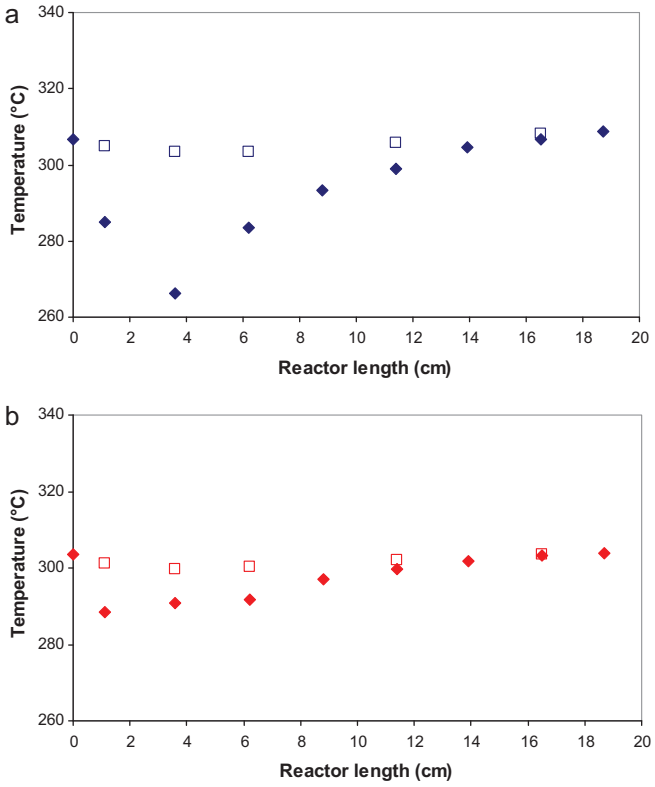

Fig. 7. DH of MCH. Variation of temperature vs. axial position. Central thermocouples (lozenges) and wall thermocouples (squares) in FeCrAl foams (a) F1: 33 ppi, $\varepsilon = 97\%$; (b) F2: 33 ppi, $\varepsilon = 81\%$.

foams. The temperature gradient ΔT showed a maximum which varied from ca. 10 to 35 °C by the only variation of the voidage, $\varepsilon = 81$ vs. 97%, respectively. The same type of experiment was repeated while varying W/F and temperature (Table 2). Pt/γ-Al_2O_3/corundum foam, as well as beads coated by Pt/γ-Al_2O_3, were also investigated. High maximum temperature gradients were observed at high W/F for beads and for the most porous of the metallic foams, but the MCH conversion (X_{MCH}) did not vary. The temperature gradient was the smallest with the denser foams (either ceramic or metallic) but X_{MCH} was lower for alumina at both W/F. The position of the control thermocouple, which laid at bed half-thickness (at 6 cm from the catalytic zone inlet), made it difficult to get exactly the same heat power, and thus to get the same wall temperature in each experiment. Moreover, the controlled temperature being near the cold point, the less conducting the bed, the higher was the temperature at wall. For example, let us compare F1 and F2 foams at low W/F ($2.6\ kg_{cat}\ s\ mol^{-1}$). The material with the lowest conductivity (F1) showed a large cold point in the center ($\Delta T = 42$, vs. 25° for F2), and thus a high T_{wall} which led to antagonist effects on the MCH conversion ($X_{MCH} = 40$ vs. 54 mol% for F2) (Table 2). For all experiments on catalytic beads, the

Table 2
Maximum temperature gradient (ΔT) and MCH conversion (X) for the three foams and for coated beads at two W/F contact times ($Q_{H_2} = 3.3 \times 10^{-4}\ mol\ s^{-1} = 3.3 \times 10^{-4}\ mol\ s^{-1}$; $T_{controller} = 300$ °C).

Packing	$W/F_{MCH} = 15.4\ kg_{cat}.s.mol^{-1}$		$W/F_{MCH} = 2.6\ kg_{cat}.s.mol^{-1}$	
	ΔT (°C)	X (%)	ΔT (°C)	X (%)
F1 (FeCrAlY)	38	98	42	40
F2 (FeCrAlY)	13	97	25	54
F3 (α-Al_2O_3)	13	78	30	40
B (zeolite)	37	97	66	54

values of Reynolds were comprised between 10 and 75. As the bead diameter were chosen to get the same pressure drop as for foams, the values of Re for foams and beads were of the same order. In the absence of a detailed modelling, which is in progress, it was difficult to correlate the MCH conversion with the conducting properties of foams. However, as a conclusion, even for highly endothermic reactions not limited by external transport, the catalytic foams seemed to significantly increase the effective conductivity of catalytic beds, the higher foam density leading to higher effective conductivity and to runs closer from being isothermal.

4. Conclusion

Using solid foams to carry catalysts is confirmed to be a good way to enhance heat and mass transfers, as shown in recent literature. The solid foam can improve the radial bed conductivity and decrease the thermal gradients. This was also demonstrated in this paper. Two different reactions, one exothermic and one endothermic, were operated with two different catalysts, and the catalytic performance of foams was compared to those of more usual catalyst shapings (powder or beads). For each reaction, experiments were performed with the same loading of active phase and in the same operating conditions. Using a catalytic stainless steel foam in the exothermic oxidative dehydrogenation of propane to propene was clearly responsible for increasing the yield of propene when compared to catalytic powder. It is assumed that hot spots were reduced, leading to more isothermal the operation. Some experiments (not shown here) were performed on unprotected (without SiO_2) 2ML-VO_x/TiO_2 foam. A similar activity was observed, in accordance with the fact that the same vanadate species were displayed on the same TiO_2 support, but the selectivity to propene was lower by ca. 10–15%. One of the beneficial effects of SiO_2 interlayer could therefore be due to a "chemical" effect. Indeed the metal was homogeneously covered by silica and the presence (or diffusion to the active surface) of iron or chromium cations, that would promote total oxidation, could be avoided. The very good mechanical stability of SiO_2/SSt plates and foams could be related to the small content of carbon in silica ($SiC_{0.01}O_{1.82}$). As most carbon was shown to be located inwards, close to stainless steel, a certain degree of plasticity could allow to accommodate the difference of dilatation coefficients between the oxidic support and the metallic substrate. Other parameters like W/F and C_2/O_2 ratio are currently varied to check the chemical regime and to increase the yield of propene as more as possible. The isothermicity due to more efficient heat transfer has to be confirmed by measuring the temperature gradient between the center of the foam and the wall of reactor, in the same way as done in MCH dehydrogenation experiments. Such temperature profiles could be obtained for this endothermic reaction in the original parallelepipedic reactor equipped with several thermocouples distributed along the bed length. The variation of temperature gradient between the reactor wall and the reactor center at different distances from the inlet was shown to depend more on the bed porosity than on the foam material. A nearly isothermal behaviour was shown with the denser foams. Though it would be risky to directly extrapolate our laboratory experiments (low Re) to larger reactors, the coating of catalysts on dense foams is a potential way to study the kinetics of highly endo or exothermic reactions at constant temperature and pressure.

Acknowledgements

The Agence nationale pour la Recherche (ANR-MILLICAT No. 06-BLAN-0216) is acknowledged for A. Essakhi and Y. Swesi grants and for financial support.

References

[1] A. Cybulski, J. Moulijn, Structured Catalysts and Reactors, Taylor & Francis, BocaRaton, USA, 2006.
[2] J.A. Moulijn, A. Stankiewicz, Structured catalysts and reactors, Catal. Today 69 (1–4) (2001).
[3] L. Kiwi-Minsker, A. Renken, Microstructured reactors for catalytic reactions, Catal. Today 110 (2005) 2–14.
[4] D. Edouard, T. Truong Huu, C. Pham Huu, F. Luck, D. Schweich, The effective thermal properties of solid foam beds: experimental and estimated temperature profiles, Int. J. Heat Mass Trans. 53 (2010) 3807–3816.
[5] G. Incera Garrido, B. Kraushaar-Czarnetzki, A general correlation for mass transfer in isotropic and anisotropic solid foams, Chem. Eng. Sci. 65 (2010) 2255–2257.
[6] F. Cavani, Catalytic selective oxidation: the forefront in the challenge for a more sustainable industrial chemistry, Catal. Today 156 (2010) 8–15.
[7] F. Cavani, N. Ballarini, A. Cericola, Oxidative dehydrogenation of ethane and propane: how far from commercial implementation? Catal. Today 127 (2007) 113–131.
[8] O. Schwarz, P.-Q. Duong, G. Schäfer, R. Schomäcker, Development of a microstructured reactor for heterogeneously catalyzed gas phase reactions: Part I. Reactor fabrication and catalytic coatings, Chem. Eng. J. 145 (2009) 420–428.
[9] R. Grabowski, S. Pietrzyk, J. Słoczynski, F. Genser, K. Wcisło, B. Grzybowska-Świerkosz, Kinetics of the propane oxidative dehydrogenation on vanadia/titania catalysts from steady-state and transient experiments, Appl. Catal. A: Gen. 232 (1–2) (2002) 277–288.
[10] A. Dinse, S. Khennache, B. Frank, C. Hess, R. Herbert, S. Wrabetz, R. Schlögl, R. Schomäcker, Oxidative dehydrogenation of propane on silica (SBA-15) supported vanadia catalysts: a kinetic investigation, J. Mol. Catal. A: Chem. 307 (1–2) (2009) 43–50.
[11] K. Routray, K.R.S.K. Reddy, G. Deo, Oxidative dehydrogenation of propane on V_2O_5/Al_2O_3 and V_2O_5/TiO_2 catalysts: understanding the effect of support by parameter estimation, Appl. Catal. A: Gen. 265 (1) (2004) 103–113.
[12] B. Frank, A. Dinse, O. Ovsitser, E.V. Kondratenko, R. Schomäcker, Mass and heat transfer effects on the oxidative dehydrogenation of propane over a low loaded VO_x/Al_2O_3 catalyst, Appl. Catal. A: Gen. 323 (2007) 66–76.
[13] G.C. Bond, P. König, The vanadium pentoxide–titanium dioxide system: Part 2. Oxidation of o-xylene on a monolayer catalyst, J. Catal. 77 (2) (1982) 309–322.
[14] G.C. Bond, Preparation and properties of vanadia/titania monolayer catalysts, Appl. Catal. A: Gen. 157 (1–2) (1997) 91–103.
[15] J.C. Védrine (Ed.), EUROCAT oxide, Catal. Today 20 (1) (1994).
[16] E. Bordes, Synergistic effects in selective oxidation catalysis: is phase cooperation resulting in site isolation? Top. Catal. 15 (2001) 131–137.
[17] T. Giornelli, A. Löfberg, E. Bordes-Richard, Grafting of VO_x/TiO_2 catalyst on anodized aluminum plates to be used in structured reactors, Thin Solid Films 479 (2005) 64–72.
[18] T. Giornelli, A. Löfberg, E. Bordes-Richard, Preparation and characterization of VO_x/TiO_2 catalytic coatings on stainless steel plates for structured catalytic reactors, Appl. Catal. A: Gen. 305 (2006) 197–203.
[19] A. Löfberg, T. Giornelli, S. Paul, E. Bordes-Richard, Catalytic coatings for structured supports and reactors: VO_x/TiO_2 catalyst coated on stainless steel for oxidative dehydrogenation of propane, Appl. Catal. A: Gen. 391 (1–2) (2011) 43–51.
[20] M. Roumanie, V. Meille, C. Pijolat, G. Tournier, C. de Bellefon, P. Pouteau, C. Delattre, Design and fabrication of a structured catalytic reactor at micrometer scale: example of methylcyclohexane dehydrogenation, Catal. Today 110 (2005) 164–170.
[21] P. Kerleau, Y. Swesi, V. Meille, I. Pitault, F. Heurtaux, Total catalytic oxidation of a side-product for an autothermal restoring hydrogen process, Catal. Today 157 (2010) 321–326.
[22] A. Shamsi, J.J. Spivey, Partial oxidation of methane on Ni–MgO catalysts supported on metal foams, Ind. Eng. Chem. Res. 44 (2005) 7298–7305.
[23] M. Maestri, A. Beretta, G. Groppi, E. Tronconi, P. Forzatti, Comparison among structured and packed-bed reactors for the catalytic partial oxidation of CH_4 at short contact times, Catal. Today 105 (2005) 709–717.
[24] V. Palma, E. Palo, P. Ciambelli, Structured catalytic substrates with radial configurations for the intensification of the WGS stage in H_2 production, Catal. Today 147S (2009) S107–S112.
[25] F.C. Moates, T.E. McMinn, J.T. Richardson, Radial reactor for trichloroethylene steam reforming, AIChE J. 45 (1999) 2411–2418.
[26] V. Meille, Review on methods to deposit catalysts on structured surfaces, Appl. Catal. A: Gen. 315 (2006) 1–17.
[27] A. Essakhi, A. Löfberg, Ph. Supiot, B. Mutel, S. Paul, V. Le Courtois, E. Bordes-Richard, Coating metallic foams and structured reactors by VOx/TiO2 oxidation catalyst: application of RPECVD, in: Proc. 10th International Symposium "Scientific Bases for the Preparation of Heterogeneous Catalysts", in: E.M. Gaigneaux, M. Devillers, S. Hermans, P. Jacobs, J. Martens, P. Ruiz (Eds.), Stud. Surf. Sci. Catal. 175 (2010) 17–24 (July 11–14).
[28] L. Guillou, D. Balloy, P. Supiot, V. Le Courtois, Preparation of a multilayered composite catalyst for Fischer–Tropsch synthesis in a micro-chamber reactor, Appl. Catal. A: Gen. 324 (2007) 42–51.
[29] T. Giornelli, A. Löfberg, L. Guillou, S. Paul, V. Le Courtois, E. Bordes-Richard, Catalytic wall reactor. Catalytic coatings of stainless steel by VO_x/TiO_2 and Co/SiO_2 catalysts, Catal. Today 128 (2007) 201–207.

[30] L. Guillou, S. Paul, V. Le Courtois, Investigation of H_2 staging effects on CO conversion and product distribution for Fischer–Tropsch synthesis in a structured microchannel reactor, Chem. Eng. J. 136 (2008) 66–76.
[31] P. Supiot, C. Vivien, A. Granier, A. Bousquet, A. Mackova, F. Boufayed, D. Escaich, P. Raynaud, Z. Stryhal, J. Pavlik, Growth and modification of organosilicon films in PECVD and PACVD reactors, Plasma Proc. Polym. 3 (2) (2006) 100–109.
[32] F. Callebert, P. Supiot, K. Asfardjani, O. Dessaux, P. Dhamelincourt, J. Laureyns, Cold remote nitrogen plasma polymerization from 1.1.3.3.tetramethyldisiloxane/oxygen mixture, J. Appl. Polym. Sci. 52 (1994) 1595–1606.
[33] A. Essakhi, A. Löfberg, P. Supiot, B. Mutel, S. Paul, V. Le Courtois, E. Bordes-Richard, Coating of structured reactors by plasma assisted polymerization of TMDSO, in: Proc. 6th Int. Symp. Polyimides and Other High Temperature/High Performance Polymers: Synthesis, Characterization and Applications, Melbourne, Florida, USA, November 9-11, Polym. Eng. Sci. 51 (2011) 940-947.
[34] A. Essakhi, A. Löfberg, S. Paul, B. Mutel, P. Supiot, V. Le Courtois, P. Rodriguez, V. Meille, E. Bordes-Richard, Materials chemistry for catalysis: coating of catalytic oxides on metallic foams, Microporous Mesoporous Mater. 140 (2011) 81–88.
[35] G.C. Bond, J. Perez Zurita, S. Flamerz, Structure and reactivity of titania-supported oxides. Part 2: Characterisation of various vanadium oxide on titania catalysts by X-ray photoelectron spectroscopy, Appl. Catal. 27 (2) (1986) 353–362.
[36] P.T. Moseley, K.R. Hyde, B.A. Bellamy, G. Tappin, The microstructure of the scale formed during the high temperature oxidation of a FeCrAlloy steel, Corros. Sci. 24 (6) (1984) 547–565.
[37] O. Sanz, F.J. Echave, M. Sánchez, A. Monzón, M. Montes, Aluminium foams as structured supports for volatile organic compounds (VOCs) oxidation, Appl. Catal. A: Gen. 340 (2008) 125–132.